Supporting Information

A Chiral Cyclometalated Iridium Star of David [2]Catenane

David P. August, Javier Jaramillo-Garcia, David A. Leigh,* Alberto Valero, and Iñigo J. Vitorica-Yrezabal

School of Chemistry, University of Manchester, Manchester M13 9PL, UK.

Email: david.leigh@manchester.ac.uk

Table of Contents

1. General Experimental Section

All reagents and solvents were purchased from Sigma-Aldrich, Alfa Aesar or Fluorochem and used without further purification unless otherwise specified. 6-Phenylpyridin-3-ol[S1] and compounds **4**,[S2] **S1**,[S2] and **S4**[S3] were synthesised following literature procedures. Dry solvents were obtained by passing through an activated alumina column on a Phoenix SDS solvent drying system (JC Meyer Solvent Systems, CA, USA). NMR spectra were recorded on a Bruker Avance III equipped with a cryoprobe (5mm CPDCH 13C-1H/D) instrument with an Oxford AS600 magnet. Chemical shifts are reported in parts per million (ppm) from high to low frequency and referenced to the residual solvent resonance. Coupling constants (J) are reported in Hertz (Hz). Standard abbreviations indicating multiplicity were used as follows: s = singlet, d = doublet, t = triplet, q = quartet, quin = quintet, sep = septet, m = multiplet, br = broad. In 13C NMR and DEPTQ, the abbreviation Cq refers to unassigned quaternary carbons. 1H assignments were made using 2D NMR methods (COSY, HSQC, HMBC, NOESY). Low resolution ESI mass spectrometry was performed with a Thermo Scientific LCQ Fleet or an Advion Expression CMS L single quadrupole MS detector. High resolution ESI (electrospray ionisation) was carried out by the mass spectrometry services at the University of Manchester. Flash column chromatography was carried out using Silica 60 Å (particle size 40-63 μm, Sigma Aldrich, UK) as the stationary phase. Analytical thin layer chromatography (TLC) was performed on pre-coated silica gel plates (0.25 mm thick, 60 g F254, Merck, Germany) and visualised using both short and long wave ultraviolet light. Size exclusion chromatography was carried out using Bio-Beads S-X1 (styrene divinylbenzene beads for size exclusion chromatography, 1% crosslinkage, 40–80 μm bead size, 600–14000 MW exclusion range, Bio-Rad, UK) as the stationary phase.

2. Abbreviations

COSY	correlation spectroscopy
DCE	1,2-dichloroethane
DCM	dichloromethane
DEPTQ	distorsionless enhancement by polarization transfer including the detection of quaternary nuclei
DMF	dimethylformamide
ESI	electrospray ionisation
HMBC	heteronuclear mulitple bond correlation
HSQC	heteronuclear single quantum coherence
LDA	lithium diisopropylamide
MS	mass spectrometry
NMR	nuclear magnetic resonance
NOESY	nuclear overhauser effect spectroscopy
TBAF	tetrabutylammonium fluoride
TBDMS	tert-butyldimethylsilyl
THF	tetrahydrofuran
TLC	thin layer chromatography

3. Synthetic Procedures

3.1 Synthesis of mesylate fragment 5

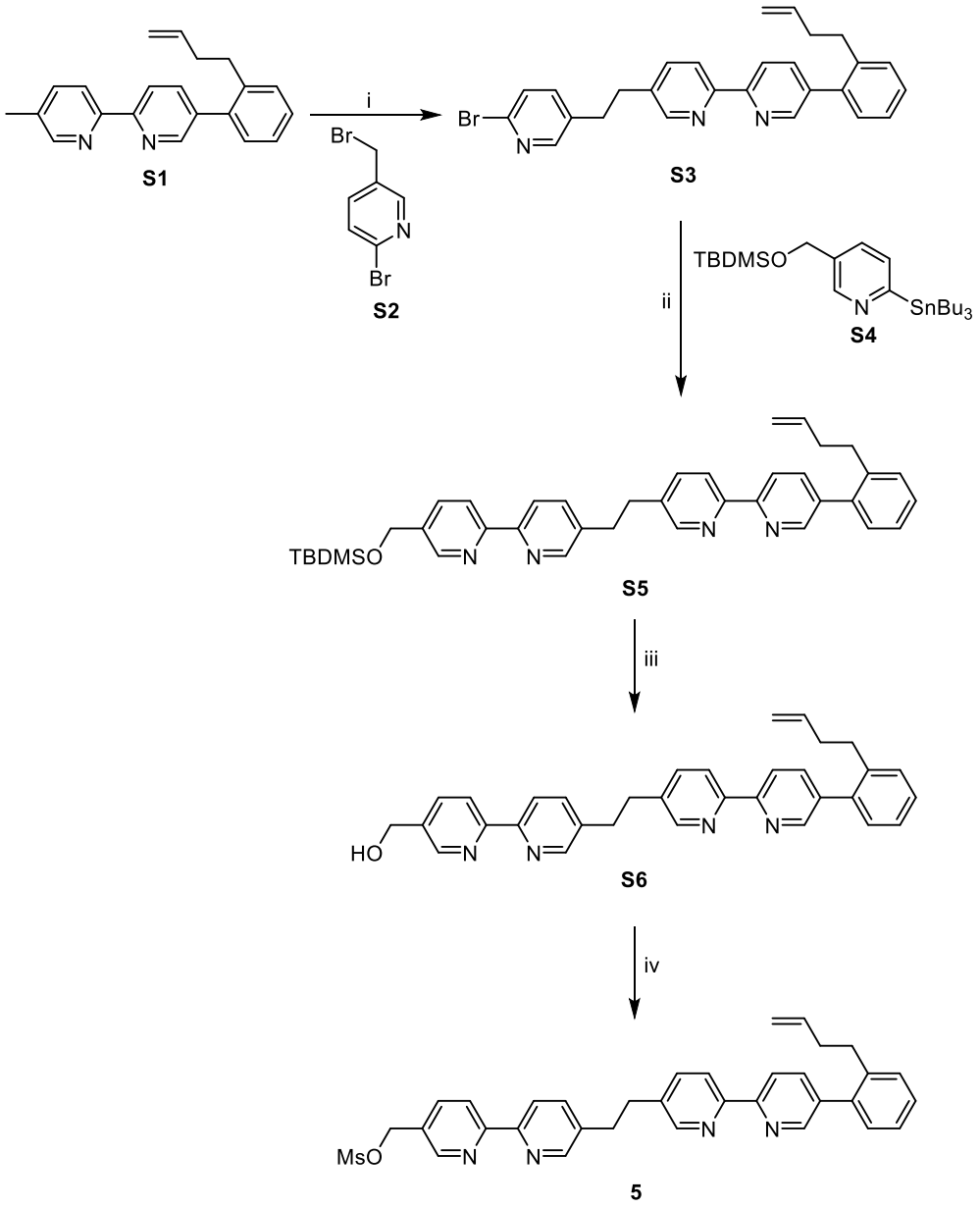

Scheme S1. Synthetic route to mesylate fragment **5**. Reaction conditions: i) LDA, THF, N_2, -78 °C, 1 h; **S2**, THF, N_2, -78 °C, 3.5 h; MeOH, -78 °C to rt; ii) **S4**, $Pd(PPh_3)_4$, toluene, N_2, reflux, 48 h; iii) TBAF, THF, N_2, rt, 1 h; iv) Ms_2O, Et_3N, DCM, N_2, 0 °C to rt, 1 h.

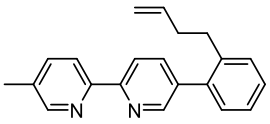

S1

Compound **S1** was prepared according to the literature procedures.[S2] The obtained characterization data was in accordance with that previously reported.

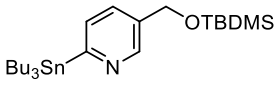

S4

Compound **S4** was prepared according to the literature procedures.[S3] The obtained characterization data was in accordance with that previously reported.

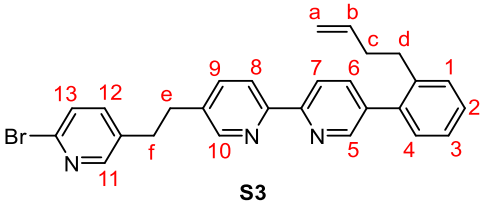

S3

Compound **S1** (1.00 g, 3.33 mmol), LDA solution (1.66 mL, 2.0 M in THF/heptane/ethylbenzene, 3.33 mmol, 1.0 equiv.) and compound **S2** (877 mg, 3.50 mmol, 1.05 equiv.) were each placed in separate flasks backfilled with nitrogen. Then, 10 mL, 10 mL and 80 mL of dry THF were added to each flask respectively. Compound **S1** and the LDA solution were cooled to -78 °C, and the LDA solution was cannulated dropwise into the compound **S1** solution. The mixture was stirred at -78 °C for 1 h. The solution of compound **S2** was then added to the mixture over 90 minutes, and the mixture was allowed to react for additional 2 h at -78 °C. The crude reaction was then quenched with methanol (25 mL) and warmed to room temperature. The solvent was removed, and the crude mixture dissolved in DCM. The organic layer was washed with distilled water and brine, dried over $MgSO_4$, filtered and its solvent removed. The mixture was then purified by flash column chromatography with petroleum ether/ethyl acetate/triethylamine 85:15:2 as eluent, to afford 1.02 g of **S3** (65% Yield). ^{1}H NMR (600 MHz, $CDCl_3$) δ 8.64 (d, *J* = 2.2 Hz, 1H, H_5), 8.47 (d, *J* = 2.2 Hz, 1H, H_{10}), 8.41 (d, *J* = 8.1 Hz, 1H, H_7), 8.36 (d, *J* = 8.1 Hz, 1H, H_8), 8.20 (d, *J* = 2.5 Hz, 1H, H_{11}), 7.78 (dd, *J* = 8.1, 2.2 Hz, 1H, H_6), 7.59 (dd, *J* = 8.1, 2.3 Hz, 1H, H_9), 7.39 (d, *J* = 8.1 Hz, 1H, H_{13}), 7.37 – 7.23 (m, 5H, H_{12}, H_1 - H_4), 5.70 (ddt, *J* = 16.9, 10.2, 6.6 Hz, 1H, H_b), 4.94 – 4.85 (m, 2H, H_a), 3.04 – 2.93 (m, 4H, H_e, H_f), 2.74 – 2.69 (m, 2H, H_d), 2.28 – 2.21 (m, 2H, H_c). ^{13}C NMR (151 MHz, $CDCl_3$) δ 154.60 (C_7-C-N), 154.56 (C_8-C-N), 150.36 (C_{11}), 149.51 (C_{10}), 149.46 (C_5), 140.12 (C_{13}-C-N), 139.77 (C_4-C-C-C_1), 138.90 (C_{12}), 138.03 (C_4-C-C-C_1), 137.76 (C_b), 137.74 (C_6), 137.50 (C_5-C-C_6), 137.15 (C_9), 135.84 (C_9-C-C_{10}), 135.41 (C_{11}-C-C_{12}), 130.33

(C_4), 129.71 (C_1), 128.41 (C_2), 127.94 (C_{13}), 126.30 (C_3), 120.94 (C_8), 120.40 (C_7), 115.25 (C_a), 35.36 (C_c), 34.32 (C_e, C_f), 33.88 (C_e, C_f), 32.61 (C_d). HRESI-MS: m/z = 492.1039 $[M+Na]^+$ (calcd. for $C_{27}H_{24}BrN_3Na$ 492.1046).

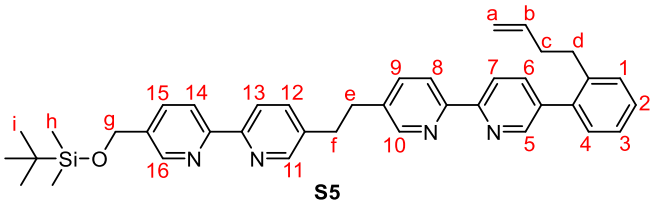

S5

Compound **S3** (0.80 g, 1.70 mmol) and compound **S4** (1.31 g, 2.55 mmol, 1.5 equiv.) were placed in a sealed vial backfilled with nitrogen. $Pd(PPh_3)_4$ (0.14 g, 0.12 mmol, 7 mol%) was added as a suspension in degassed anhydrous toluene (5 mL), and the mixture was heated to reflux and stirred for 48 h. After cooling to room temperature, the solvent was removed and the crude mixture was purified by flash column chromatography with petroleum ether/ethyl acetate/triethylamine 85:15:2 as eluent, to afford 0.68 g of **S5** (64% Yield). ^{1}H NMR (600 MHz, $CDCl_3$) δ 8.63 (d, *J* = 2.2 Hz, 1H, H_5), 8.62 (d, *J* = 2.3 Hz, 1H, H_{16}), 8.51 (d, *J* = 2.4 Hz, 1H, H_{11}), 8.49 (d, *J* = 2.3 Hz, 1H, H_{10}), 8.41 (d, *J* = 8.1 Hz, 1H, H_7), 8.35 (d, *J* = 8.1 Hz, 1H, H_{13}), 8.33 (d, *J* = 8.1 Hz, 1H, H_{14}), 8.30 (d, *J* = 8.1 Hz, 1H, H_8), 7.78 – 7.74 (m, 2H, H_6, H_{15}), 7.62 (dd, *J* = 8.1, 2.3 Hz, 1H, H_{12}), 7.59 (dd, *J* = 8.1, 2.3 Hz, 1H, H_9), 7.38 – 7.22 (m, 4H, H_1 - H_4), 5.70 (ddt, *J* = 16.9, 10.2, 6.6 Hz, 1H, H_b), 4.94 – 4.87 (m, 2H, H_a), 4.82 (s, 2H, H_g), 3.05 (s, 4H, H_e, H_f), 2.74 – 2.69 (m, 2H, H_d), 2.26 – 2.21 (m, 2H, H_c), 0.95 (s, 9H, H_i), 0.12 (s, 6H, H_h). ^{13}C NMR (151 MHz, Chloroform-*d*) δ 155.09 (C_{14}-C-N), 154.72 (C_7-C-N), 154.55 (C_8-C-N), 154.35 (C_{13}-C-N), 149.56 (C_{11}), 149.46 (C_{10}), 149.40 (C_5), 147.44 (C_{16}), 139.76 (C_4-C-C-C_1), 138.07 (C_4-C-C-C_1), 137.75 (C_b), 137.68 (C_6), 137.36 (C_5-C-C_6), 137.17 (C_{12}), 137.11 (C_9), 136.74 (C_{15}-C-C_{16}), 136.34 (C_{11}-C-C_{12}), 136.11 (C_9-C-C_{10}), 135.04 (C_{15}), 130.32 (C_4), 129.68 (C_1), 128.35 (C_2), 126.27 (C_3), 120.86 (C_{13}), 120.80 (C_8), 120.61 (C_{14}), 120.36 (C_7), 115.23 (C_a), 62.92 (C_g), 35.35 (C_c), 34.52, 34.50 (C_e, C_f), 32.60 (C_d), 26.03 (C_i), 18.50 (Si-C-C_i), -5.10 (C_h). HRESI-MS: m/z = 635.3168 $[M+Na]^+$ (calcd. for $C_{39}H_{44}N_4NaOSi$ 635.3177).

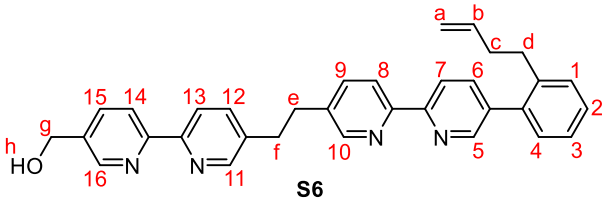

S6

Compound **S5** (0.68 g, 1.10 mmol) was placed in a flask backfilled with nitrogen and dissolved in 15 mL of dry THF. Then tetrabutylammonium fluoride solution (1.21 mL, 1.0 M in THF, 1.21 mmol, 1.1 equiv.) was added dropwise. The mixture was stirred at room temperature for 1 h, and then quenched with water (15 mL) and a small amount of calcium carbonate. The crude mixture was partitioned in DCM/water and the organic layer was extracted. The organic layer was then washed with distilled water, dried over Na_2SO_4, filtered and the solvent removed to afford 0.53 g of **S6** (97% Yield). ^{1}H NMR (600 MHz, $CDCl_3$) δ 8.64 (d, *J* = 2.3 Hz, 1H, H_{16}), 8.63 (d, *J* = 2.3 Hz, 1H, H_5), 8.50 (d, *J* = 2.3 Hz, 1H, H_{10}), 8.49 (d, *J* = 2.4 Hz, 1H, H_{11}), 8.41 (d, *J* = 8.1 Hz, 1H, H_7), 8.35 (d, *J* = 8.1 Hz, 1H, H_{14}), 8.34 (d, *J* = 8.1 Hz, 1H, H_8), 8.30 (d, *J* = 8.2 Hz, 1H, H_{13}), 7.83 (dd, *J* = 8.1, 2.3 Hz, 1H, H_{15}), 7.77 (dd, *J* = 8.1, 2.3 Hz,

1H, H_6), 7.62 (dd, *J* = 8.1, 2.3 Hz, 1H, H_9), 7.60 (dd, *J* = 8.1, 2.3 Hz, 1H, H_{12}), 7.39 – 7.22 (m, 4H, H_1 - H_4), 5.69 (ddt, *J* = 16.9, 10.2, 6.6 Hz, 1H, H_b), 4.94 – 4.85 (m, 2H, H_a), 4.79 (s, 2H, H_g), 3.05 (s, 4H, H_e, H_f), 2.74 – 2.69 (m, 2H, H_d), 2.26 – 2.21 (m, 2H, H_c), 2.13 – 2.02 (br s, 1H, H_h). ^{13}C NMR (151 MHz, $CDCl_3$) δ 155.67 (C_{14}-C-N), 154.70 (C_7-C-N), 154.37 (C_8-C-N), 154.34 (C_{13}-C-N), 149.56 (C_{10}), 149.50 (C_{11}), 149.42 (C_5), 148.13 (C_{16}), 139.77 (C_4-C-C-C_1), 138.06 (C_4-C-C-C_1), 137.76 (C_b), 137.71 (C_6), 137.40 (C_5-C-C_6), 137.20, 137.18 (C_9, C_{12}), 136.33, 136.32 (C_9-C-C_{10}, C_{11}-C-C_{12}), 136.09 (C_{15}-C-C_{16}), 135.89 (C_{15}), 130.33 (C_4), 129.69 (C_1), 128.37 (C_2), 126.28 (C_3), 120.94 (C_{13}), 120.90, 120.87 (C_8, C_{14}), 120.38 (C_7), 115.24 (C_a), 62.89 (C_g), 35.35 (C_c), 34.50 (C_e, C_f), 32.61 (C_d). HRESI-MS: m/z = 521.2316 $[M+Na]^+$ (calcd. for $C_{33}H_{30}N_4NaO$ 521.2312).

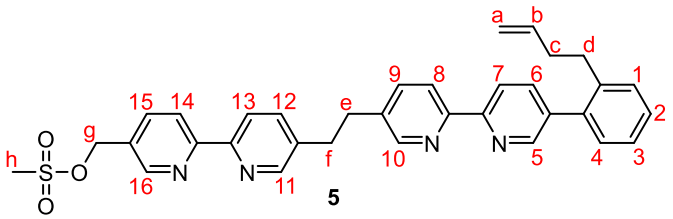

5

Compound **S6** (100 mg, 0.20 mmol) and mesyl anhydride (52 mg, 0.30 mmol, 1.5 equiv.) were placed in a sealed vial backfilled with nitrogen and dissolved in 4 mL of dry DCM. The solution was cooled to 0 °C and then dry triethylamine (42 µL, 30 mg, 0.30 mmol, 1.5 equiv.) was added dropwise. The mixture was allowed to warm to room temperature and stirred for 1 h. The mixture was quenched with water (6 mL), and partitioned in DCM/water. The organic layer was extracted, washed with distilled water, dried over Na_2SO_4, filtered and the solvent removed to afford 115 mg of **5** (99% Yield). ^{1}H NMR (600 MHz, $CDCl_3$) δ 8.71 (d, *J* = 2.2 Hz, 1H, H_{16}), 8.68 (d, *J* = 2.1 Hz, 1H, H_5), 8.59 (br s, 1H, H_{10}), 8.53 (d, *J* = 2.2 Hz, 1H, H_{11}), 8.45 (d, *J* = 8.1 Hz, 1H, H_7), 8.44 (d, *J* = 8.2 Hz, 1H, H_{14}), 8.40 (d, *J* = 8.1 Hz, 1H, H_8), 8.35 (d, *J* = 8.1 Hz, 1H, H_{13}), 7.90 (dd, *J* = 8.2, 2.3 Hz, 1H, H_{15}), 7.82 (dd, *J* = 8.1, 2.2 Hz, 1H, H_6), 7.69 (dd, *J* = 8.1, 2.2 Hz, 1H, H_9), 7.64 (dd, *J* = 8.1, 2.3 Hz, 1H, H_{12}), 7.40 – 7.20 (m, 4H, H_1 - H_4), 5.69 (ddt, *J* = 16.9, 10.2, 6.6 Hz, 1H, H_b), 5.32 (s, 2H, H_g), 4.94 – 4.86 (m, 2H, H_a), 3.09 (s, 4H, H_e, H_f), 3.01 (s, 3H, H_h), 2.73 – 2.68 (m, 2H, H_d), 2.27 – 2.20 (m, 2H, H_c). ^{13}C NMR (151 MHz, $CDCl_3$) δ 156.70 (C_{14}-C-N), 153.49 (C_{13}-C-N), 153.24 (br, C_7-C-N, C_8-C-N), 149.43 (C_{16}), 149.32 (C_{11}), 149.19 (C_5), 148.86 (br, C_{10}), 139.71 (C_4-C-C-C_1), 138.32 (C_6), 138.21 (br, C_9), 138.02 (C_5-C-C_6, C_4-C-C-C_1), 137.68 (C_{15}), 137.66 (C_b), 137.62 (C_{12}), 136.80 (C_9-C-C_{10}, C_{11}-C-C_{12}), 130.28 (C_4), 129.74 (C_1), 129.28 (C_{15}-C-C_{16}), 128.58 (C_2), 126.35 (C_3), 121.47 (C_8), 121.41 (C_{13}), 121.14 (C_{14}), 120.84 (C_7), 115.30 (C_a), 68.42 (C_g), 38.59 (C_h), 35.30 (C_c), 34.33, 34.31 (C_e, C_f), 32.56 (C_d). HRESI-MS: m/z = 599.2081 $[M+Na]^+$ (calcd. for $C_{34}H_{32}N_4NaO_3S$ 599.2087).

3.2 Synthesis and chiral resolution of iridium starting materials

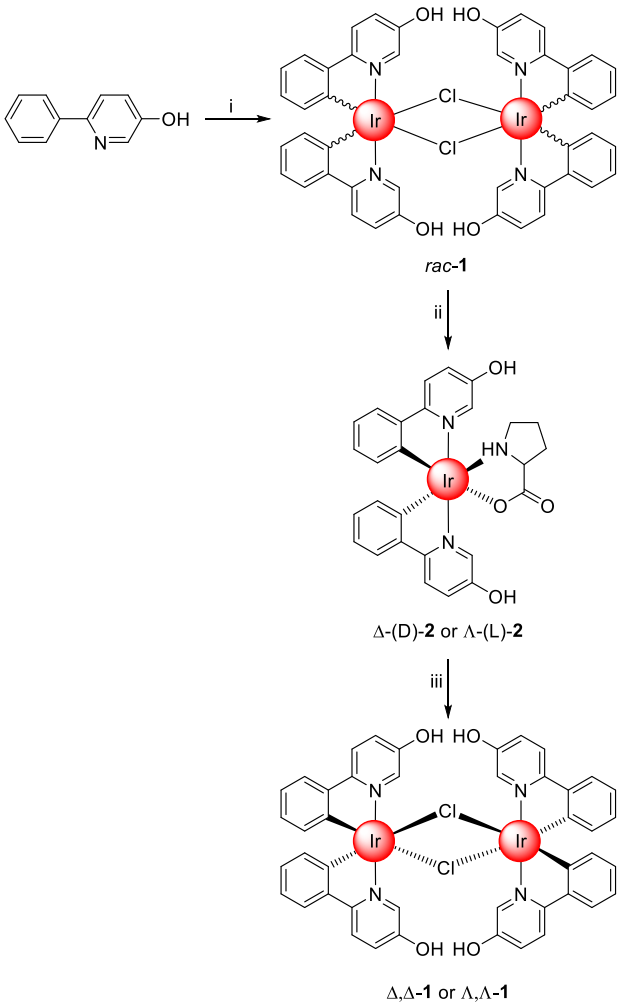

Scheme S2. General route for the synthesis and chiral resolution of complex **1**. Reaction conditions: i) $IrCl_3$, 2-methoxyethanol/water, N_2, reflux, 24 h; ii) (D)- or (L)-proline, NaOMe, MeOH, rt, 2 h; iii) HCl conc., MeOH, rt, 1 h.

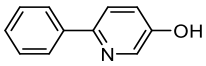

6-Phenylpyridin-3-ol was prepared according to literature procedures.[S1] The characterization data obtained was in accordance with that previously reported.

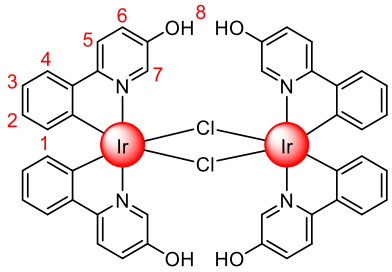

rac-**1**

Iridium(III) chloride anhydrous (2.42 g, 8.1 mmol) and 6-phenylpyridin-3-ol (2.77 g, 16.2 mmol, 2 equiv.) were placed in a flask fitted with a condenser and dissolved in 2-methoxyethanol (37.5 mL) and distilled water (12.5 mL). The reaction was set under a N_2 atmosphere, and the solution was degassed by N_2 bubbling for 30 minutes. Then the mixture was stirred at reflux for 24 h. The reaction was then cooled and poured onto 150 mL of distilled water. The yellow solid was filtered over Celite®, washed with excess water, taken into acetone and the solvent removed to afford 3.90 g of *rac*-**1** (85% Yield). ^{1}H NMR (600 MHz, Acetone-d_6) δ 8.91 (d, J = 2.5 Hz, 4H, H_7), 8.84 (s, 4H, H_8), 7.95 (d, J = 8.9 Hz, 4H, H_5), 7.50 (dd, J = 8.8, 2.7 Hz, 4H, H_6), 7.45 (dd, J = 7.8, 1.3 Hz, 4H, H_4), 6.69 – 6.62 (m, 4H, H_3), 6.48 – 6.41 (m, 4H, H_2), 5.89 (dd, J = 7.8, 1.2 Hz, 4H, H_1). ^{13}C NMR (151 MHz, Acetone-d_6) δ 160.70 (C_5-C-N), 153.03 (C_6-C-C_7), 145.87 (C_4-C-C-C_1), 143.87 (C_1-C-Ir), 140.20 (C_7), 131.13 (C_1), 127.81 (C_2), 125.23 (C_6), 122.95 (C_4), 121.56 (C_3), 120.09 (C_5). Compound *rac*-**3** was observed as a mixture of the mononuclear complexes $[Ir(ppyOH)_2]^+$, $[Ir(ppyOH)_2(CH_3CN)]^+$ and $[Ir(ppyOH)_2(CH_3CN)_2]^+$ in ESI-MS. HRESI-MS: m/z = 533.0819 $[Ir(ppyOH)_2]^+$ (calcd. for $C_{22}H_{16}IrN_2O_2$ 533.0836).

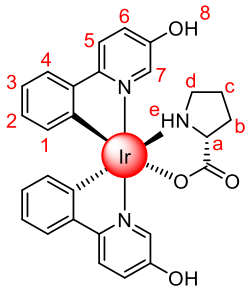

Δ-(*D*)-**2**

Compound *rac*-**1** (1.76 g, 1.56 mmol), D-proline (0.45 g, 3.90 mmol, 2.5 equiv.) and sodium methoxide (0.21 g, 3.90 mmol, 2.5 equiv.) were placed in a flask and dissolved in methanol (200 mL). The mixture was stirred at room temperature for 2 h. Then the mixture was dry-loaded onto silica from the methanol solution and purified by flash column chromatography with dichloromethane/methanol 95:5 as eluent, to afford 0.19 g of Δ-(D)-**2** (9% Yield). ^{1}H NMR (600 MHz, CD_3OD) δ 8.48 (d, *J* = 2.6 Hz, 1H, H_7), 8.33 (d, *J* = 2.7 Hz, 1H, $H_{7'}$), 7.90 (d, *J* = 8.9 Hz, 1H, $H_{5'}$), 7.86 (d, *J* = 8.9 Hz, 1H, H_5), 7.49 (d, *J* = 7.2 Hz, 1H, $H_{4'}$), 7.45 (d, *J* = 7.7 Hz, 1H, H_4), 7.42 (dd, *J* = 8.9, 2.6 Hz, 2H, H_6, $H_{6'}$), 6.78 – 6.72 (m, 2H, H_3, $H_{3'}$), 6.62 – 6.56 (m, 2H, H_2, $H_{2'}$), 6.36 (d, *J* = 7.6 Hz, 1H, $H_{1'}$), 6.01 (d, *J* = 7.6 Hz, 1H, H_1), 4.11 (dd, *J* = 9.2, 7.3 Hz, 1H, H_a), 2.44 – 2.37 (m, 1H, H_d), 2.35 – 2.27 (m, 1H, H_b), 1.90 – 1.77 (m, 2H, $H_{b'}$, $H_{d'}$), 1.57 – 1.50 (m, 2H, H_c). ^{13}C NMR (151 MHz, CD_3OD) δ 187.93 (C_a-COO), 162.61 (C_5-C-N), 161.46 ($C_{5'}$-C-N), 154.89 ($C_{6'}$-C-$C_{7'}$), 154.65 (C_6-C-C_7), 149.14 (C_1-C-Ir), 146.37 (C_4-C-C-C_1), 145.80 ($C_{4'}$-C-C-$C_{1'}$), 143.46 ($C_{1'}$-C-Ir), 138.81 (C_7), 136.56 ($C_{7'}$), 133.66 ($C_{1'}$), 133.24 (C_1), 128.77, 128.70 (C_2, $C_{2'}$), 126.06, 125.57 (C_6, $C_{6'}$), 123.70 ($C_{4'}$), 123.54 (C_4), 122.03, 121.53 (C_3, $C_{3'}$), 121.01 ($C_{5'}$), 120.56 (C_5), 63.19 (C_a), 49.56 (C_d), 32.56 (C_b), 27.68 (C_c). HRESI-MS: m/z = 686.1015 $[M+K]^+$ (calcd. for $C_{27}H_{24}IrN_3KO_4$ 686.1028).

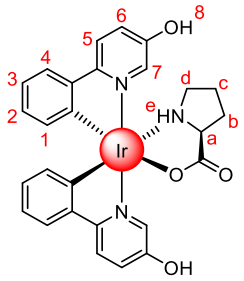

Λ-(*L*)-**2**

Compound *rac*-**1** (1.03 g, 0.91 mmol), (*L*)-proline (0.26 g, 2.3 mmol, 2.5 equiv.) and sodium methoxide (0.12 g, 2.3 mmol, 2.5 equiv.) were placed in a flask and dissolved in methanol (150 mL). The mixture was stirred at room temperature for 2 h. Then the mixture was dry-loaded onto silica from the methanol solution and purified by flash column chromatography with dichloromethane/methanol 95:5 as eluent, to afford 0.17 g of Λ-(L)-**2** (15% Yield). ^{1}H NMR (600 MHz, CD_3OD) δ 8.48 (d, *J* = 2.6 Hz, 1H, H_7), 8.33 (d, *J* = 2.7 Hz, 1H, $H_{7'}$), 7.90 (d, *J* = 8.9 Hz, 1H, $H_{5'}$), 7.86 (d, *J* = 8.9 Hz, 1H, $_{H5}$), 7.49 (dd, *J* = 7.9, 1.3 Hz, 1H, $H_{4'}$), 7.45 (dd, *J* = 7.8, 1.3 Hz, 1H, H_4), 7.42 (dd, *J* = 8.9, 2.6 Hz, 2H, H_6, $H_{6'}$), 6.78 – 6.72 (m, 2H, H_3, $H_{3'}$), 6.62 – 6.56 (m, 2H, H_2, $H_{2'}$), 6.36 (dd, *J* = 7.7, 1.2 Hz, 1H, $H_{1'}$), 6.01 (dd, *J* = 7.7, 1.2 Hz, 1H, H_1), 4.11 (dd, *J* = 9.1, 7.3 Hz, 1H, H_a), 2.44 – 2.38 (m, 1H, H_d), 2.35 – 2.26 (m, 1H, H_b), 1.92 – 1.76 (m, 2H, $H_{b'}$, $H_{d'}$), 1.60 – 1.48 (m, 2H, H_c). ^{13}C NMR (151 MHz, CD_3OD) δ 187.91 (C_a-COO), 162.65 (C_5-C-N), 161.48 ($C_{5'}$-C-N), 154.89 ($C_{6'}$-C-$C_{7'}$), 154.63 (C_6-C-C_7), 149.13 (C_1-C-Ir), 146.37 (C_4-C-C-C_1), 145.81 ($C_{4'}$-C-C-$C_{1'}$), 143.48 ($C_{1'}$-C-Ir), 138.82 (C_7), 136.59 ($C_{7'}$), 133.66 ($C_{1'}$), 133.24 (C_1), 128.78, 128.71 (C_2, $C_{2'}$), 126.07, 125.58 (C_6, $C_{6'}$), 123.70($C_{4'}$), 123.55 (C_4), 122.03, 121.53 (C_3, $C_{3'}$), 121.00 ($C_{5'}$), 120.55 (C_5), 63.21 (C_a), 49.56 (C_d), 32.56 (C_b), 27.67 (C_c). Compound Λ-(L)-**2** presented significant loss of the L-proline ligand in ESI-MS, where a mixture of the mononuclear complexes $[Ir(ppyOH)_2]^+$ and $[Ir(ppyOH)_2(CH_3CN)]^+$ was observed together with the expected molecular ion. HRESI-MS: m/z = 670.1284 $[M+Na]^+$ (calcd. for $C_{27}H_{24}IrN_3NaO_4$ 670.1288).

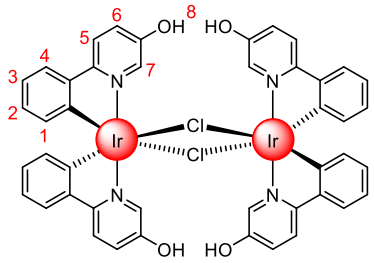

Δ,Δ-**1**

Compound Δ-(D)-**2** (0.19 g, 0.29 mmol) was placed in a flask and dissolved in methanol (20 mL), then concentrated hydrochloric acid (2 mL) was added and the mixture was stirred at room temperature for 1 h. Distilled water was added until precipitation and the yellow solid was filtered on Celite®, washed with excess water, taken into acetone and the solvent removed to afford 0.15 g of Δ,Δ-**1** (92% Yield). ^{1}H NMR (600 MHz, Acetone-d_6) δ 8.91 (d, J = 2.7 Hz, 4H, H_7), 8.84 (br s, 4H, H_8), 7.95 (d, J = 8.8 Hz, 4H, H_5), 7.50 (dd, J = 8.8, 2.7 Hz, 4H, H_6), 7.45 (dd, J = 7.8, 1.4 Hz, 4H, H_4), 6.69 – 6.62 (m, 4H, H_3), 6.48 – 6.41 (m, 4H, H_2), 5.89 (dd, J = 7.8, 1.2 Hz, 4H, H_1). ^{13}C NMR (151 MHz, Acetone-d_6) δ 160.71 (C_5-C-N), 153.03 (C_6-C-C_7), 145.86 (C_4-C-C-C_1), 143.86 (C_1-C-Ir), 140.19 (C_7), 131.13 (C_1), 127.81 (C_2), 125.23 (C_6), 122.95 (C_4), 121.56 (C_3), 120.09 (C_5). Compound Δ,Δ-**1** was observed as a mixture of the mononuclear complexes $[Ir(ppyOH)_2]^+$, $[Ir(ppyOH)_2(CH_3CN)]^+$ and $[Ir(ppyOH)_2(CH_3CN)_2]^+$ in ESI-MS. HRESI-MS: m/z = 533.0830 $[Ir(ppyOH)_2]^+$ (calcd. for $C_{22}H_{16}IrN_2O_2$ 533.0836).

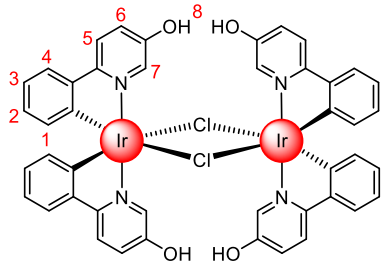

Λ,Λ-**1**

Compound Λ-(L)-**2** (0.17 g, 0.27 mmol) was placed in a flask and dissolved in methanol (20 mL), then concentrated hydrochloric acid (2 mL) was added and the mixture was stirred at room temperature for 1 h. Distilled water was added until precipitation and the yellow solid was filtered on Celite®, washed with excess water, taken into acetone and the solvent removed to afford 0.11 g of Λ,Λ-**1** (72% Yield). ^{1}H NMR (600 MHz, Acetone-d_6) δ 8.91 (d, J = 2.7 Hz, 4H, H_7), 8.85 (br s, 4H, H_8), 7.95 (d, J = 8.9 Hz, 4H, H_5), 7.50 (dd, J = 8.8, 2.7 Hz, 4H, H_6), 7.45 (dd, J = 7.8, 1.4 Hz, 4H, H_4), 6.69 – 6.62 (m, 4H, H_3), 6.47 – 6.41 (m, 4H, H_2), 5.89 (dd, J = 7.8, 1.2 Hz, 4H, H_1). ^{13}C NMR (151 MHz, Acetone-d_6) δ 160.71 (C_5-C-N), 153.00 (C_6-C-C_7), 145.87 (C_4-C-C-C_1), 143.87 (C_1-C-Ir), 140.18 (C_7), 131.13 (C_1), 127.81 (C_2), 125.21 (C_6), 122.95 (C_4), 121.55 (C_3), 120.09 (C_5). Compound Λ,Λ-**1** was observed as a mixture of the mononuclear complexes $[Ir(ppyOH)_2]^+$, $[Ir(ppyOH)_2(CH_3CN)]^+$ and $[Ir(ppyOH)_2(CH_3CN)_2]^+$ in ESI-MS. HRESI-MS: m/z = 533.0819 $[Ir(ppyOH)_2]^+$ (calcd. for $C_{22}H_{16}IrN_2O_2$ 533.0836).

3.3 Synthesis of iridium-containing building blocks

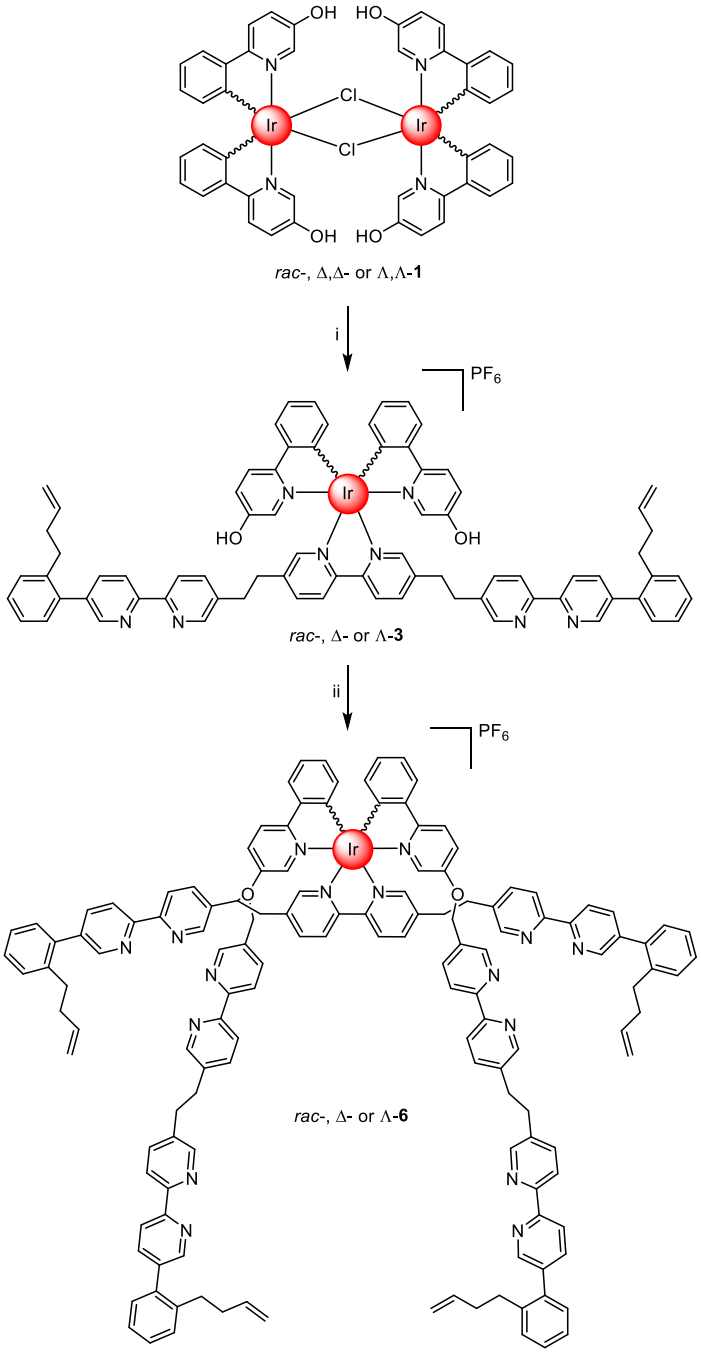

Scheme S3. General synthetic route for iridium containing building blocks. Reaction conditions: i) **4**, DCM/MeOH, rt, 24 h; then KPF_6; ii) **5**, K_2CO_3, DMF, N_2, 60 °C, 21 h.

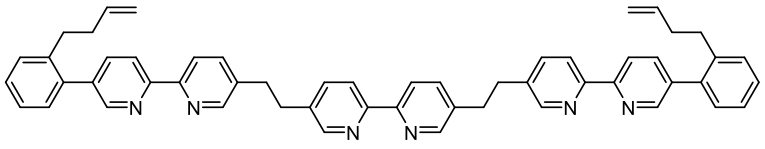

4

Compound **4** was prepared according to literature procedures.[S2] The obtained characterization data was in accordance with that previously reported.

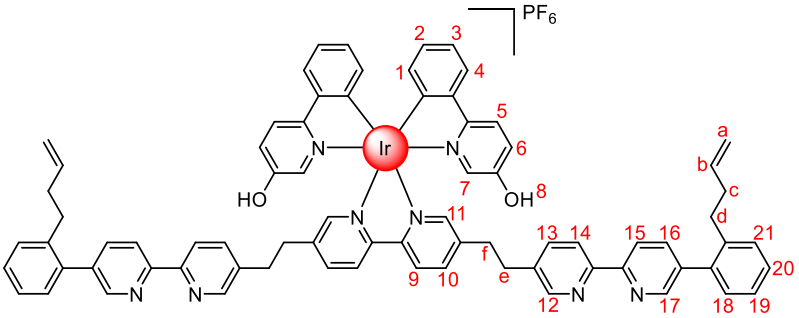

rac-**3**

Compound **4** (500 mg, 0.64 mmol) was placed in a flask and dissolved in dichloromethane (60 mL). Then compound *rac*-**1** (542 mg, 0.48 mmol, 1.5 equiv. with respect to iridium) was slowly added while stirring as a solution in methanol (60 mL) over 24 h at room temperature. After the addition was completed, potassium hexafluorophosphate (1.18 g, 6.4 mmol, 10 equiv.) was added as a solid, and the mixture stirred for 10 minutes. The solvent was removed and the residue was redissolved in dichloromethane, filtered, and purified by size-exclusion column chromatography with dichloromethane as eluent to afford 395 mg of a mixture with around a 10:1 ratio of compound *rac*-**3** with another regioisomer (42% Yield). See Section 4 for a detailed explanation on regioisomer formation. ^{1}H NMR (600 MHz, $CDCl_3$) δ 8.61 (d, *J* = 2.0 Hz, 2H, H_{17}), 8.39 (d, *J* = 5.2 Hz, 2H, H_9 or H_{14}), 8.38 (d, *J* = 5.1 Hz, 2H, H_9 or H_{14}), 8.13 (d, *J* = 7.9 Hz, 2H, H_{15}), 7.86 – 7.80 (m, 4H, H_{11} or H_{12}, H_{10} or H_{13}), 7.75 (dd, *J* = 8.1, 2.3 Hz, 2H, H_{16}), 7.71 (dd, *J* = 8.3, 2.1 Hz, 2H, H_{10} or H_{13}), 7.59 (d, *J* = 9.0 Hz, 2H, H_5), 7.44 – 7.41 (m, 2H, H_4), 7.39 – 7.32 (m, 4H, H_{20}, H_{21}), 7.31 – 7.27 (m, 2H, H_{19}), 7.23 – 7.18 (m, 4H, H_6, H_{18}), 7.13 (s, 2H, H_{11} or H_{12}), 6.98 – 6.94 (m, 4H, H_2, H_3), 6.77 (d, *J* = 2.5 Hz, 2H, H_7), 5.94 – 5.91 (m, 2H, H_1), 5.65 (ddt, *J* = 16.9, 10.3, 6.6 Hz, 2H, H_b), 4.90 – 4.81 (m, 4H, H_a), 3.12 – 2.69 (m, 8H, H_e, H_f), 2.69 – 2.59 (m, 4H, H_d), 2.26 – 2.19 (m, 4H, H_c). ^{13}C NMR (151 MHz, $CDCl_3$) δ 160.04 (C_5-C-N), 154.86 (C_9-C-N or C_{14}-C-N), 153.99 (C_9-C-N or C_{14}-C-N), 153.15 (C_6-C-C_7), 152.53 (C_{15}-C-N), 149.92 (C_{11} or C_{12}), 149.78 (C_{17}), 148.20 (C_q), 147.98 (C_{11} or C_{12}), 143.59 (C_q), 140.37 (C_{10} or C_{13}), 140.26 (C_{10}-C-C_{11} or C_{12}-C-C_{13}), 139.58 (C_{21}-C-C_d), 138.71 (C_{10} or C_{13}), 137.98 (C_{16}-C-C_{17}), 137.59, 137.56 (C_7, C_{16}, C_b, C_q), 135.86 (C_{10}-C-C_{11} or C_{12}-C-C_{13}), 131.27 (C_1), 130.27 (C_{18}), 129.96 (C_2 or C_3), 129.72 (C_{21}), 128.59 (C_{20}), 127.95 (C_6), 126.38 (C_{19}), 124.93 (C_9 or C_{14}), 124.15 (C_9 or C_{14}), 123.49 (C_4), 122.47 (C_2 or C_3), 121.11 (C_{15}), 120.24 (C_5), 115.40 (C_a), 35.32 (C_c), 34.60, 33.43 (C_e, C_f), 32.54 (C_d). Despite extensive use of additional 2D and NOE NMR techniques, it was not possible to distinguish between the H_9/H_{10}/H_{11} and H_{12}/H_{13}/H_{14} pyridine ring systems. HRESI-MS: m/z = 1313.4795 $[M\text{-}PF_6]^+$ (calcd. for $C_{76}H_{64}IrN_8O_2$ 1313.4776).

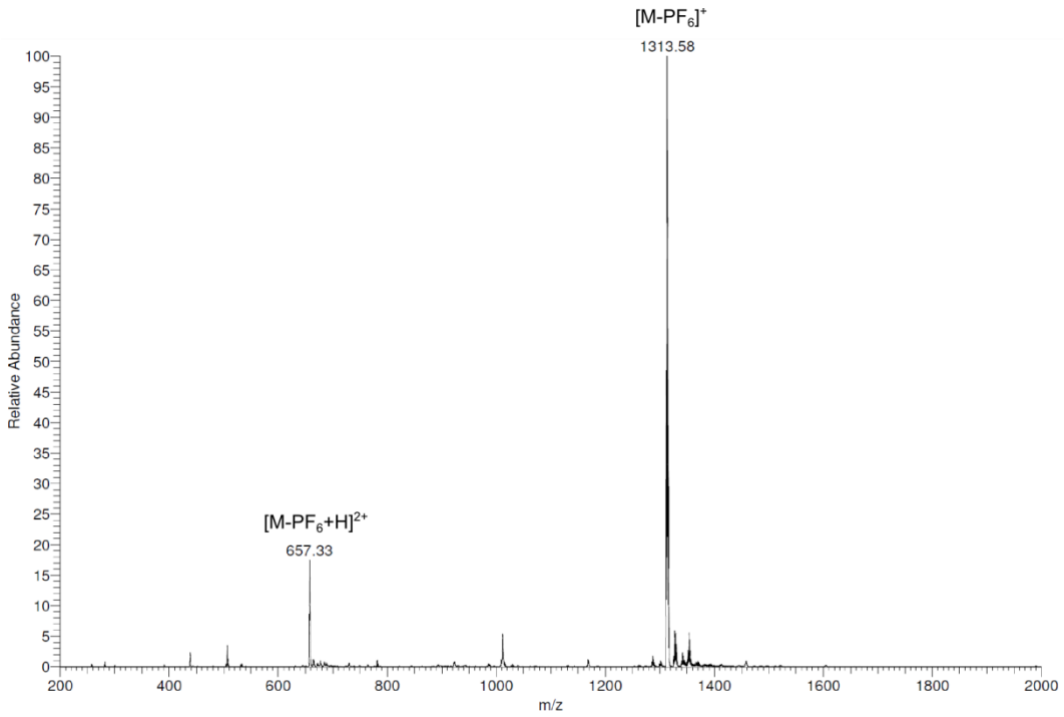

Figure S1. Low-resolution ESI-MS of *rac*-**3**. Calculated peaks (m/z): 1313.48 $[M\text{-}PF_6]^+$; 657.24 $[M\text{-}PF_6\text{+}H]^{2+}$.

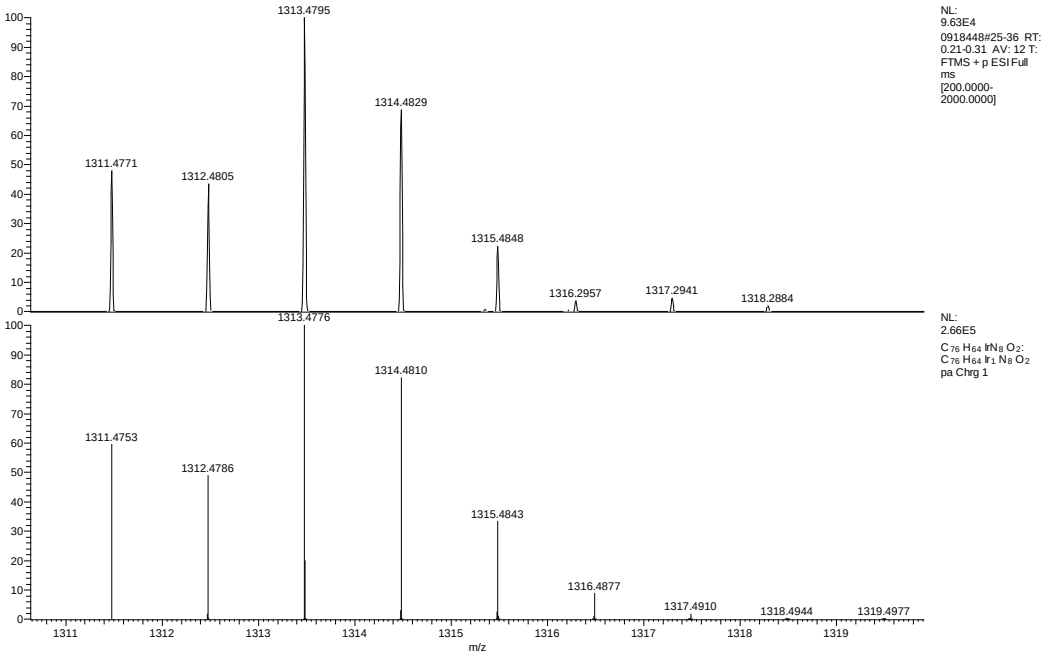

Figure S2. High-resolution ESI-MS of the $[M\text{-}PF_6]^+$ peak of *rac*-**3**. Experimental spectrum (top, observed m/z 1313.4795) and calculated spectrum (bottom, theoretical m/z 1313.4776).

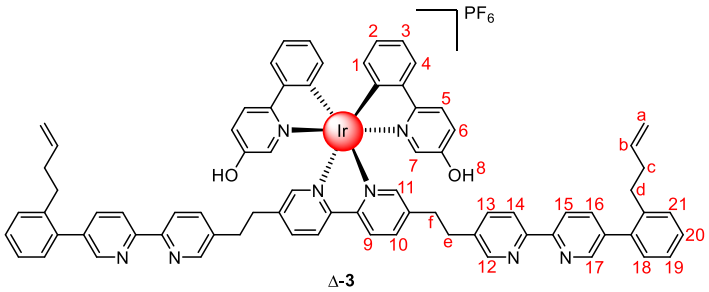

Δ-**3**

Compound **4** (82 mg, 0.10 mmol) was placed in a flask and dissolved in dichloromethane (12 mL). Then compound Δ,Δ-**1** (89 mg, 0.08 mmol, 1.5 equiv. with respect to iridium) was slowly added while stirring as a solution in methanol (12 mL) over 24 h at room temperature. After the addition was completed, potassium hexafluorophosphate (0.19 g, 1.0 mmol, 10 equiv.) was added as a solid, and the mixture stirred for 10 minutes. The solvent was removed and the residue was redissolved in dichloromethane, filtered, and purified by size-exclusion column chromatography with dichloromethane as eluent to afford 54 mg of a mixture around 10:1 ratio of compound Δ-**3** with another regioisomer (35% Yield). See Section 4 for a detailed explanation on regioisomer formation. ^{1}H NMR (600 MHz, $CDCl_3$) δ 8.61 (d, *J* = 1.4 Hz, 2H, H_{17}), 8.38 (d, *J* = 8.3 Hz, 2H, H_9 or H_{14}), 8.37 (d, *J* = 8.3 Hz, 2H, H_9 or H_{14}), 8.14 (dd, *J* = 8.1, 0.8 Hz, 2H, H_{15}), 7.85 (d, *J* = 1.7 Hz, 2H, H_{11} or H_{12}), 7.82 (dd, *J* = 8.4, 2.0 Hz, 2H, H_{10} or H_{13}), 7.75 (dd, *J* = 8.1, 2.2 Hz, 2H, H_{16}), 7.71 (dd, *J* = 8.2, 2.2 Hz, 2H, H_{10} or H_{13}), 7.59 (d, *J* = 9.0 Hz, 2H, H_5), 7.43 – 7.40 (m, 2H, H_4), 7.38 – 7.32 (m, 4H, H_{20}, H_{21}), 7.29 (td, *J* = 7.3, 1.7 Hz, 2H, H_{19}), 7.23 – 7.18 (m, 4H, H_6, H_{18}), 7.14 (d, *J* = 2.0 Hz, 2H, H_{11} or H_{12}), 6.97 – 6.95 (m, 4H, H_2, H_3), 6.80 (d, *J* = 2.6 Hz, 2H, H_7), 5.95 – 5.92 (m, 2H, H_1), 5.65 (ddt, *J* = 16.9, 10.2, 6.6 Hz, 2H, H_b), 4.91 – 4.80 (m, 4H, H_a), 3.11 – 2.69 (m, 8H, H_e, H_f), 2.69 – 2.62 (m, 4H, H_d), 2.25 – 2.19 (m, 4H, H_c). ^{13}C NMR (151 MHz, $CDCl_3$) δ 159.99 (C_5-C-N), 154.85 (C_9-C-N or C_{14}-C-N), 153.97 (C_9-C-N or C_{14}-C-N), 153.19 (C_6-C-C_7), 152.63 (C_{15}-C-N), 149.94 (C_{11} or C_{12}), 149.78 (C_{17}), 148.20 (C_q), 148.03 (C_{11} or C_{12}), 143.61 (C_q), 140.31 (C_{10} or C_{13}, C_{10}-C-C_{11} or C_{12}-C-C_{13}), 139.58 (C_{21}-C-C_d), 138.63 (C_{10} or C_{13}), 137.94 (C_{16}-C-C_{17}), 137.60, 137.56, 137.54 (C_7, C_{16}, C_b, C_q), 135.86 (C_{10}-C-C_{11} or C_{12}-C-C_{13}), 131.28 (C_1), 130.27 (C_{18}), 129.92 (C_2 or C_3), 129.72 (C_{21}), 128.58 (C_{20}), 127.87 (C_6), 126.37 (C_{19}), 124.87 (C_9 or C_{14}), 124.03 (C_9 or C_{14}), 123.47 (C_4), 122.46 (C_2 or C_3), 121.07 (C_{15}), 120.22 (C_5), 115.39 (C_a), 35.32 (C_c), 34.58, 33.40 (C_e, C_f), 32.54 (C_d). Despite extensive use of additional 2D and NOE NMR techniques, it was not possible to distinguish between the H_9/H_{10}/H_{11} and H_{12}/H_{13}/H_{14} pyridine ring systems. HRESI-MS: m/z = 1313.4762 $[M\text{-}PF_6]^+$ (calcd. for $C_{76}H_{64}IrN_8O_2$ 1313.4776).

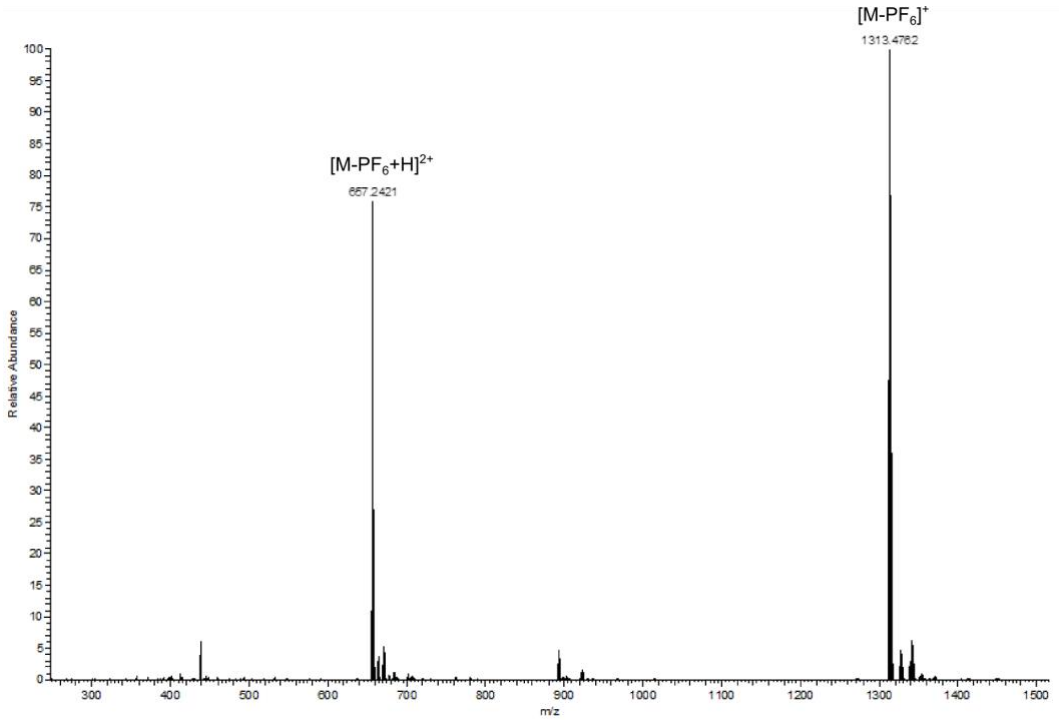

Figure S3. High-resolution ESI-MS of Δ-**3**. Calculated peaks (m/z): 1313.4776 $[M\text{-}PF_6]^+$; 657.2424 $[M\text{-}PF_6{+}H]^{2+}$.

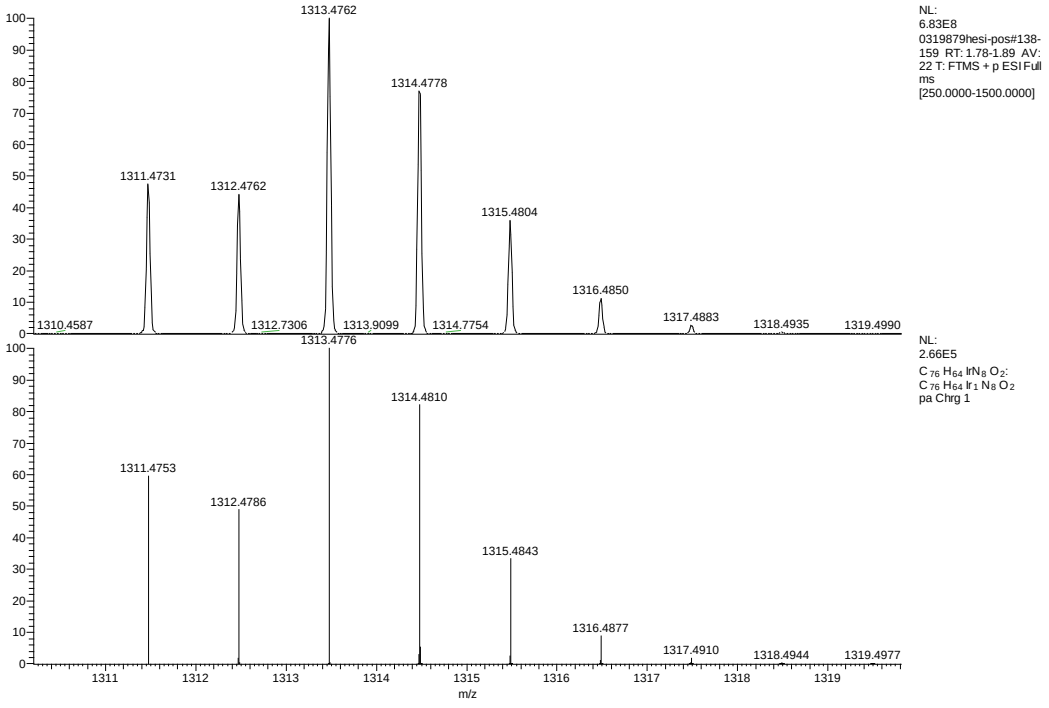

Figure S4. High-resolution ESI-MS of the $[M\text{-}PF_6]^+$ peak of Δ-**3**. Experimental spectrum (top, observed m/z 1313.4762) and calculated spectrum (bottom, theoretical m/z 1313.4776).

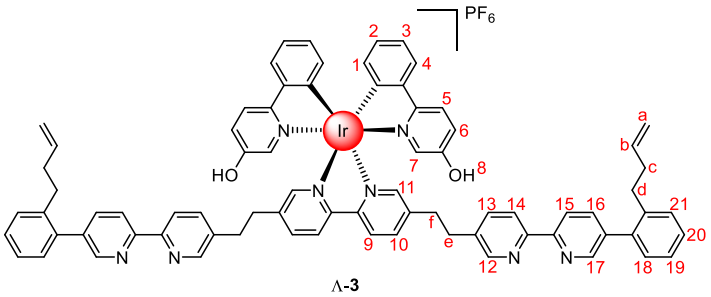

Λ-**3**

Compound **4** (66 mg, 0.08 mmol) was placed in a flask and dissolved in dichloromethane (10 mL). Then compound Λ,Λ-**1** (71 mg, 0.06 mmol, 1.5 equiv. with respect to iridium) was slowly added while stirring as a solution in methanol (10 mL) over 24 h at room temperature. After the addition was completed, potassium hexafluorophosphate (0.15 g, 0.8 mmol, 10 equiv.) was added as a solid, and the mixture stirred for 10 minutes. The solvent was removed and the residue was redissolved in dichloromethane, filtered, and purified by size-exclusion column chromatography with dichloromethane as eluent to afford 57 mg of a mixture around 10:1 ratio of compound Λ-**3** with another regioisomer (46% Yield). See Section 4 for a detailed explanation on regioisomer formation. ^{1}H NMR (600 MHz, $CDCl_3$) δ 8.61 (dd, *J* = 2.2, 0.8 Hz, 2H, H_{17}), 8.38 (d, *J* = 8.3 Hz, 2H, H_9 or H_{14}), 8.37 (d, *J* = 8.3 Hz, 2H, H_9 or H_{14}), 8.13 (dd, *J* = 8.1, 0.8 Hz, 2H, H_{15}), 7.84 (d, *J* = 1.8 Hz, 2H, H_{11} or H_{12}), 7.84 – 7.79 (m, 2H, H_{10} or H_{13}), 7.75 (dd, *J* = 8.1, 2.3 Hz, 2H, H_{16}), 7.71 (dd, *J* = 8.2, 2.2 Hz, 2H, H_{10} or H_{13}), 7.59 (d, *J* = 9.0 Hz, 2H, H_5), 7.44 – 7.41 (m, 2H, H_4), 7.39 – 7.32 (m, 4H, H_{20}, H_{21}), 7.31 – 7.27 (m, 2H, H_{19}), 7.23 – 7.18 (m, 4H, H_6, H_{18}), 7.12 (d, *J* = 2.1 Hz, 2H, H_{11} or H_{12}), 6.98 – 6.95 (m, 4H, H_2, H_3), 6.78 (d, *J* = 2.5 Hz, 2H, H_7), 5.95 – 5.91 (m, 2H, H_1), 5.65 (ddt, *J* = 16.9, 10.2, 6.6 Hz, 2H, H_b), 4.91 – 4.79 (m, 4H, H_a), 3.10 – 2.69 (m, 8H, H_e, H_f), 2.69 – 2.61 (m, 4H, H_d), 2.25 – 2.19 (m, 4H, H_c). ^{13}C NMR (151 MHz, $CDCl_3$) δ 160.03 (C_5-C-N), 154.84 (C_9-C-N or C_{14}-C-N), 153.97 (C_9-C-N or C_{14}-C-N), 153.16 (C_6-C-C_7), 152.58 (C_{15}-C-N), 149.93 (C_{11} or C_{12}), 149.77 (C_1[7]), 148.20 (C_q), 148.00 (C_{11} or C_{12}), 143.60 (C_q), 140.34 (C_{10} or C_{13}), 140.30 (C_{10}-C-C_{11} or C_{12}-C-C_{13}), 139.58 (C_{21}-C-C_d), 138.69 (C_{10} or C_{13}), 137.96 (C_{16}-C-C_{17}), 137.59, 137.56 (C_7, C_{16}, C_b, C_q), 135.88 (C_{10}-C-C_{11} or C_{12}-C-C_{13}), 131.27 (C_1), 130.27 (C_{18}), 129.94 (C_2 or C_3), 129.72 (C_{21}), 128.59 (C_{20}), 127.92 (C_6), 126.38 (C_{19}), 124.88 (C_9 or C_{14}), 124.09 (C_9 or C_{14}), 123.48 (C_4), 122.47 (C_2 or C_3), 121.09 (C_{15}), 120.23 (C_5), 115.40 (C_a), 35.32 (C_c), 34.58, 33.41 (C_e, C_f), 32.54 (C_d). Despite extensive use of additional 2D and NOE NMR techniques, it was not possible to distinguish between the H_9/H_{10}/H_{11} and H_{12}/H_{13}/H_{14} pyridine ring systems. HRESI-MS: m/z = 1313.4787 $[M\text{-}PF_6]^+$ (calcd. for $C_{76}H_{64}IrN_8O_2$ 1313.4776).

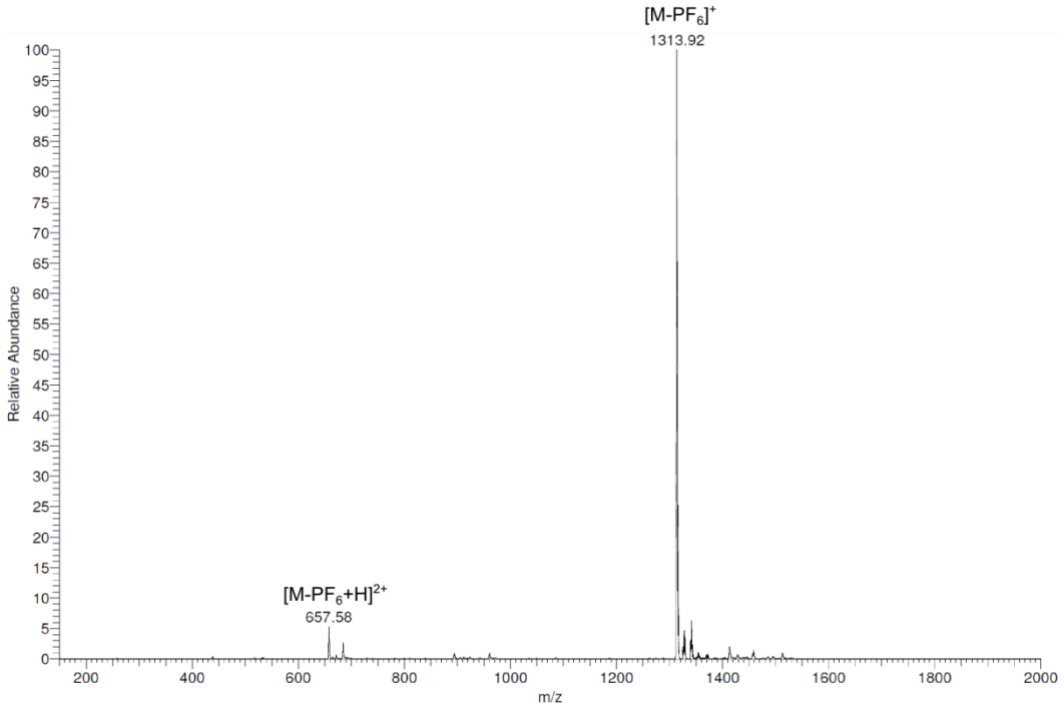

Figure S5. Low-resolution ESI-MS of Λ-**3**. Calculated peaks (m/z): 1313.48 $[M\text{-}PF_6]^+$; 657.24 $[M\text{-}PF_6\text{+}H]^{2+}$.

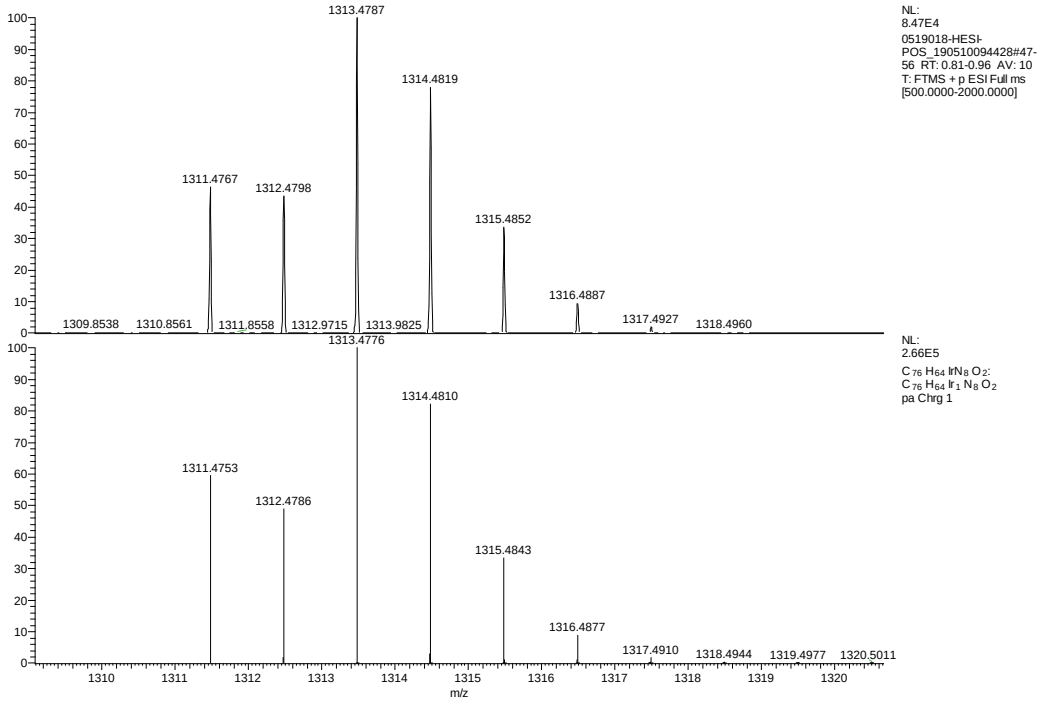

Figure S6. High-resolution ESI-MS of the $[M\text{-}PF_6]^+$ peak of Λ-**3**. Experimental spectrum (top, observed m/z 1313.4787) and calculated spectrum (bottom, theoretical m/z 1313.4776).

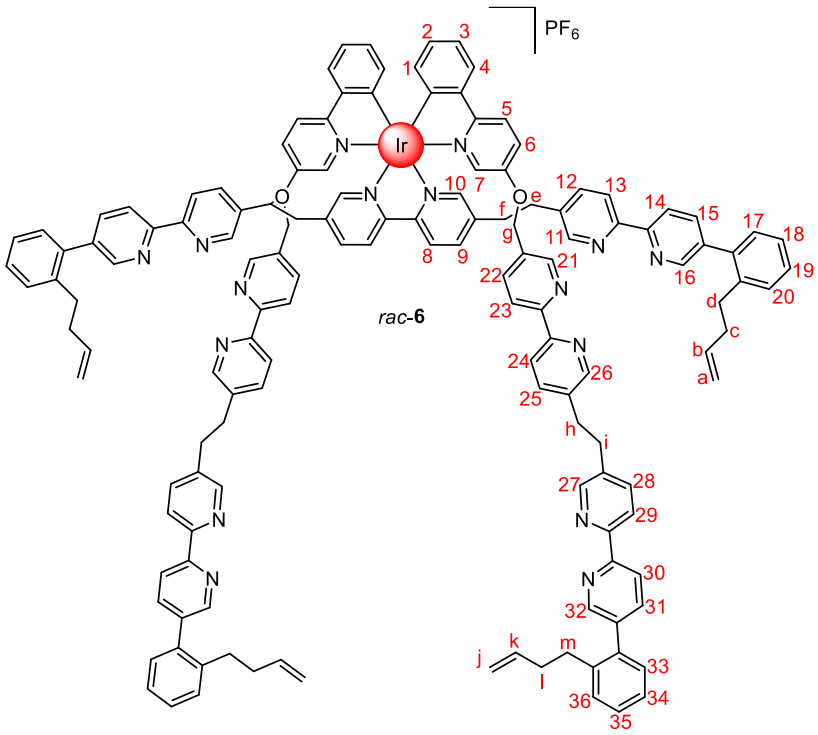

Compound *rac*-**3** (222 mg, 0.15 mmol), compound **5** (220 mg, 0.38 mmol, 2.5 equiv.) and potassium carbonate anhydrous (105 mg, 0.76 mmol, 5.0 equiv.) were placed in a sealed vial backfilled with N_2. The solids were dissolved in dry DMF (10 mL) and the mixture was heated at 60 °C for 21 h while stirring. The solvent was then removed, and the residue was redissolved in dichloromethane, filtered off, and purified by size-exclusion column chromatography with dichloromethane as eluent to afford 343 mg of a mixture of compound *rac*-**6** with other regioisomers which was taken forward without additional purification (93% Yield). HRESI-MS: m/z = 758.9847 $[M\text{-}PF_6+2H]^{3+}$ (calcd. for $C_{142}H_{122}IrN_{16}O_2$ 758.9861).

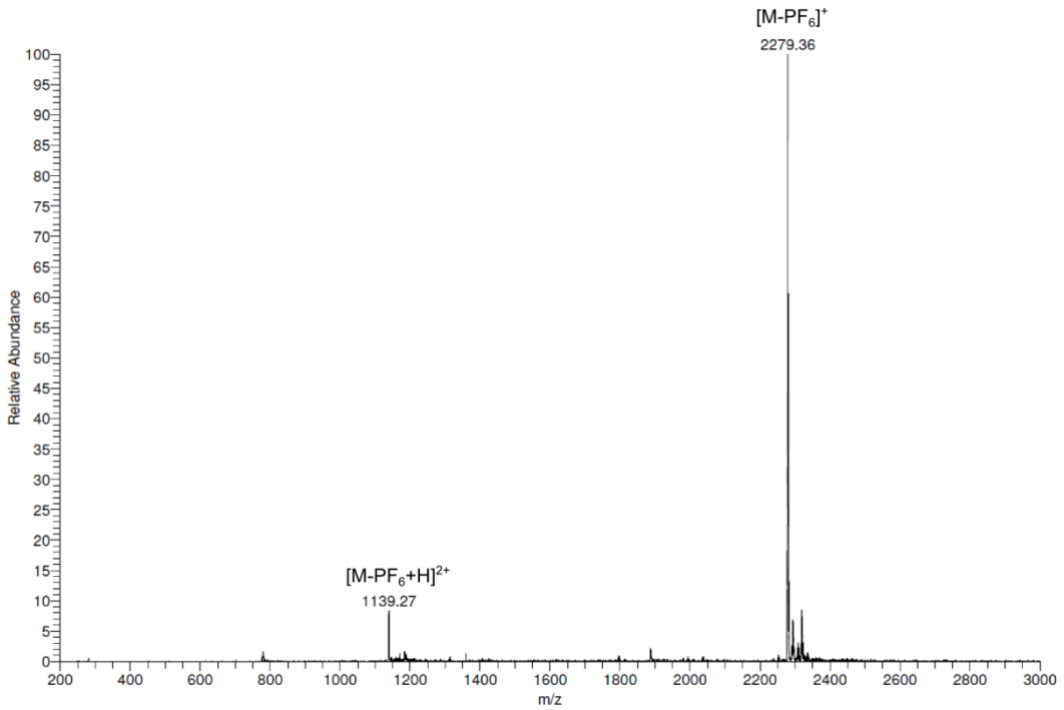

Figure S7. Low-resolution ESI-MS of *rac*-**6**. Calculated peaks (m/z): 2274.94 $[M\text{-}PF_6]^+$; 1137.98 $[M\text{-}PF_6\text{+}H]^{2+}$.

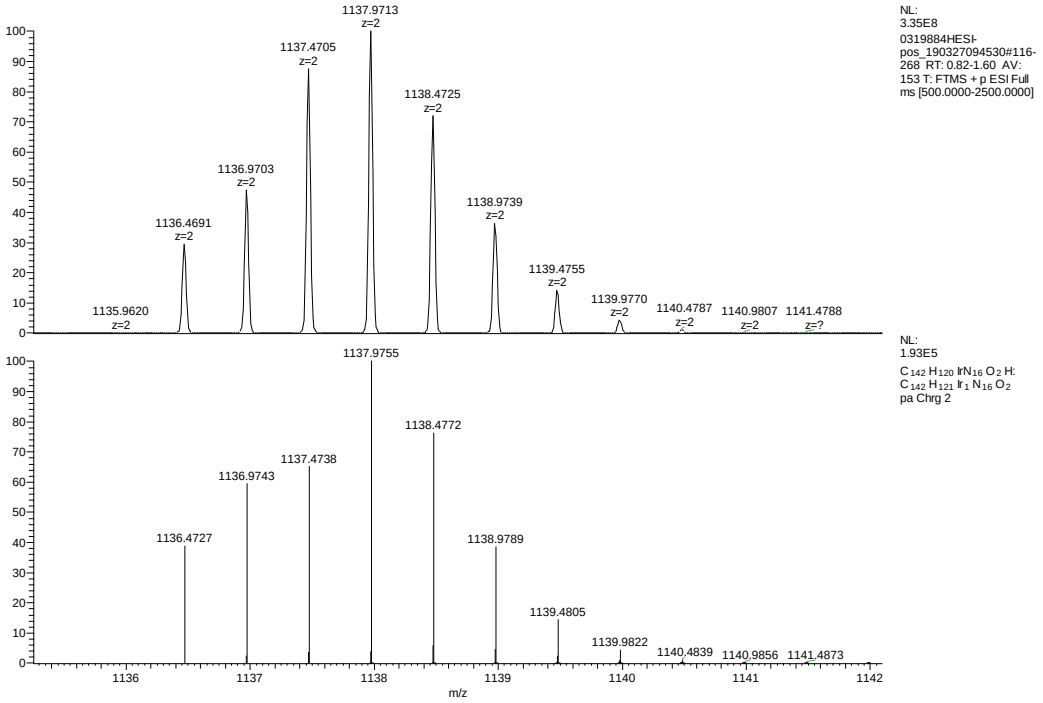

Figure S8. High-resolution ESI-MS of the $[M\text{-}PF_6\text{+}H]^{2+}$ peak of *rac*-**6**. Experimental spectrum (top, observed m/z 1137.9713) and calculated spectrum (bottom, theoretical m/z 1137.9755).

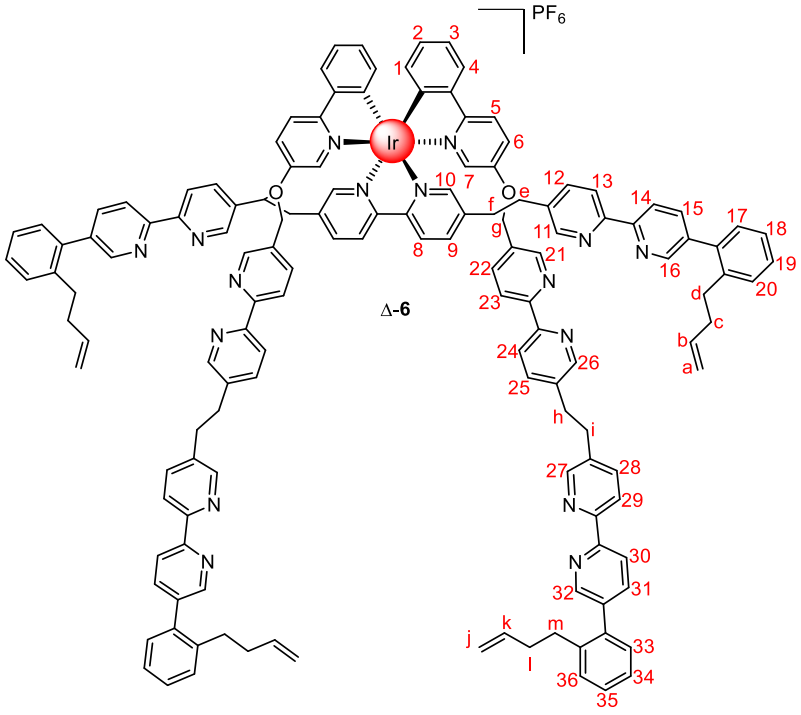

Compound Δ-**3** (54 mg, 0.04 mmol), compound **5** (53 mg, 0.09 mmol, 2.5 equiv.) and potassium carbonate anhydrous (26 mg, 0.18 mmol, 5.0 equiv.) were placed in a sealed vial backfilled with N_2. The solids were dissolved in dry DMF (2 mL) and the mixture was heated at 60 °C for 21 h while stirring. The solvent was then removed, and the residue was redissolved in dichloromethane, filtered off, and purified by size-exclusion column chromatography with dichloromethane as eluent to afford 57 mg of a mixture of compound Δ-**6** with other regioisomers which was taken forward without additional purification (64% Yield). HRESI-MS: m/z = 2274.9441 $[M\text{-}PF_6]^+$ (calcd. for $C_{142}H_{120}IrN_{16}O_2$ 2274.9437).

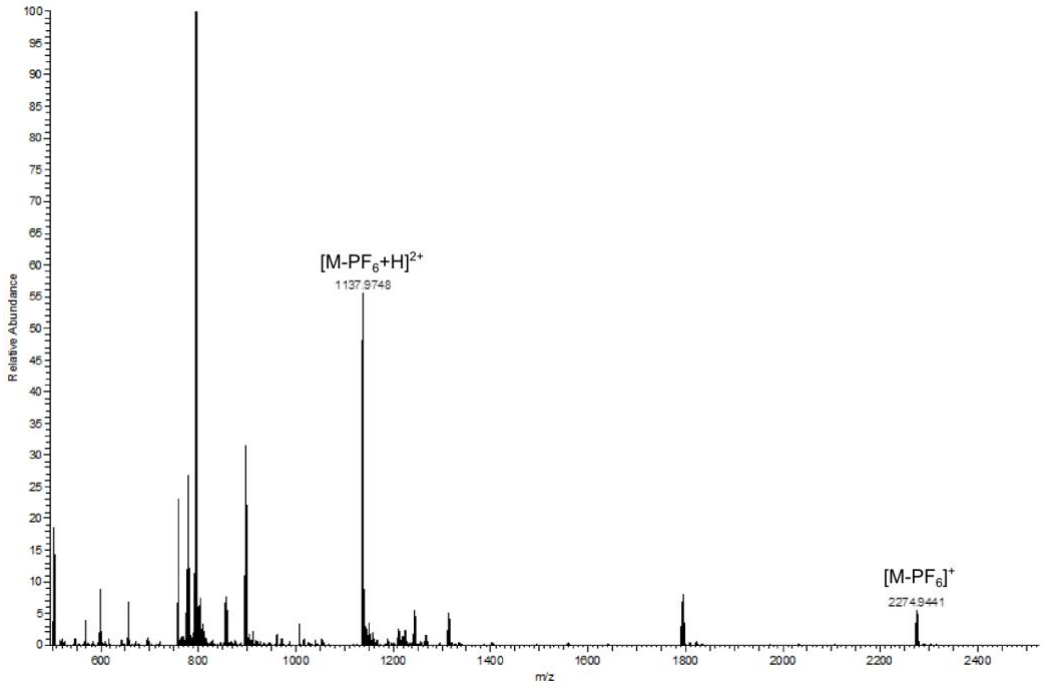

Figure S9. High-resolution ESI-MS of Δ-**6**. Calculated peaks (m/z): 2274.9437 $[M\text{-}PF_6]^+$; 1137.9755 $[M\text{-}PF_6{+}H]^{2+}$.

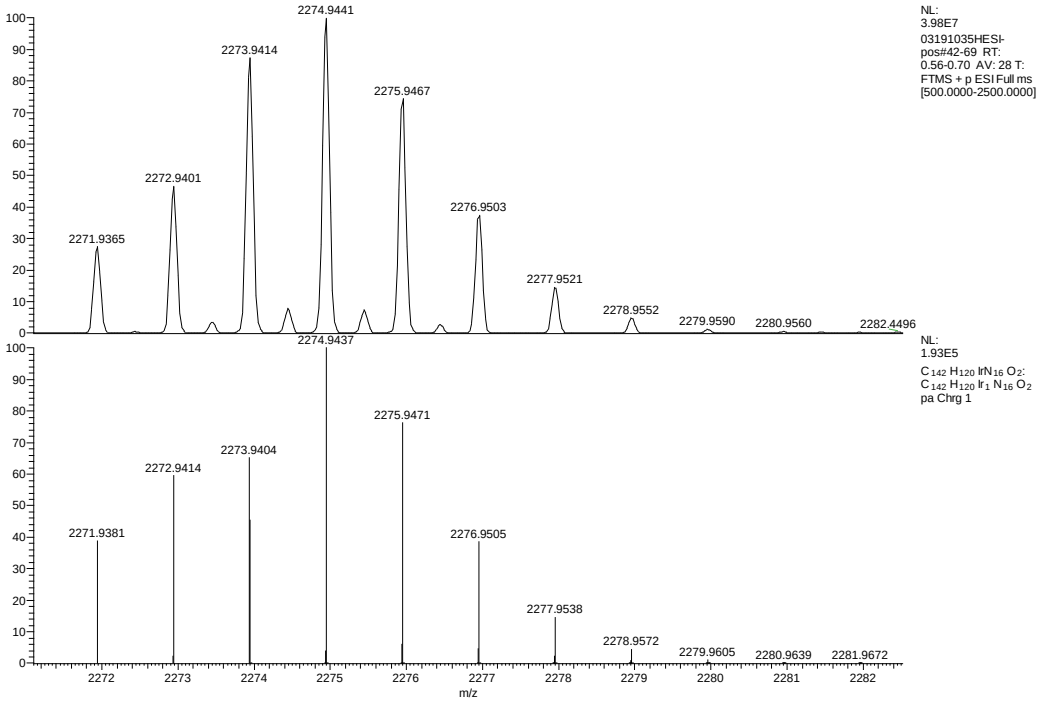

Figure S10. High-resolution ESI-MS of the $[M\text{-}PF_6]^+$ peak of Δ-**6**. Experimental spectrum (top, observed m/z 2274.9441) and calculated spectrum (bottom, theoretical m/z 2274.9437).

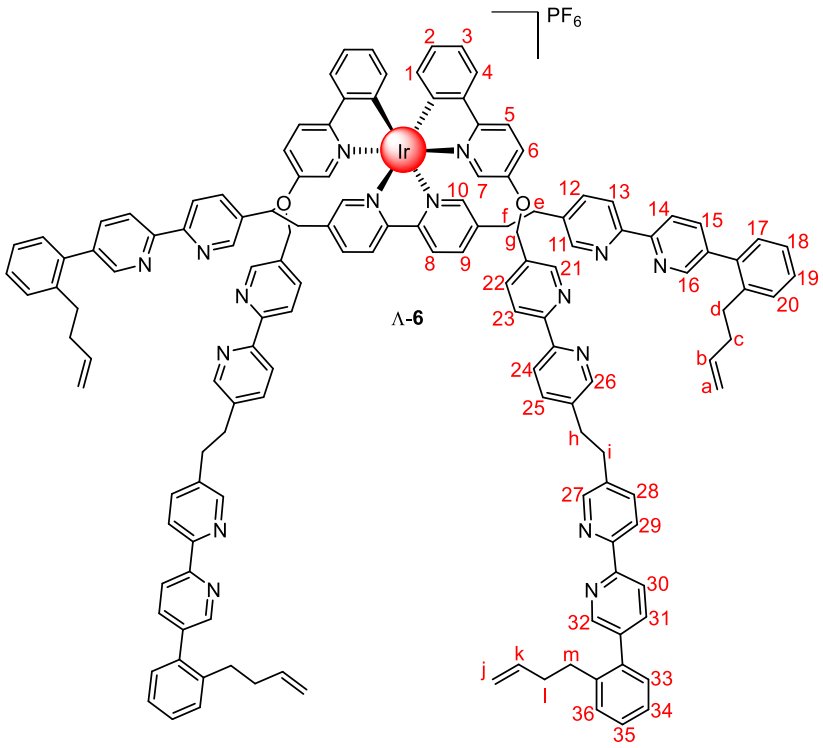

Compound Λ-**3** (57 mg, 0.04 mmol), compound **5** (56 mg, 0.10 mmol, 2.5 equiv.) and potassium carbonate anhydrous (27 mg, 0.20 mmol, 5.0 equiv.) were placed in a sealed vial backfilled with N_2. The solids were dissolved in dry DMF (2 mL) and the mixture was heated at 60 °C for 21 h while stirring. The solvent was then removed, and the residue was redissolved in dichloromethane, filtered off, and purified by size-exclusion column chromatography with dichloromethane as eluent to afford 59 mg of a mixture of compound Λ-**6** with other regioisomers which was taken forward without additional purification (62% Yield). HRESI-MS: m/z = 2271.9330 $[M\text{-}PF_6]^+$ (calcd. for $C_{142}H_{120}IrN_{16}O_2$ 2271.9381).

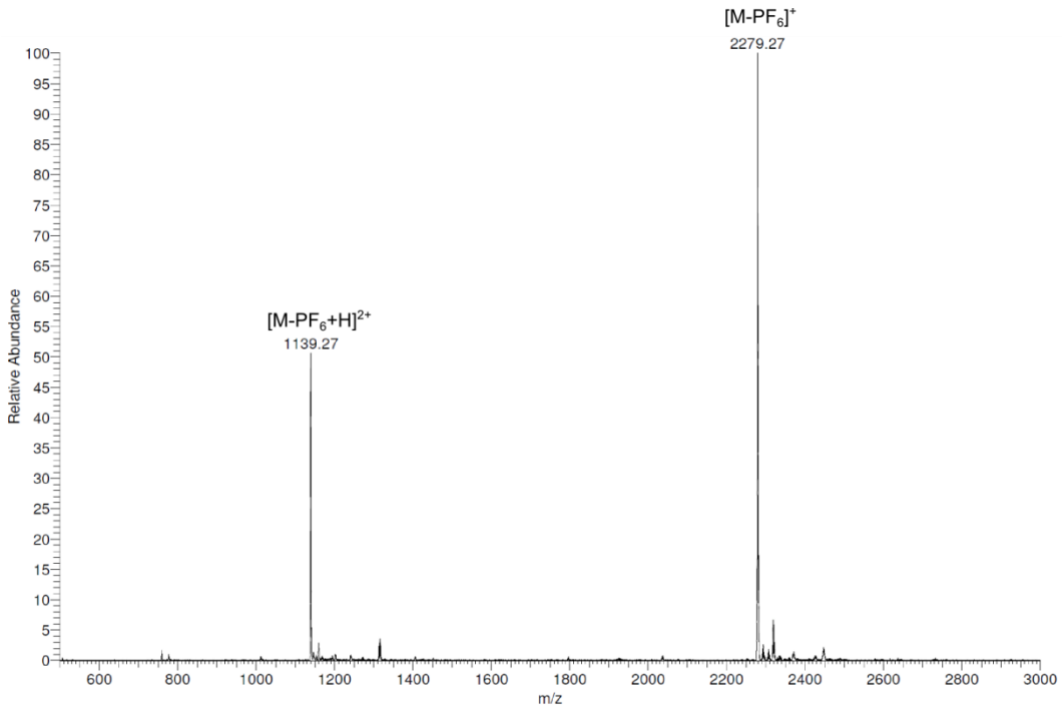

Figure S11. Low-resolution ESI-MS of Λ-**6**. Calculated peaks (m/z): 2274.94 $[M\text{-}PF_6]^+$; 1137.98 $[M\text{-}PF_6\text{+}H]^{2+}$.

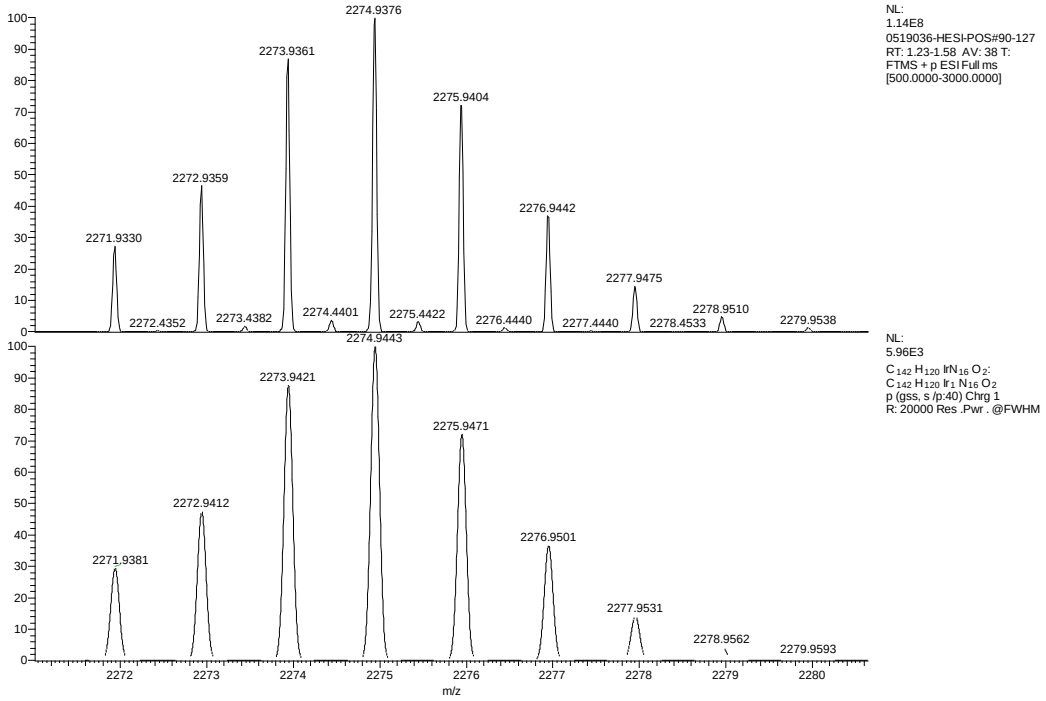

Figure S12. High-resolution ESI-MS of the $[M\text{-}PF_6]^+$ peak of Λ-**6**. Experimental spectrum (top, observed m/z 2274.9376) and calculated spectrum (bottom, theoretical m/z 2274.9443).

3.4 Synthesis of Ir_2Zn_4 open helicates

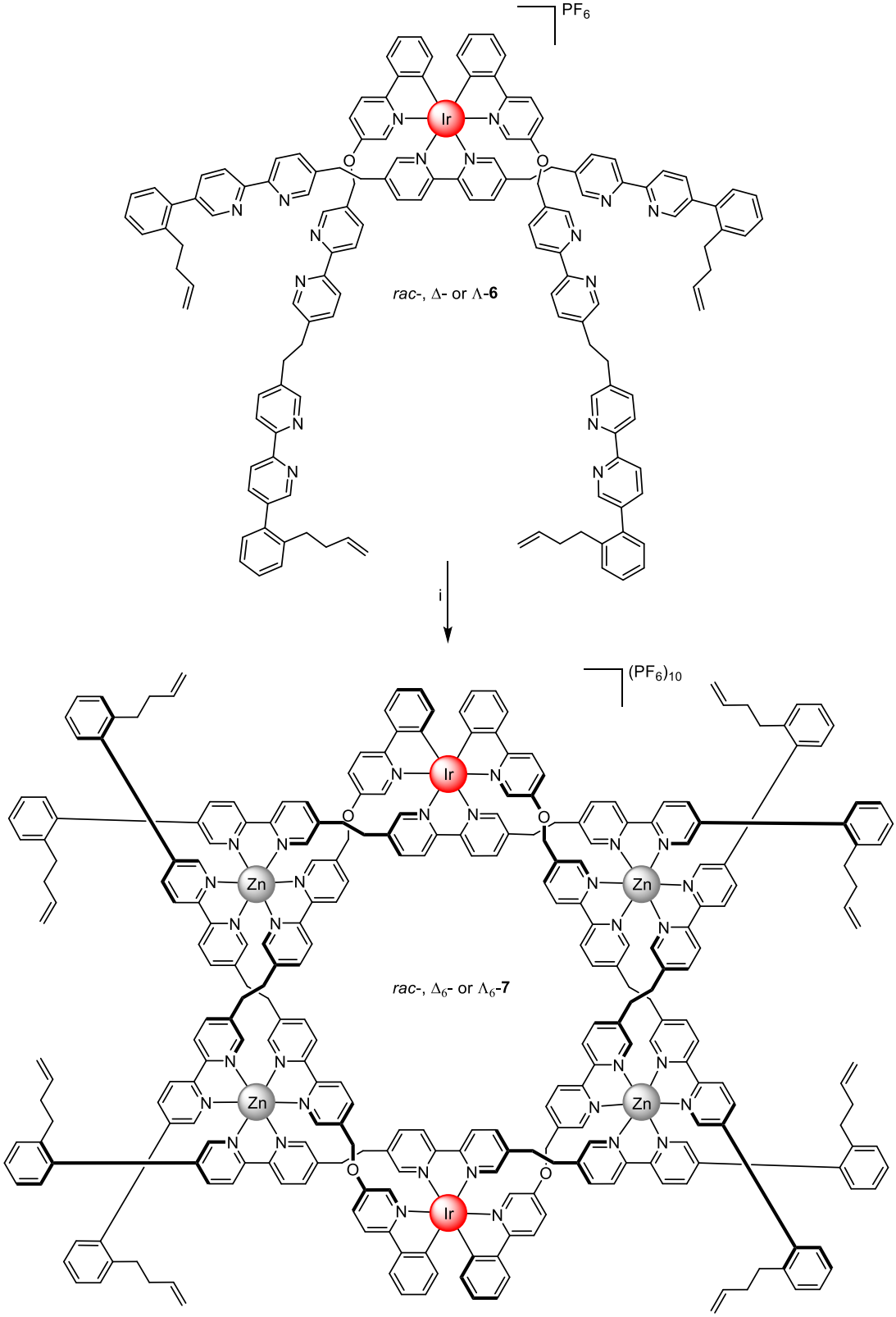

Scheme S4. Synthetic route for heterometallic open helicate **7**. Reaction conditions: i) $Zn(OTf)_2$, MeCN, 60 °C, 24 h; then KPF_6.

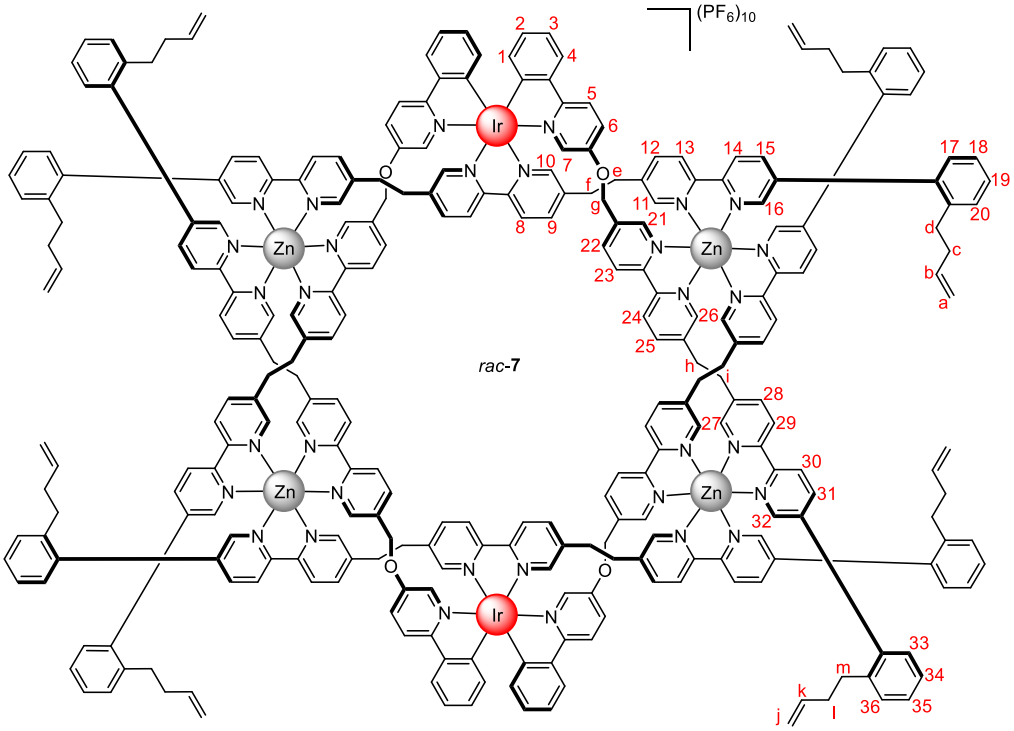

Compound *rac*-**6** (78 mg, 0.032 mmol) and zinc triflate (26 mg, 0.072 mmol, 2.25 equiv.) were dissolved in acetonitrile (6 mL) and placed in a sealed vial. The mixture was stirred at 60 °C for 24 h. After allowing the mixture to cool down, a saturated potassium hexafluorophosphate solution in methanol was added until a precipitate formed. The solid was then filtered on Celite®, washed with excess water, methanol and dichloromethane, and taken into DMF. The solvent was removed to afford 95 mg of *rac*-**7** (95%). ^{1}H NMR (600 MHz, CD_3CN) δ 8.87 (br, 4H, H_{23}), 8.81 (br, 4H, H_{24}), 8.76 – 8.69 (m, 8H, H_8, H_{30}), 8.68 (d, *J* = 8.4 Hz, 4H, H_{14}), 8.42 (dd, *J* = 8.2, 2.1 Hz, 4H, H_{31}), 8.41 (dd, *J* = 8.2, 2.1 Hz, 4H, H_{15}), 8.26 (d, *J* = 8.3 Hz, 4H, H_{29}), 8.12 (d, *J* = 8.3 Hz, 4H, H_{13}), 7.99 (d, *J* = 9.1 Hz, 4H, H_5), 7.92 (d, *J* = 7.7 Hz, 4H, H_4), 7.87 (s, 4H, H_{32}), 7.81 (s, 4H, H_{16}), 7.77 (d, *J* = 8.0 Hz, 4H, H_{25}), 7.71 (d, *J* = 8.1 Hz, 4H, H_{22}), 7.61 (d, *J* = 7.7 Hz, 4H, H_9), 7.42 – 7.25 (m, 44H, H_{10}, H_{18} - H_{20}, H_{21}, H_{26}, H_{28}, H_{33} – H_{36}), 7.22 – 7.16 (m, 8H, H_{17}, H_3), 7.06 (d, *J* = 9.1 Hz, 4H, H_{12}), 6.99 – 6.95 (m, 8H, H_{11}, H_2), 6.92 (s, 4H, H_{27}), 6.88 (dd, *J* = 8.9, 2.7 Hz, 4H, H_6), 6.30 (s, 4H, H_7), 6.14 (d, *J* = 7.7 Hz, 4H, H_1), 5.53 (ddt, *J* = 17.0, 10.4, 6.5 Hz, 4H, H_b), 5.45 (ddt, *J* = 16.9, 10.3, 6.5 Hz, 4H, H_k), 5.28 (d, *J* = 15.9 Hz, 4H, H_g), 4.85 – 4.70 (m, 20H, $H_{g'}$, H_a, H_j), 3.19 – 2.49 (m, 32H, H_e, H_f, H_h, H_i), 2.44 – 2.38 (m, 8H, H_d), 2.38 – 2.30 (m, 8H, H_m), 2.04 – 1.98 (m, 8H, H_c), 1.97 – 1.90 (m, 8H, H_l). DEPTQ (151 MHz, Acetonitrile-d_3) δ 162.49 (C_5-C-N), 152.52 (C_8-C-N), 151.98 (C_{10}), 151.71 (C_6-C-C_7), 149.53 (C_1-C-Ir), 149.06 (C_{32}), 148.78 (C_{16}), 148.20 (C_{26}), 147.73 (C_{14}-C-N, C_{29}-C-N, C_{30}-C-N), 147.61 (C_{27}), 147.56 (C_{11}, C_{21}, C_{23}-C-N), 147.09 (C_{13}-C-N), 145.82 (C_{24}-C-N), 144.19 (C_{31}, C_4-C-C-C_1), 144.11 (C_{15}), 143.32 (C_{12}), 143.13 (C_{25}), 142.45 (C_{28}), 142.37 (C_{31}-C-C_{32}), 142.26 (C_{15}-C-C_{16}), 141.41 (C_{22}), 141.17 (C_9-C-C_{10}), 140.80 (C_{25}-C-C_{26}), 140.61 (C_9), 140.06, 140.03 (C_{17}-C-C-C_{20}, C_{33}-C-C-C_{36}), 139.74 (C_{27}-C-C_{28}), 139.62 (C_{11}-C-C_{12}), 138.32 (C_b), 138.27 (C_k), 137.43 (C_{21}-C-C_{22}), 136.06, 136.03 (C_{17}-C-C-C_{20}, C_{33}-C-C-C_{36}), 135.34 (C_7), 132.81 (C_1), 131.19 (C_{33}), 131.13 (C_2), 131.10 (C_{17}), 130.75, 130.71 (C_{20}, C_{36}), 130.38 (C_{19}, C_{35}), 129.17 (C_6), 127.44 (C_{18}, C_{34}), 125.40 (C_4), 124.65 (C_8), 124.11 (C_{14}), 124.06 (C_3, C_{30}), 123.91 (C_{13}), 123.64 (C_{24}, C_{29}), 123.35 (C_{23}), 121.99 (C_5), 115.94 (C_a, C_j), 67.09 (C_g), 35.24, 35.19 (C_c, C_l), 32.63, 32.59 (C_d, C_m), 29.75, 29.56, 29.29, 28.92 (C_e, C_f, C_h, C_i). DOSY (600 MHz, CD_3CN) D = 4.12 x 10^{-10} m^2/s, hydrodynamic radius = 14.4 Å. HRESI-MS: m/z = 1420.0956 $[M\text{-}4PF_6]^{4+}$ (calcd. for $C_{284}H_{240}F_{36}Ir_2N_{32}O_4P_6Zn_4$ 1420.0981).

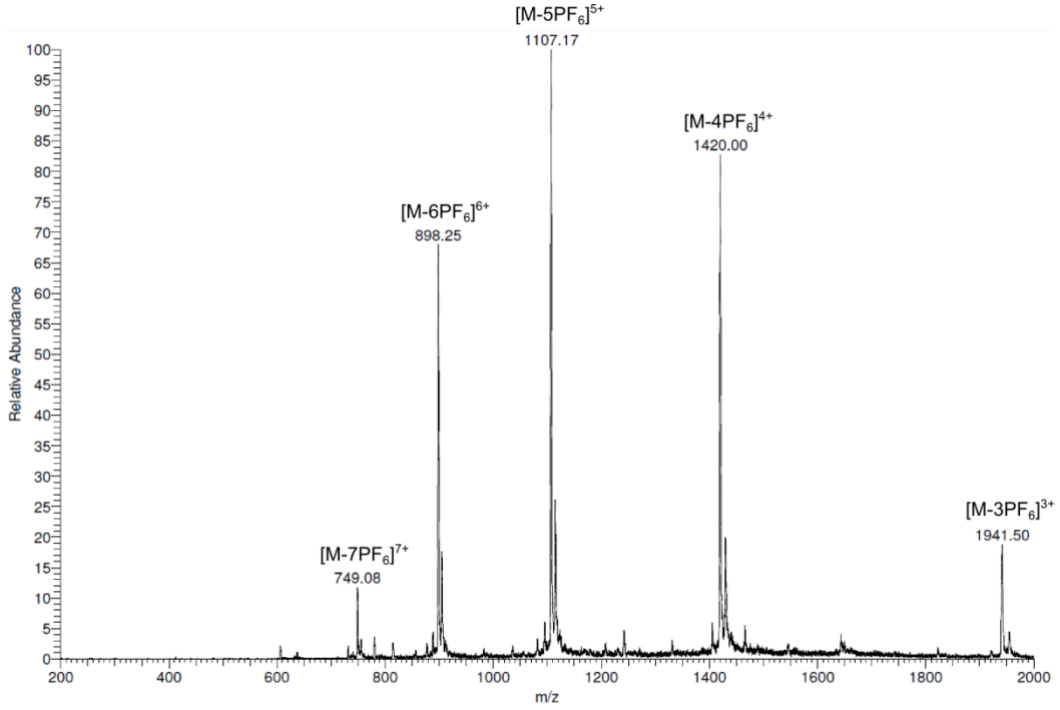

Figure S13. Low-resolution ESI-MS of *rac*-**7**. Calculated peaks (m/z): 1939.45 $[M\text{-}3PF_6]^{3+}$; 1418.35 $[M\text{-}4PF_6]^{4+}$; 1105.69 $[M\text{-}5PF_6]^{5+}$; 897.25 $[M\text{-}6PF_6]^{6+}$; 748.36 $[M\text{-}7PF_6]^{7+}$.

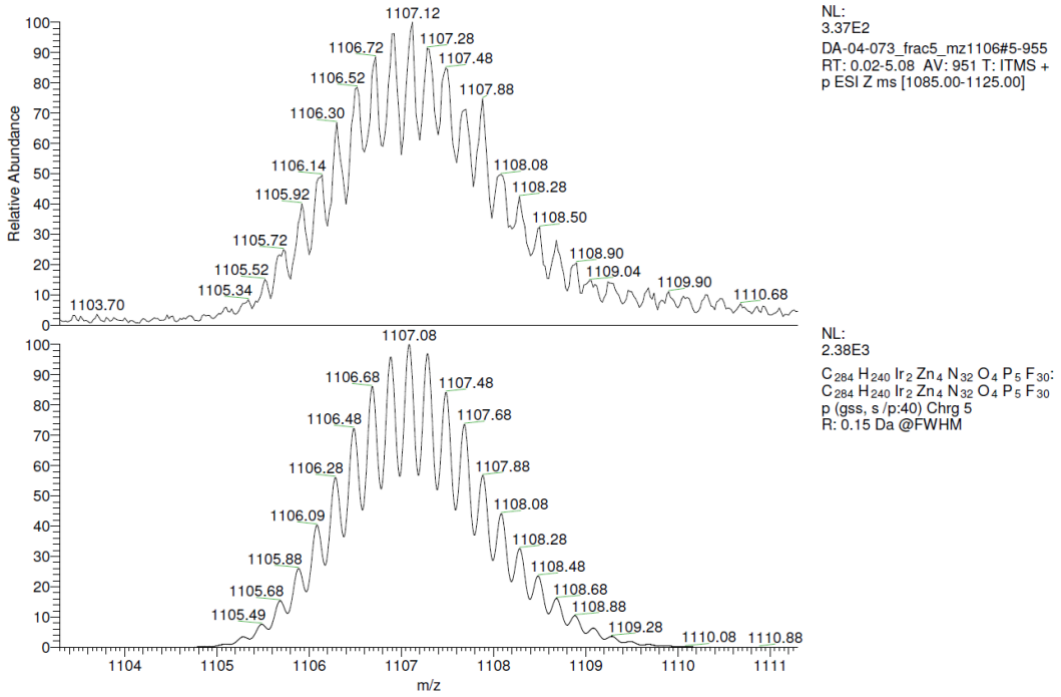

Figure S14. Low-resolution ESI-MS of the $[M\text{-}5PF_6]^{5+}$ peak of *rac*-**7**. Experimental spectrum (top, observed m/z 1107.12) and calculated spectrum (bottom, theoretical m/z 1107.08).

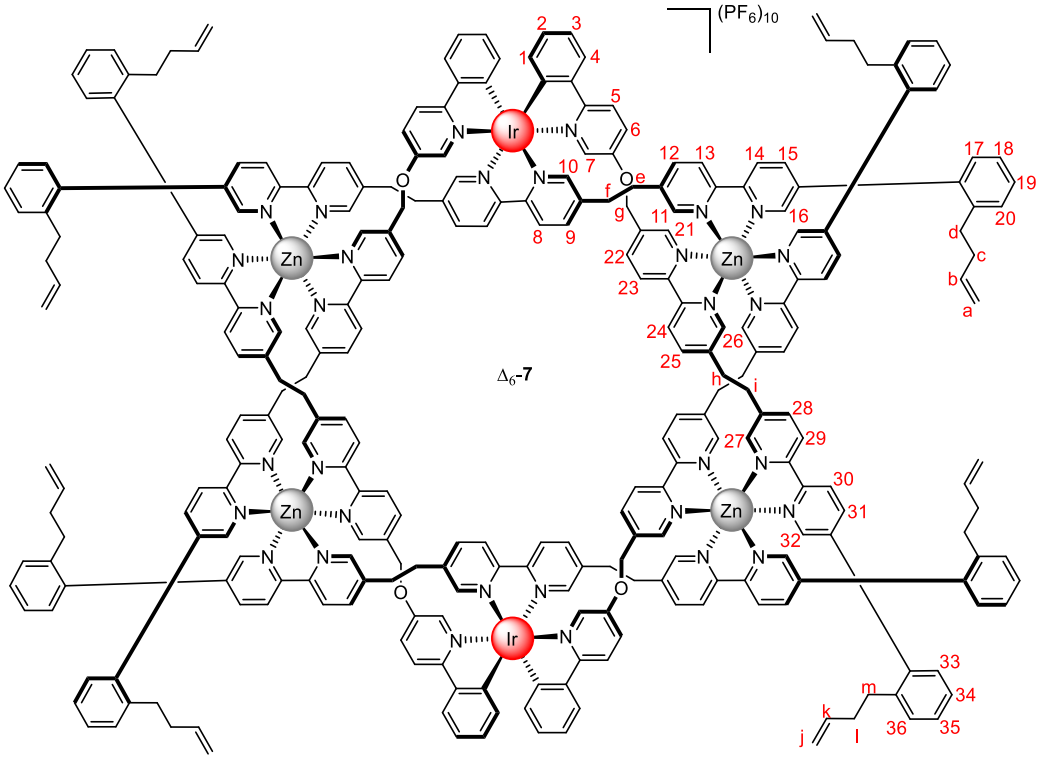

Compound Δ-**6** (47 mg, 0.020 mmol) and zinc triflate (16 mg, 0.044 mmol, 2.25 equiv.) were dissolved in acetonitrile (4 mL) and placed in a sealed vial. The mixture was stirred at 60 °C for 24 h. After allowing the mixture to cool down, a saturated potassium hexafluorophosphate solution in methanol was added until a precipitate formed. The solid was then filtered on Celite®, washed with excess water, methanol and dichloromethane, and taken into DMF. The solvent was removed to afford 57 mg of Δ_6-**7** (92% Yield). ^{1}H NMR (600 MHz, CD_3CN) δ 8.86 (br, 4H, H_{23}), 8.80 (br, 4H, H_{24}), 8.77 – 8.70 (m, 8H, H_8, H_{30}), 8.68 (d, *J* = 8.4 Hz, 4H, H_{14}), 8.42 (dd, *J* = 8.0, 2.2 Hz, 4H, H_{31}), 8.41 (dd, *J* = 8.0, 2.2 Hz, 4H, H_{15}), 8.26 (d, *J* = 8.3 Hz, 4H, H_{29}), 8.12 (d, *J* = 8.2 Hz, 4H, H_{13}), 7.99 (d, *J* = 9.1 Hz, 4H, H_5), 7.92 (d, *J* = 7.7 Hz, 4H, H_4), 7.88 (d, *J* = 2.1 Hz, 4H, H_{32}), 7.82 (d, *J* = 2.1 Hz, 4H, H_{16}), 7.77 (d, *J* = 8.4 Hz, 4H, H_{25}), 7.71 (d, *J* = 7.1 Hz, 4H, H_{22}), 7.61 (d, *J* = 7.4 Hz, 4H, H_9), 7.43 – 7.25 (m, 44H, H_{10}, H_{18} - H_{20}, H_{21}, H_{26}, H_{28}, H_{33} – H_{36}), 7.22 – 7.17 (m, 8H, H_{17}, H_3), 7.07 (dd, *J* = 8.5, 2.1 Hz, 4H, H_{12}), 7.01 – 6.95 (m, 8H, H_{11}, H_2), 6.92 (s, 4H, H_{27}), 6.88 (dd, *J* = 9.0, 2.7 Hz, 4H, H_6), 6.31 (d, *J* = 2.7 Hz, 4H, H_7), 6.15 (d, *J* = 7.7 Hz, 4H, H_1), 5.53 (ddt, *J* = 16.9, 10.3, 6.5 Hz, 4H, H_b), 5.46 (ddt, *J* = 16.9, 10.3, 6.5 Hz, 4H, H_k), 5.28 (d, *J* = 15.9 Hz, 4H, H_g), 4.86 – 4.71 (m, 20H, $H_{g'}$, H_a, H_j), 3.20 – 2.51 (m, 32H, H_e, H_f, H_h, H_i), 2.45 – 2.38 (m, 8H, H_d), 2.38 – 2.31 (m, 8H, H_m), 2.04 – 1.98 (m, 8H, H_c), 1.98 – 1.91 (m, 8H, H_l). DEPTQ (151 MHz, CD_3CN) δ 162.51 (C_5-C-N), 152.52 (C_8-C-N), 151.98 (C_{10}), 151.71 (C_6-C-C_7), 149.53 (C_1-C-Ir), 149.07 (C_{32}), 148.79 (C_{16}), 148.20 (C_{26}), 147.74 (C_{14}-C-N, C_{30}-C-N), 147.68 (C_{29}-C-N), 147.61 (C_{27}), 147.54 (C_{11}, C_{23}-C-N), 147.48 (C_{21}), 147.12 (C_{13}-C-N), 145.83 (C_{24}-C-N), 144.20 (C_{31}, C_4-C-C-C_1), 144.13 (C_{15}), 143.29 (C_{12}), 143.08 (C_{25}), 142.42 (C_{28}), 142.38 (C_{31}-C-C_{32}), 142.27 (C_{15}-C-C_{16}), 141.40 (C_{22}), 141.18 (C_9-C-C_{10}), 140.81 (C_{25}-C-C_{26}), 140.57 (C_9), 140.07, 140.04 (C_{17}-C-C-C_{20}, C_{33}-C-C-C_{36}), 139.74 (C_{27}-C-C_{28}), 139.62 (C_{11}-C-C_{12}), 138.33 (C_b), 138.27 (C_k), 137.44 (C_{21}-C-C_{22}), 136.06, 136.02 (C_{17}-C-C-C_{20}, C_{33}-C-C-C_{36}), 135.33 (C_7), 132.82 (C_1), 131.17 (C_{33}, C_2), 131.10 (C_{17}), 130.76, 130.73 (C_{20}, C_{36}), 130.40 (C_{19}, C_{35}), 129.18 (C_6), 127.44 (C_{18}, C_{34}), 125.41 (C_4), 124.62 (C_8), 124.12 (C_{14}), 124.07 (C_3, C_{30}), 123.93 (C_{13}), 123.65 (C_{24}, C_{29}), 123.28 (C_{23}), 122.01 (C_5), 115.94 (C_a, C_j), 67.10 (C_g), 35.25, 35.20 (C_c, C_l), 32.64, 32.60 (C_d, C_m), 29.80, 29.60, 29.32, 28.95 (C_e, C_f, C_h, C_i). HRESI-MS: m/z = 1107.0849 $[M-5PF_6]^{5+}$ (calcd. for $C_{284}H_{240}F_{30}Ir_2N_{32}O_4P_5Zn_4$ 1107.0836).

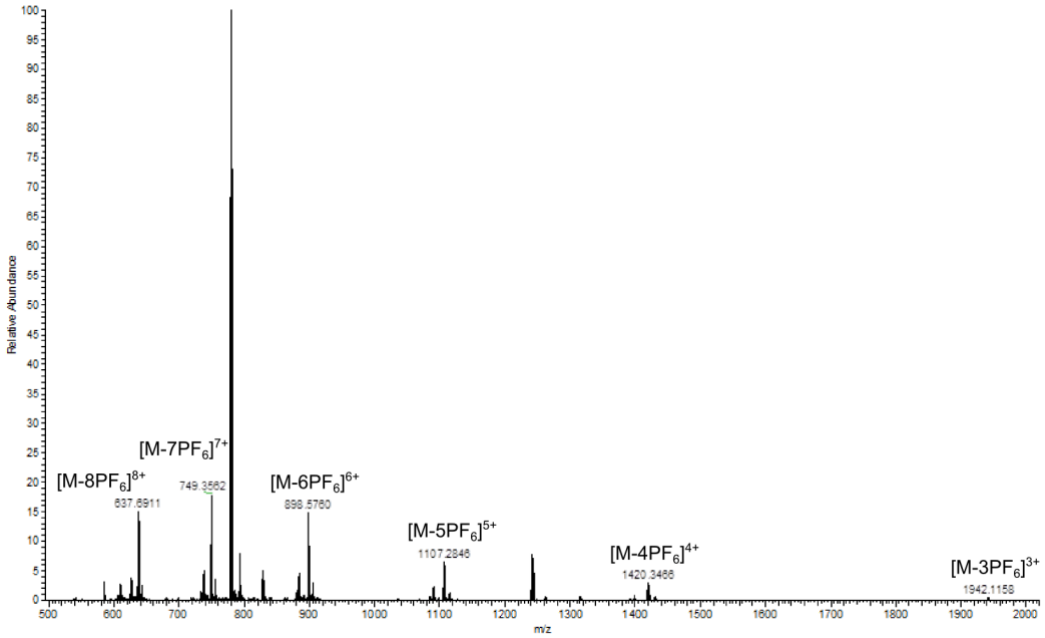

Figure S15. High-resolution ESI-MS of Δ_6-**7**. Calculated peaks (m/z): 1939.45 $[M\text{-}3PF_6]^{3+}$; 1418.35 $[M\text{-}4PF_6]^{4+}$; 1105.69 $[M\text{-}5PF_6]^{5+}$; 897.25 $[M\text{-}6PF_6]^{6+}$; 748.36 $[M\text{-}7PF_6]^{7+}$; 636.70 $[M\text{-}8PF_6]^{8+}$.

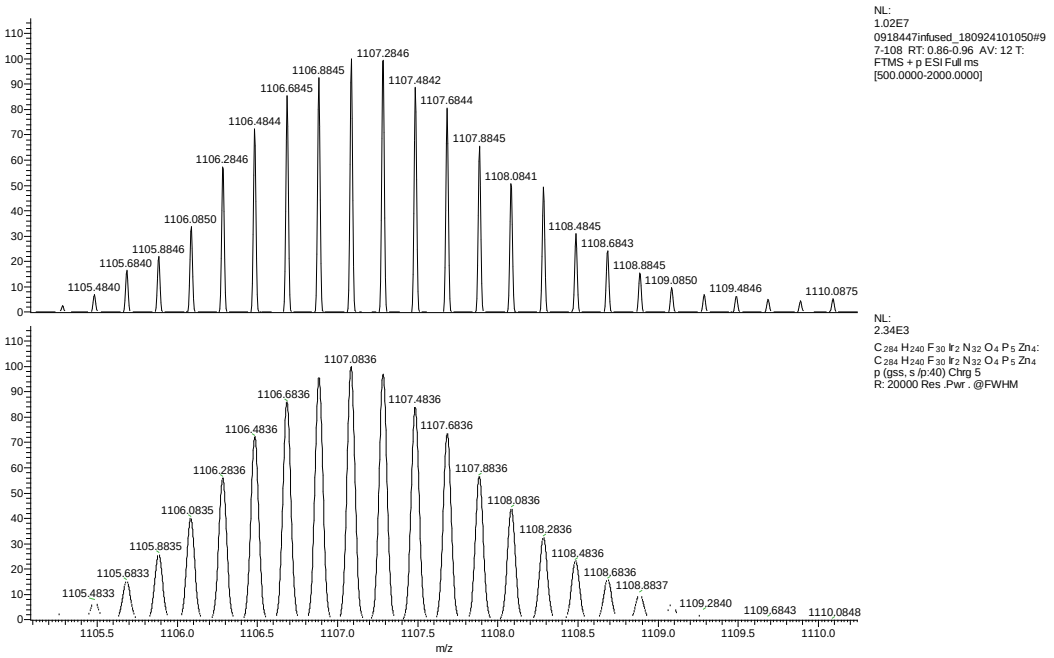

Figure S16. High-resolution ESI-MS of the $[M\text{-}5PF_6]^{5+}$ peak of Δ_6-**7**. Experimental spectrum (top, observed m/z 1107.0849) and calculated spectrum (bottom, theoretical m/z 1107.0836).

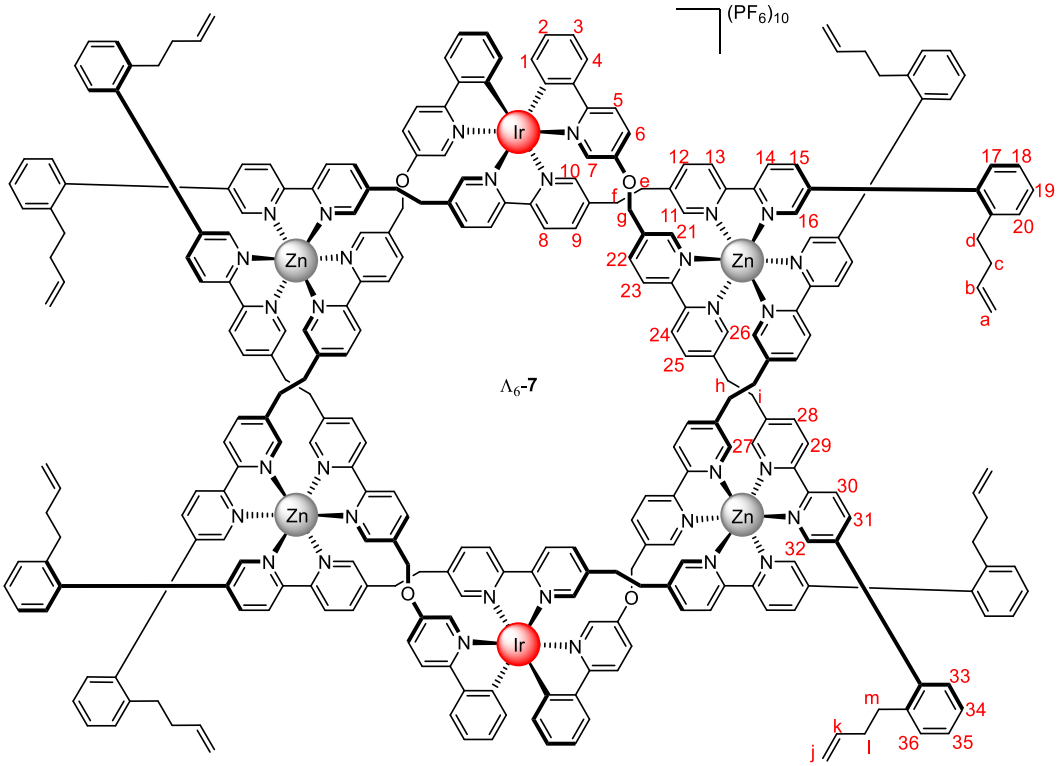

Compound Λ-**6** (49 mg, 0.020 mmol) and zinc triflate (17 mg, 0.046 mmol, 2.25 equiv.) were dissolved in acetonitrile (4 mL) and placed in a sealed vial. The mixture was stirred at 60 °C for 24 h. After allowing the mixture to cool down, a saturated potassium hexafluorophosphate solution in methanol was added until a precipitate formed. The solid was then filtered on Celite®, washed with excess water, methanol and dichloromethane, and taken into DMF. The solvent was removed to afford 61 mg of Λ_6-**7** (96% Yield). ^{1}H NMR (600 MHz, CD_3CN) δ 8.87 (br d, *J* = 8.2 Hz, 4H, H_{23}), 8.81 (br d, *J* = 8.1 Hz, 4H, H_{24}), 8.75 – 8.70 (m, 8H, H_8, H_{30}), 8.68 (d, *J* = 8.4 Hz, 4H, H_{14}), 8.42 (dd, *J* = 7.9, 2.1 Hz, 4H, H_{31}), 8.41 (dd, *J* = 7.9, 2.1 Hz, 4H, H_{15}), 8.26 (d, *J* = 8.3 Hz, 4H, H_{29}), 8.12 (d, *J* = 8.2 Hz, 4H, H_{13}), 7.99 (d, *J* = 9.1 Hz, 4H, H_5), 7.92 (d, *J* = 7.6 Hz, 4H, H_4), 7.88 (d, *J* = 2.1 Hz, 4H, H_{32}), 7.82 (d, *J* = 2.1 Hz, 4H, H_{16}), 7.76 (d, *J* = 8.2 Hz, 4H, H_{25}), 7.70 (d, *J* = 7.6 Hz, 4H, H_{22}), 7.60 (d, *J* = 8.0 Hz, 4H, H_9), 7.41 – 7.24 (m, 44H, H_{10}, H_{18} - H_{20}, H_{21}, H_{26}, H_{28}, H_{33} – H_{36}), 7.22 – 7.17 (m, 8H, H_{17}, H_3), 7.06 (dd, *J* = 8.1, 2.1 Hz, 4H, H_{12}), 7.00 – 6.96 (m, 8H, H_{11}, H_2), 6.92 (d, *J* = 2.1 Hz, 4H, H_{27}), 6.88 (dd, *J* = 9.0, 2.7 Hz, 4H, H_6), 6.31 (d, *J* = 2.7 Hz, 4H, H_7), 6.15 (d, *J* = 7.7 Hz, 4H, H_1), 5.53 (ddt, *J* = 16.9, 10.3, 6.5 Hz, 4H, H_b), 5.45 (ddt, *J* = 16.9, 10.3, 6.5 Hz, 4H, H_k), 5.27 (d, *J* = 15.8 Hz, 4H, H_g), 4.85 – 4.71 (m, 20H, $H_{g'}$, H_a, H_j), 3.18 – 2.51 (m, 32H, H_e, H_f, H_h, H_i), 2.45 – 2.38 (m, 8H, H_d), 2.38 – 2.30 (m, 8H, H_m), 2.04 – 1.98 (m, 8H, H_c), 1.97 – 1.90 (m, 8H, H_l). DEPTQ (151 MHz, CD_3CN) δ 162.52 (C_5-C-N), 152.54 (C_8-C-N), 151.97 (C_{10}), 151.72 (C_6-C-C_7), 149.56 (C_1-C-Ir), 149.08 (C_{32}), 148.80 (C_{16}), 148.19 (C_{26}), 147.75 (C_{14}-C-N, C_{30}-C-N), 147.68 (C_{29}-C-N), 147.62 (C_{27}), 147.56 (C_{11}), 147.51 (C_{23}-C-N), 147.47 (C_{21}), 147.12 (C_{13}-C-N), 145.84 (C_{24}-C-N), 144.20 (C_{31}, C_4-C-C-C_1), 144.15 (C_{15}), 143.29 (C_{12}), 143.08 (C_{25}), 142.41 (C_{28}), 142.38 (C_{31}-C-C_{32}), 142.28 (C_{15}-C-C_{16}), 141.40 (C_{22}), 141.18 (C_9-C-C_{10}), 140.81 (C_{25}-C-C_{26}), 140.58 (C_9), 140.08, 140.04 (C_{17}-C-C-C_{20}, C_{33}-C-C-C_{36}), 139.76 (C_{27}-C-C_{28}), 139.63 (C_{11}-C-C_{12}), 138.34 (C_b), 138.28 (C_k), 137.44 (C_{21}-C-C_{22}), 136.07, 136.03 (C_{17}-C-C-C_{20}, C_{33}-C-C-C_{36}), 135.35 (C_7), 132.83 (C_1), 131.19 (C_{33}), 131.14 (C_2), 131.10 (C_{17}), 130.77, 130.72 (C_{20}, C_{36}), 130.40 (C_{19}, C_{35}), 129.18 (C_6), 127.45, 127.43 (C_{18}, C_{34}), 125.41 (C_4), 124.65 (C_8), 124.12 (C_{14}), 124.07 (C_3, C_{30}), 123.92 (C_{13}), 123.72 (C_{24}), 123.66 (C_{29}), 123.33 (C_{23}), 122.01 (C_5), 115.95 (C_a), 115.94 (C_j), 67.11 (C_g), 35.25, 35.20 (C_c, C_l), 32.64, 32.60 (C_d, C_m), 29.80, 29.61, 29.32, 28.95 (C_e, C_f, C_h, C_i). HRESI-MS: m/z = 1420.0965 $[M\text{-}4PF_6]^{4+}$ (calcd. for $C_{284}H_{240}F_{36}Ir_2N_{32}O_4P_6Zn_4$ 1420.0965).

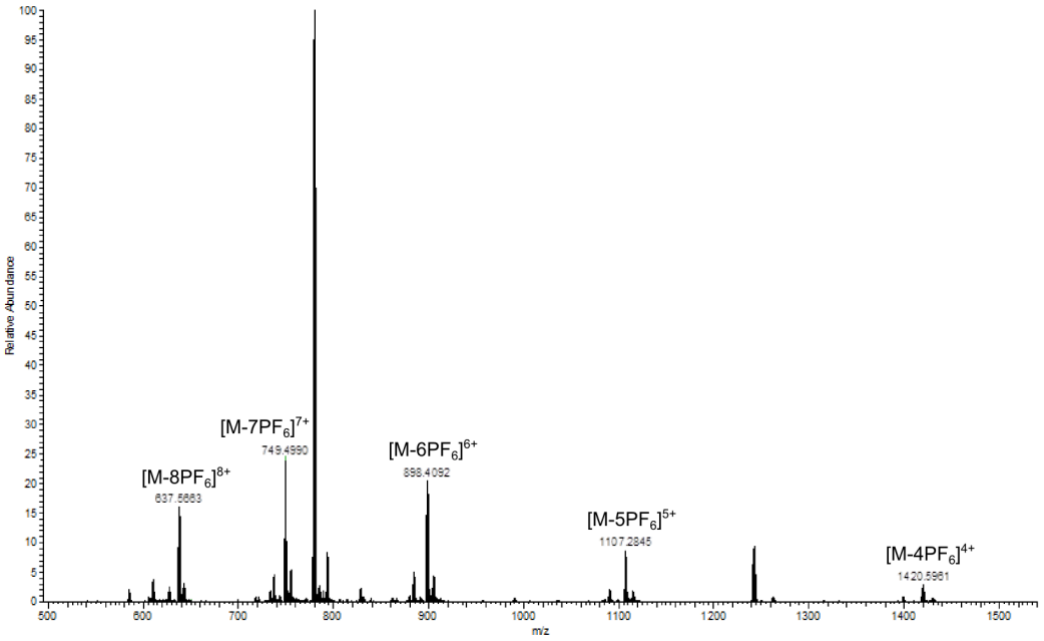

Figure S17. High-resolution ESI-MS of Λ_6-**7**. Calculated peaks (m/z): 1418.35 $[M\text{-}4PF_6]^{4+}$; 1105.69 $[M\text{-}5PF_6]^{5+}$; 897.25 $[M\text{-}6PF_6]^{6+}$; 748.36 $[M\text{-}7PF_6]^{7+}$; 636.70 $[M\text{-}8PF_6]^{8+}$.

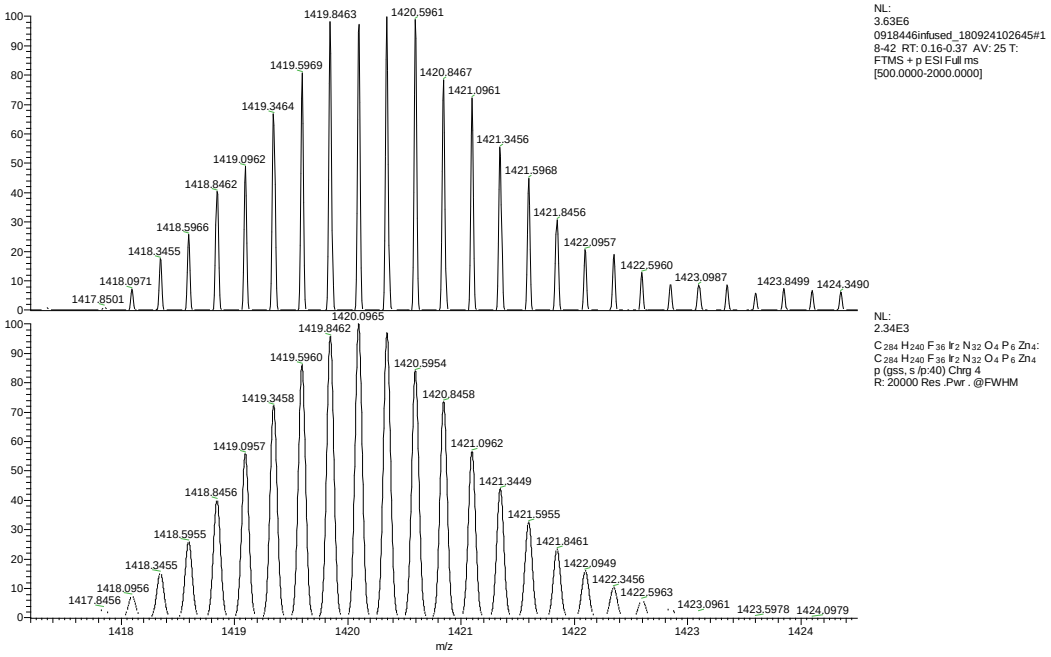

Figure S18. High-resolution ESI-MS of the $[M\text{-}4PF_6]^{4+}$ peak of Λ_6-**7**. Experimental spectrum (top, observed m/z 1420.0965) and calculated spectrum (bottom, theoretical m/z 1420.0965).

3.5 Synthesis of an Ir_2Zn_4 Star of David catenane

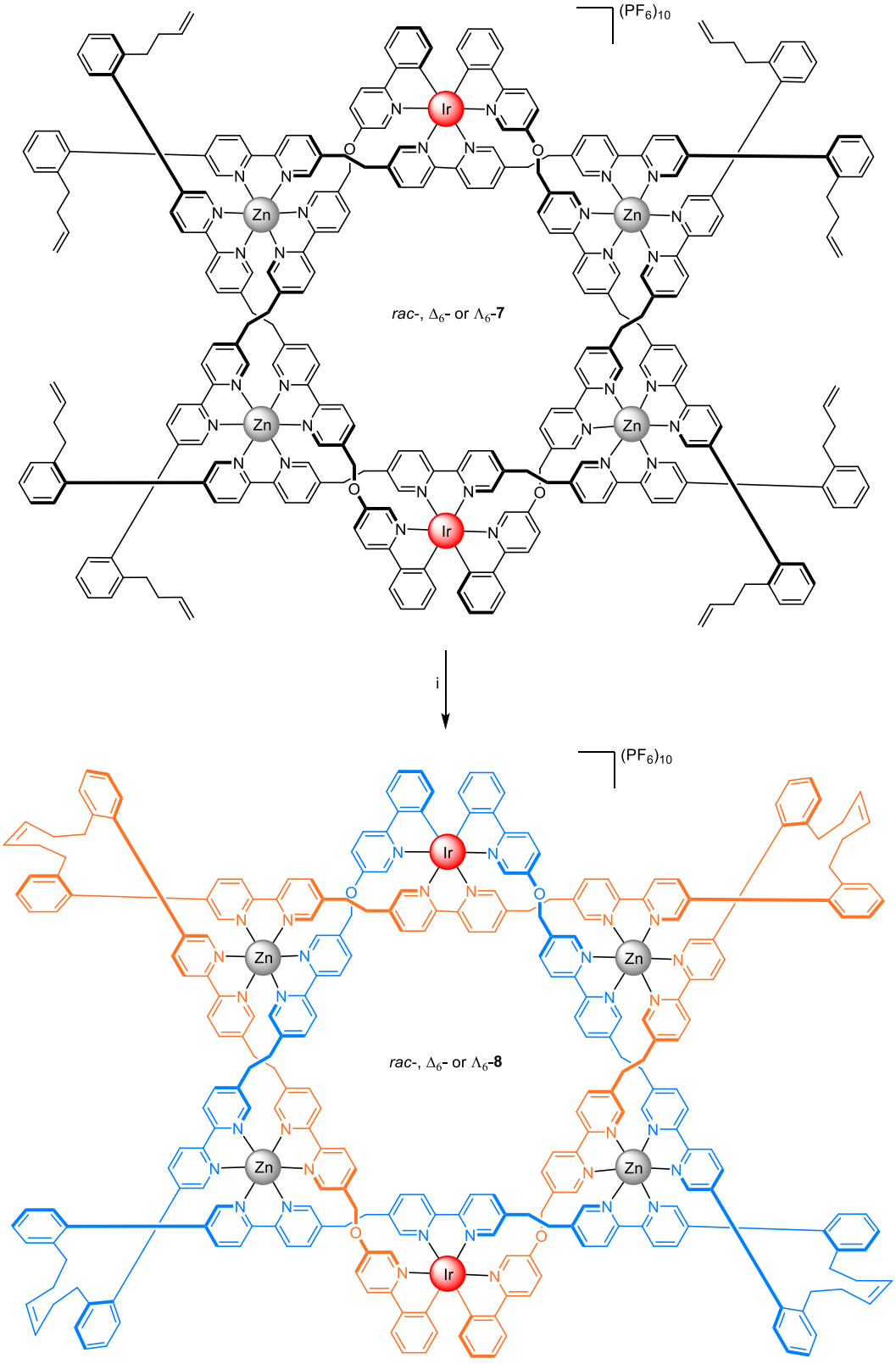

Scheme S5. Synthetic route for closed heterometallic helicate **8**. Reaction conditions: i) Hoveyda-Grubbs 2nd generation catalyst, DCE/$MeNO_2$, N_2, 60 °C, 24 h; then KPF_6.

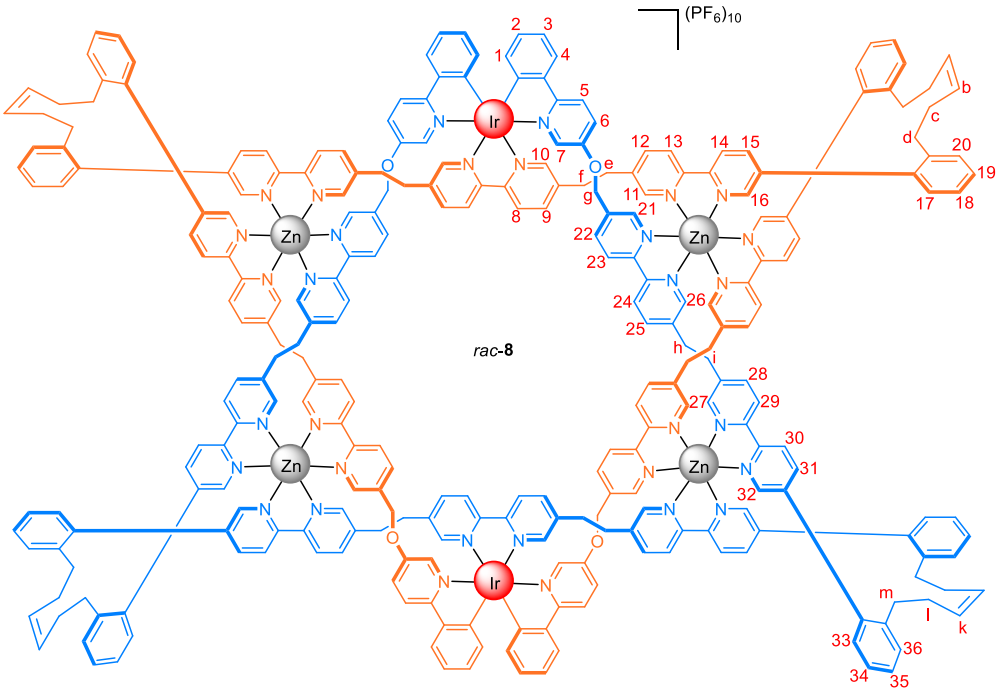

Compound *rac*-**7** (95 mg, 0.015 mmol) and Hoveyda-Grubbs 2nd generation catalyst (7.6 mg, 0.012 mmol, 0.80 equiv.) were placed in a sealed vial and dissolved in degassed anhydrous 1, 2-dichloroethane (7.5 mL) and nitromethane (7.5 mL). The mixture was stirred at 60 °C for 24 h. After allowing the mixture to cool down, ethyl vinyl ether (8 mL) was added to quench the catalyst and the mixture was stirred for 30 minutes before removing the solvents. The solid residue was sonicated in chloroform (25 mL) and filtered on Celite®, then washed with excess chloroform and taken into acetonitrile. A saturated potassium hexafluorophosphate solution in methanol was added until a precipitate formed. The solid was then filtered on Celite®, washed with excess water, methanol and chloroform, and taken into acetonitrile. The solvent was removed to afford 65 mg of *rac*-**8** (69% Yield). ^{1}H NMR (600 MHz, CD_3CN) δ 9.07 – 8.79 (br, 12H, H_8, H_{23}, H_{24}), 8.78 – 8.66 (m, 8H, H_{14}, H_{30}), 8.47 – 8.35 (m, 8H, H_{15}, H_{31}), 8.35 – 8.24 (m, 4H, H_{29}), 8.20 – 8.10 (m, 4H, H_{13}), 8.00 (d, J = 9.1 Hz, 4H, H_5), 7.93 (d, J = 7.9 Hz, 4H, H_4), 7.83 – 7.59 (m, 20H, H_9, H_{16}, H_{22}, H_{25}, H_{32}), 7.56 – 7.15 (m, 52H, H_3, H_{10}, H_{17} – H_{20}, H_{21}, H_{26}, H_{28}, H_{33} – H_{36}), 7.12 – 7.02 (m, 4H, H_{12}), 7.01 – 6.78 (m, 16H, H_2, H_6, H_{11}, H_{27}), 6.36 – 6.25 (m, 4H, H_7), 6.19 – 6.09 (m, 4H, H_1), 5.30 (d, J = 15.8 Hz, 4H, H_g), 4.89/4.59 (s, 8H, H_b, H_k), 4.84 – 4.76 (m, 4H, $H_{g'}$), 3.22 – 2.51 (m, 32H, H_e, H_f, H_h, H_i), 2.46 – 2.30/1.60 – 1.29 (m, 16H, H_d, H_m), 1.89 – 1.60 (m, 16H, H_c, H_l). DEPTQ (151 MHz, CD_3CN) δ 162.45 (C_5-C-N), 152.59 (C_8-C-N), 152.00 (C_{10}), 151.86, 151.81 (C_6-C-C_7), 149.52 (C_1-C-Ir), 149.41, 149.21, 149.13 (C_{16}, C_{32}), 148.53, 148.48, 148.44 (C_{26}), 147.78, 147.76, 147.71, 147.67 (C_{10}, C_{11}, C_{21}, C_{27}), 147.48, 147.42, 147.12, 147.06, 145.76, 145.71 (C_q), 144.89, 144.83, 144.50, 144.47 (C_{15}, C_{31}), 144.15 (C_q), 143.53, 143.42, 143.38, 143.23, 143.15, 143.09, 143.05 (C_{12}, C_{25}), 142.75, 142.64 (C_q), 142.40 (C_{28}), 142.26 (C_q), 141.48 (C_{22}), 141.15, 140.98, 140.93, 140.85, 140.80 (C_q), 140.68 (C_9), 140.33, 139.90, 139.85, 139.67, 139.60, 137.37, 136.40, 136.35 (C_q), 135.59, 135.56 (C_7), 132.82 (C_1), 131.31, 131.27 (C_{17} – C_{20}, C_{33} – C_{36}), 131.11 (C_2), 131.07, 130.76, 130.61 (C_{17} – C_{20}, C_{33} – C_{36}), 129.79, 129.48 (C_b, C_k), 129.25, 129.22 (C_6), 127.64, 127.56, 127.41, 127.33 (C_{17} – C_{20}, C_{33} – C_{36}), 125.37 (C_4), 124.78, 124.74, 124.71 (C_8), 124.09, 124.05, 123.83, 123.78, 123.70, 123.55, 123.49, 123.35, 123.33, 123.29 (C_3, C_{13}, C_{14}, C_{23}, C_{24}, C_{29}, C_{30}), 122.06, 122.05 (C_5), 67.16 (C_g), 36.03 (C_c, C_l), 33.99, 33.90 (C_d, C_m), 29.69, 29.37, 29.32, 28.93 (C_e, C_f, C_h, C_i). DOSY (600 MHz, CD_3CN) D = 4.06 x 10^{-10} m^2/s, hydrodynamic radius = 14.6 Å. HRESI-MS: m/z = 1392.0643 $[M\text{-}4PF_6]^{4+}$ (calcd. for $C_{276}H_{224}F_{36}Ir_2N_{32}O_4P_6Zn_4$ 1392.0647).

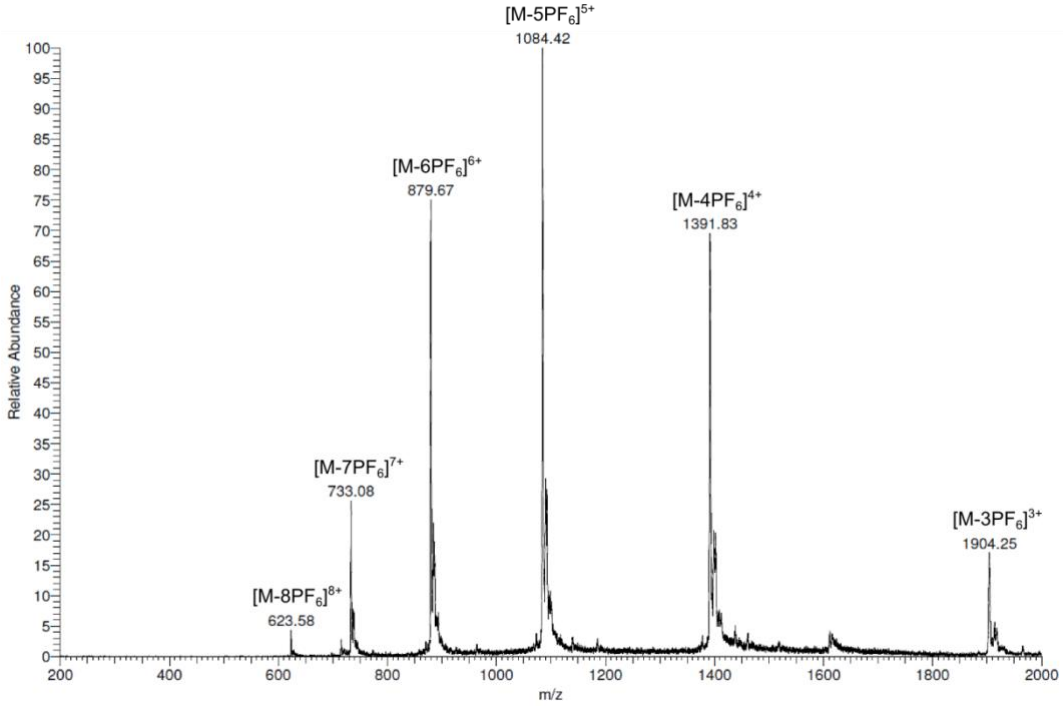

Figure S19. Low-resolution ESI-MS of *rac*-**8**. Calculated peaks (m/z): 1902.08 $[M–3PF_6]^{3+}$; 1390.32 $[M–4PF_6]^{4+}$; 1083.26 $[M–5PF_6]^{5+}$; 878.56 $[M–6PF_6]^{6+}$; 732.34 $[M–7PF_6]^{7+}$; 622.68 $[M–8PF_6]^{8+}$.

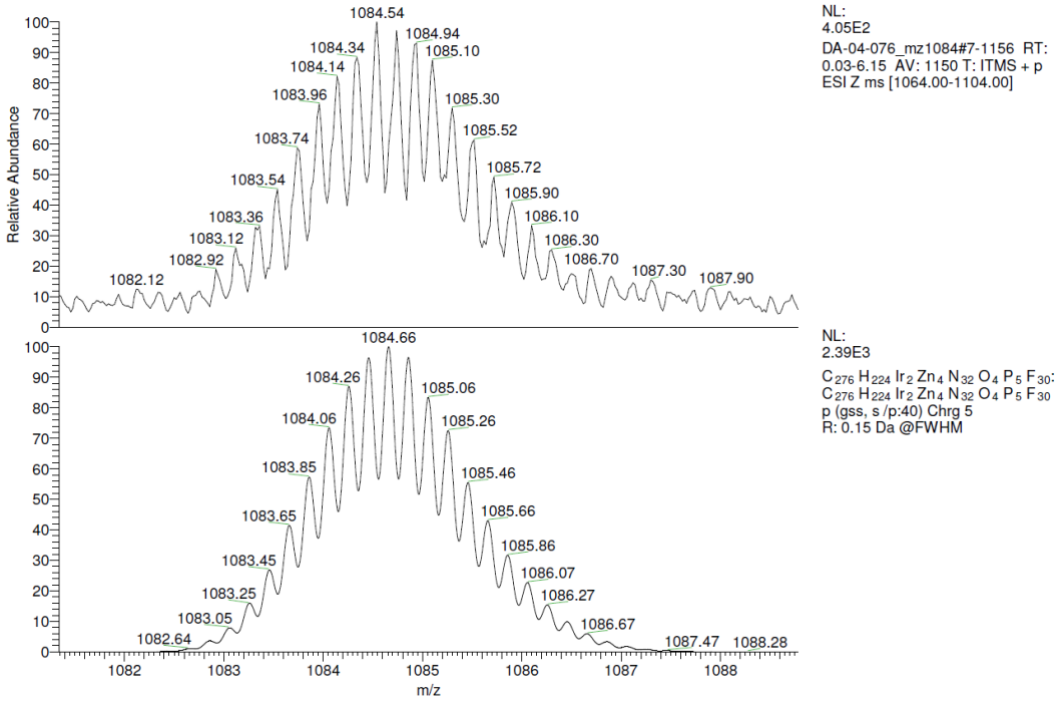

Figure S20. Low-resolution ESI-MS of the $[M-5PF_6]^{5+}$ peak of *rac*-**8**. Experimental spectrum (top, observed m/z 1084.54) and calculated spectrum (bottom, theoretical m/z 1084.66).

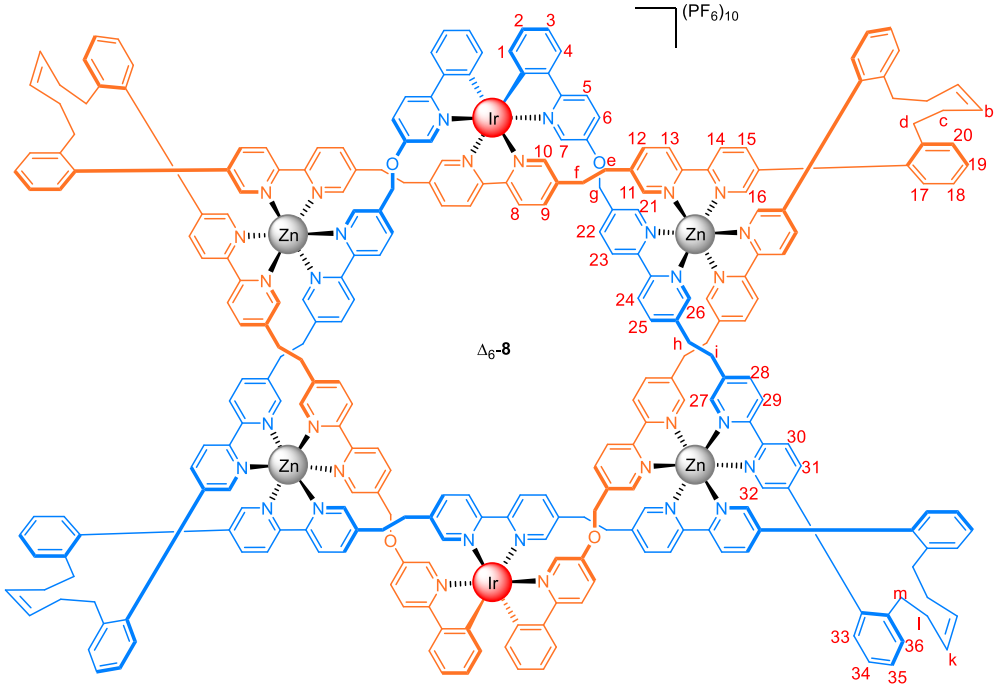

Compound Δ_6-**7** (46 mg, 7.4 µmol) and Hoveyda-Grubbs 2nd generation catalyst (3.7 mg, 5.9 µmol, 0.80 equiv.) were placed in a sealed vial and dissolved in degassed anhydrous 1, 2-dichloroethane (4 mL) and nitromethane (4 mL). The mixture was stirred at 60 °C for 24 h. After allowing the mixture to cool down, ethyl vinyl ether (4 mL) was added and the mixture was stirred for 30 minutes before removing the solvents. The solid residue was sonicated in chloroform (25 mL) and filtered on Celite®, then washed with excess chloroform and taken into acetonitrile. A saturated potassium hexafluorophosphate solution in methanol was added until a precipitate formed. The solid was then filtered on Celite®, washed with excess water, methanol and chloroform, and taken into acetonitrile. The solvent was removed to afford 22 mg of Δ_6-**8** (48% Yield). ^{1}H NMR (600 MHz, CD_3CN) δ 9.06 – 8.78 (br, 12H, H_8, H_{23}, H_{24}), 8.77 – 8.66 (m, 8H, H_{14}, H_{30}), 8.48 – 8.36 (m, 8H, H_{15}, H_{31}), 8.34 – 8.24 (m, 4H, H_{29}), 8.20 – 8.11 (m, 4H, H_{13}), 8.00 (d, *J* = 9.1 Hz, 4H, H_5), 7.93 (d, *J* = 7.9 Hz, 4H, H_4), 7.84 – 7.59 (m, 20H, H_9, H_{16}, H_{22}, H_{25}, H_{32}), 7.57 – 7.16 (m, 52H, H_3, H_{10}, H_{17} – H_{20}, H_{21}, H_{26}, H_{28}, H_{33} – H_{36}), 7.12 – 7.03 (m, 4H, H_{12}), 7.01 – 6.79 (m, 16H, H_2, H_6, H_{11}, H_{27}), 6.32 (s, 4H, H_7), 6.16 (s, 4H, H_1), 5.30 (d, *J* = 15.8 Hz, 4H, H_g), 4.89/4.59 (s, 8H, H_b, H_k), 4.81 (dd, *J* = 15.6, 4.5 Hz, 4H, $H_{g'}$), 3.20 – 2.48 (m, 32H, H_e, H_f, H_h, H_i), 2.46 – 2.29/1.61 – 1.29 (m, 16H, H_d, H_m), 1.90 – 1.62 (m, 16H, H_c, H_l). DEPTQ (151 MHz, CD_3CN) δ 162.41 (C_5-C-N), 152.65, 152.62, 152.60, 152.55 (C_8-C-N), 151.95, 151.93 (C_{10}), 151.79, 151.77 (C_6-C-C_7), 149.52 (C_1-C-Ir), 149.36, 149.16, 149.07 (C_{16}, C_{32}), 148.44, 148.40 (C_{26}), 147.79, 147.74, 147.71, 147.65 (C_{10}, C_{11}, C_{21}, C_{27}), 147.47, 147.44, 147.06, 147.03, 147.02, 145.83, 145.78, 145.72 (C_q), 144.86, 144.80, 144.47 (C_{15}, C_{31}), 144.11 (C_q), 143.41, 143.39, 143.35, 143.28, 143.23, 143.19, 143.14, 143.06 (C_{12}, C_{25}), 142.71 (C_q), 142.65, 142.43, 142.40 (C_{28}), 142.22 (C_q), 141.48 (C_{22}), 141.16, 141.14, 141.04, 141.01, 140.80, 140.77 (C_q), 140.69, 140.67 (C_9), 140.30, 140.28, 139.86, 139.82, 139.63, 139.60, 139.55, 137.36, 137.30, 137.26, 136.38, 136.35, 136.31 (C_q), 135.58, 135.56, 135.53 (C_7), 132.77 (C_1), 131.29, 131.26 (C_{17} – C_{20}, C_{33} – C_{36}), 131.08 (C_2), 131.01, 130.97, 130.75, 130.62, 130.56 (C_{17} – C_{20}, C_{33} – C_{36}), 129.76, 129.74, 129.44 (C_b, C_k), 129.20, 129.18 (C_6), 127.62, 127.54, 127.39, 127.30 (C_{17} – C_{20}, C_{33} – C_{36}), 125.34 (C_4), 124.08, 124.06, 124.01, 123.80, 123.77, 123.75, 123.67, 123.56, 123.49, 123.44 (C_3, C_{13}, C_{14}, C_{23}, C_{24}, C_{29}, C_{30}), 122.02, 121.99 (C_5), 67.14 (C_g), 36.02 (C_c, C_l), 33.97, 33.92, 33.86 (C_d, C_m), 29.60, 29.34, 29.30, 29.20, 28.92, 28.86 (C_e, C_f, C_h, C_i). C_8 was not observed. HRESI-MS: m/z = 1392.0628 $[M\text{-}4PF_6]^{4+}$ (calcd. for $C_{276}H_{224}F_{36}Ir_2N_{32}O_4P_6Zn_4$ 1392.0647).

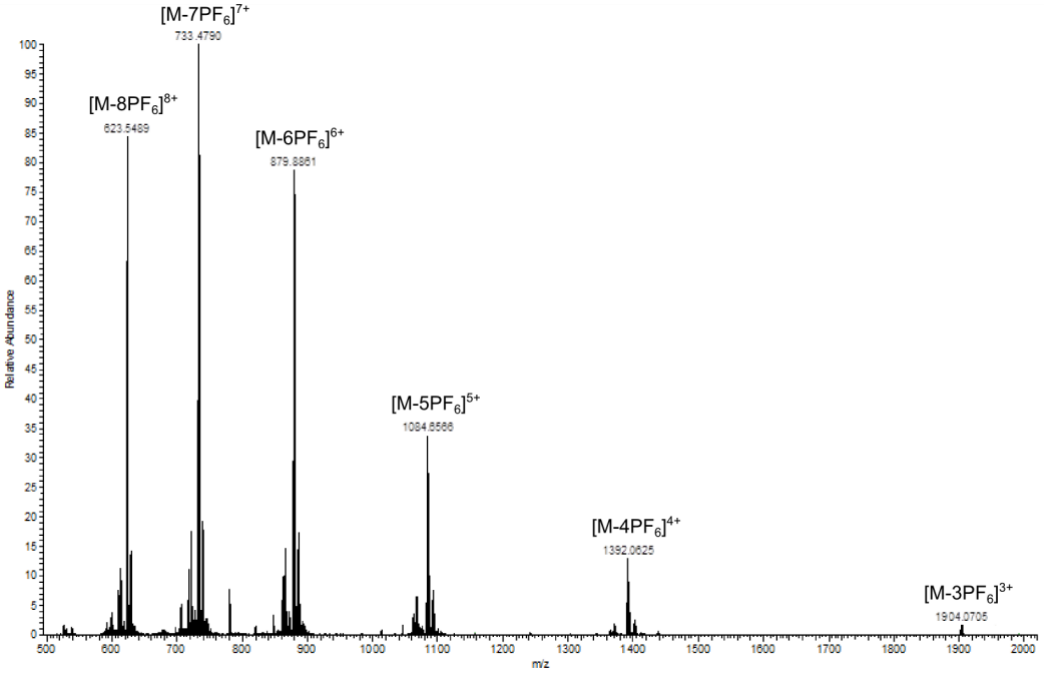

Figure S21. High-resolution ESI-MS of Δ_6-**8**. Calculated peaks (m/z): 1902.08 $[M–3PF_6]^{3+}$; 1390.32 $[M–4PF_6]^{4+}$; 1083.26 $[M–5PF_6]^{5+}$; 878.56 $[M–6PF_6]^{6+}$; 732.34 $[M–7PF_6]^{7+}$; 622.68 $[M–8PF_6]^{8+}$.

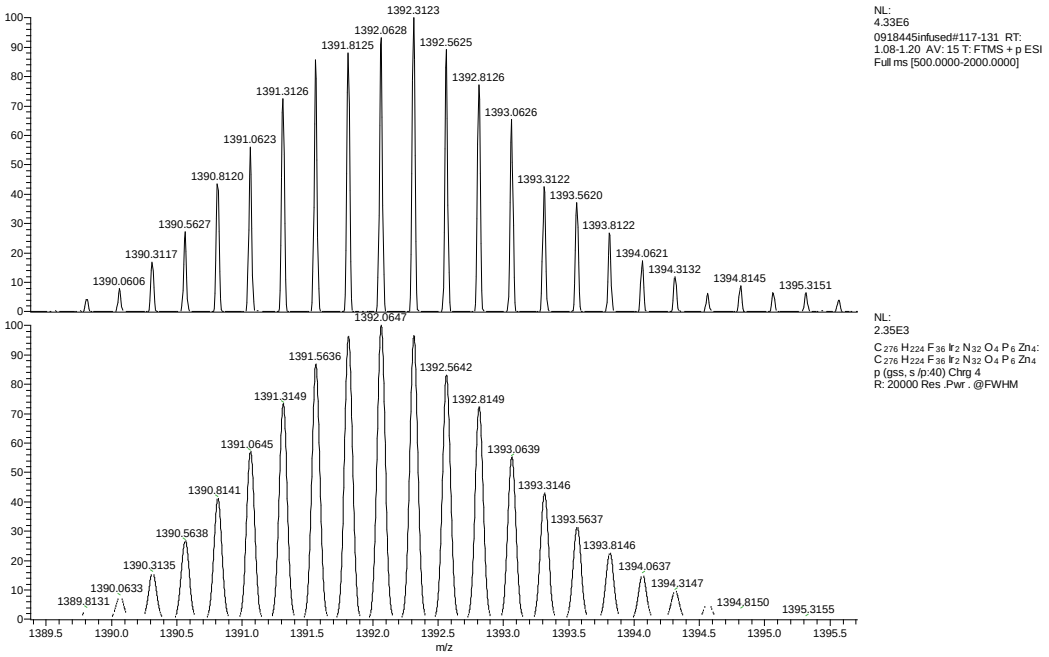

Figure S22. High-resolution ESI-MS of the $[M\text{-}4PF_6]^{4+}$ peak of Δ_6-**8**. Experimental spectrum (top, observed m/z 1392.0628) and calculated spectrum (bottom, theoretical m/z 1392.0647).

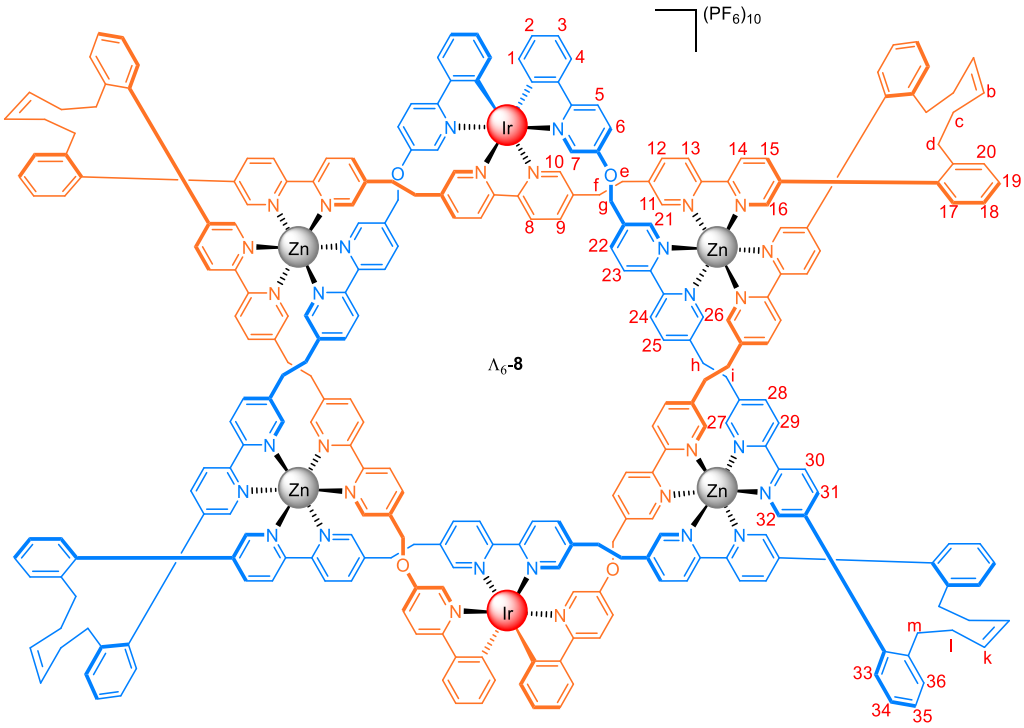

Compound Λ_6-**7** (51 mg, 8.2 µmol) and Hoveyda-Grubbs 2nd generation catalyst (4.1 mg, 6.5 µmol, 0.80 equiv.) were placed in a sealed vial and dissolved in degassed anhydrous 1, 2-dichloroethane (4 mL) and nitromethane (4 mL). The mixture was stirred at 60 °C for 24 h. After allowing the mixture to cool down, ethyl vinyl ether (4 mL) was added and the mixture was stirred for 30 minutes before removing the solvents. The solid residue was sonicated in chloroform (25 mL) and filtered on Celite®, then washed with excess chloroform and taken into acetonitrile. A saturated potassium hexafluorophosphate solution in methanol was added until a precipitate formed. The solid was then filtered on Celite®, washed with excess water, methanol and chloroform, and taken into acetonitrile. The solvent was removed to afford 22 mg of Λ_6-**8** (44% Yield). ^{1}H NMR (600 MHz, CD_3CN) δ 8.94 – 8.78 (br, 12H, H_8, H_{23}, H_{24}), 8.77 – 8.66 (m, 8H, H_{14}, H_{30}), 8.47 – 8.36 (m, 8H, H_{15}, H_{31}), 8.34 – 8.25 (m, 4H, H_{29}), 8.21 – 8.12 (m, 4H, H_{13}), 8.00 (d, J = 9.1 Hz, 4H, H_5), 7.93 (d, J = 7.9 Hz, 4H, H_4), 7.84 – 7.58 (m, 20H, H_9, H_{16}, H_{22}, H_{25}, H_{32}), 7.56 – 7.16 (m, 52H, H_3, H_{10}, H_{17} – H_{20}, H_{21}, H_{26}, H_{28}, H_{33} – H_{36}), 7.12 – 7.02 (m, 4H, H_{12}), 7.01 – 6.79 (m, 16H, H_2, H_6, H_{11}, H_{27}), 6.33 (s, 4H, H_7), 6.16 (s, 4H, H_1), 5.33 – 5.24 (m, 4H, H_g), 4.90/4.59 (s, 8H, H_b, H_k), 4.85 – 4.77 (m, 4H, $H_{g'}$), 3.19 – 2.48 (m, 32H, H_e, H_f, H_h, H_i), 2.47 – 2.24/1.61 – 1.24 (m, 16H, H_d, H_m), 1.88 – 1.62 (m, 16H, H_c, H_l). DEPTQ (151 MHz, CD_3CN) δ 162.41 (C_5-C-N), 152.54, 152.51 (C_8-C-N), 151.98, 151.95 (C_{10}), 151.83, 151.79 (C_6-C-C_7), 149.52 (C_1-C-Ir), 149.38, 149.20, 149.18, 149.12 (C_{16}, C_{32}), 148.49, 148.46, 148.44 (C_{26}), 147.76, 147.74, 147.67, 147.62, 147.44 (C_{10}, C_{11}, C_{21}, C_{27}), 147.42, 147.36, 147.10, 147.06, 147.03, 145.70, 145.66 (C_q), 144.88, 144.80, 144.48, 144.44 (C_{15}, C_{31}), 144.12 (C_q), 143.32, 143.23, 143.15, 143.12, 143.01 (C_{12}, C_{25}), 142.71, 142.61, 142.59 (C_q), 142.36 (C_{28}), 142.22 (C_q), 141.42 (C_{22}), 141.14, 140.82, 140.77, 140.62, 140.59 (C_q), 140.32 (C_9), 139.86, 139.81, 139.64, 139.58, 137.36, 136.37, 136.33 (C_q), 135.56, 135.52 (C_7), 132.81, 132.79 (C_1), 131.30, 131.26 (C_{17} – C_{20}, C_{33} – C_{36}), 131.08 (C_2), 131.04, 130.99, 130.77, 130.74, 130.65, 130.63, 130.58 (C_{17} – C_{20}, C_{33} – C_{36}), 129.77, 129.74, 129.45 (C_b, C_k), 129.22, 129.19 (C_6), 127.61, 127.54, 127.38, 127.30 (C_{17} – C_{20}, C_{33} – C_{36}), 125.35 (C_4), 124.63, 124.59, 124.53 (C_8), 124.06, 124.03, 123.80, 123.68, 123.53, 123.48, 123.42, 123.15, 123.11 (C_3, C_{13}, C_{14}, C_{23}, C_{24}, C_{29}, C_{30}), 122.04, 122.01 (C_5), 67.12 (C_g), 36.02 (C_c, C_l), 33.97, 33.94, 33.88 (C_d, C_m), 29.70, 29.65, 29.34, 29.30, 29.20, 28.94, 28.88 (C_e, C_f, C_h, C_i). HRESI-MS: m/z = 1392.0643 $[M\text{-}4PF_6]^{4+}$ (calcd. for $C_{276}H_{224}F_{36}Ir_2N_{32}O_4P_6Zn_4$ 1392.0647).

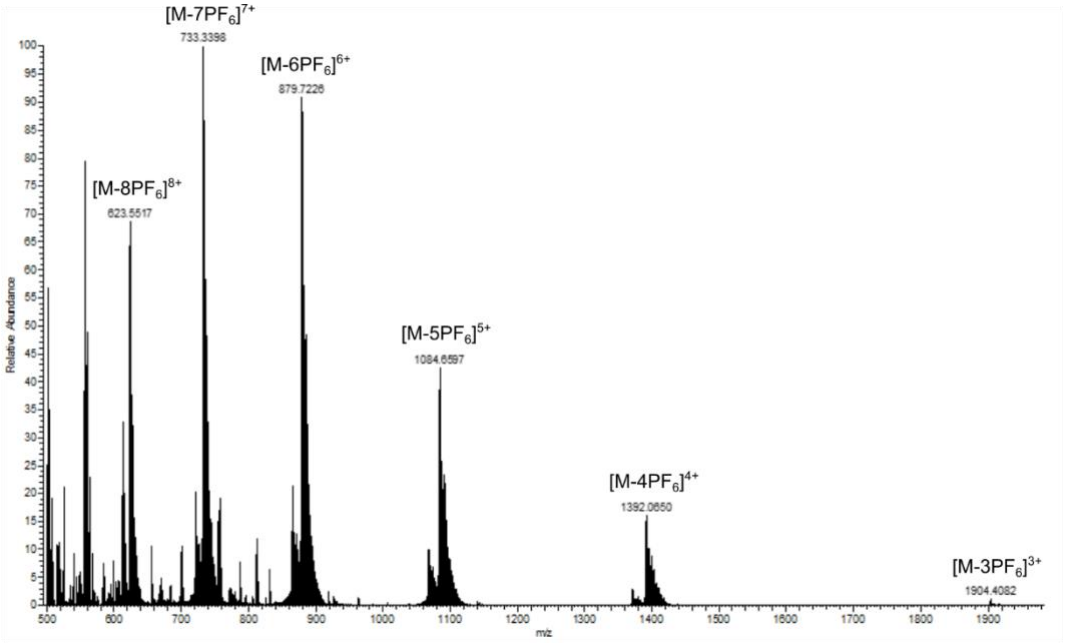

Figure S23. High-resolution ESI-MS of Λ_6-**8**. Calculated peaks (m/z): 1902.08 $[M–3PF_6]^{3+}$; 1390.32 $[M–4PF_6]^{4+}$; 1083.26 $[M–5PF_6]^{5+}$; 878.56 $[M–6PF_6]^{6+}$; 732.34 $[M–7PF_6]^{7+}$; 622.68 $[M–8PF_6]^{8+}$.

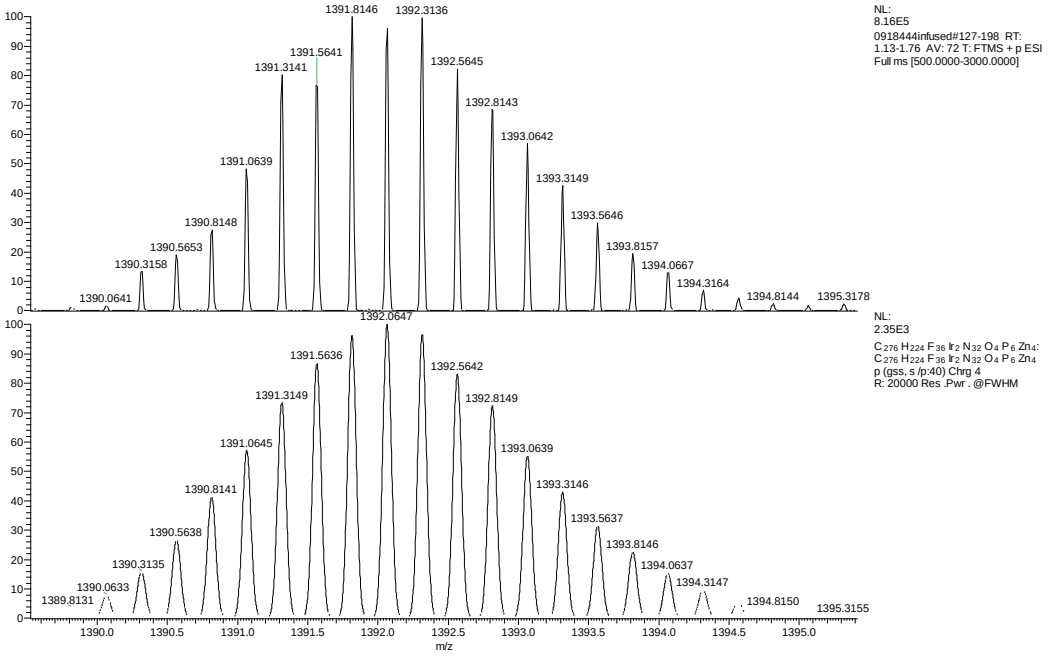

Figure S24. High-resolution ESI-MS of the $[M-4PF_6]^{4+}$ peak of Λ_6-**8**. Experimental spectrum (top, observed m/z 1392.0643) and calculated spectrum (bottom, theoretical m/z 1392.0647).

3.6 Synthesis of an Iridium Star of David [2]Catenane

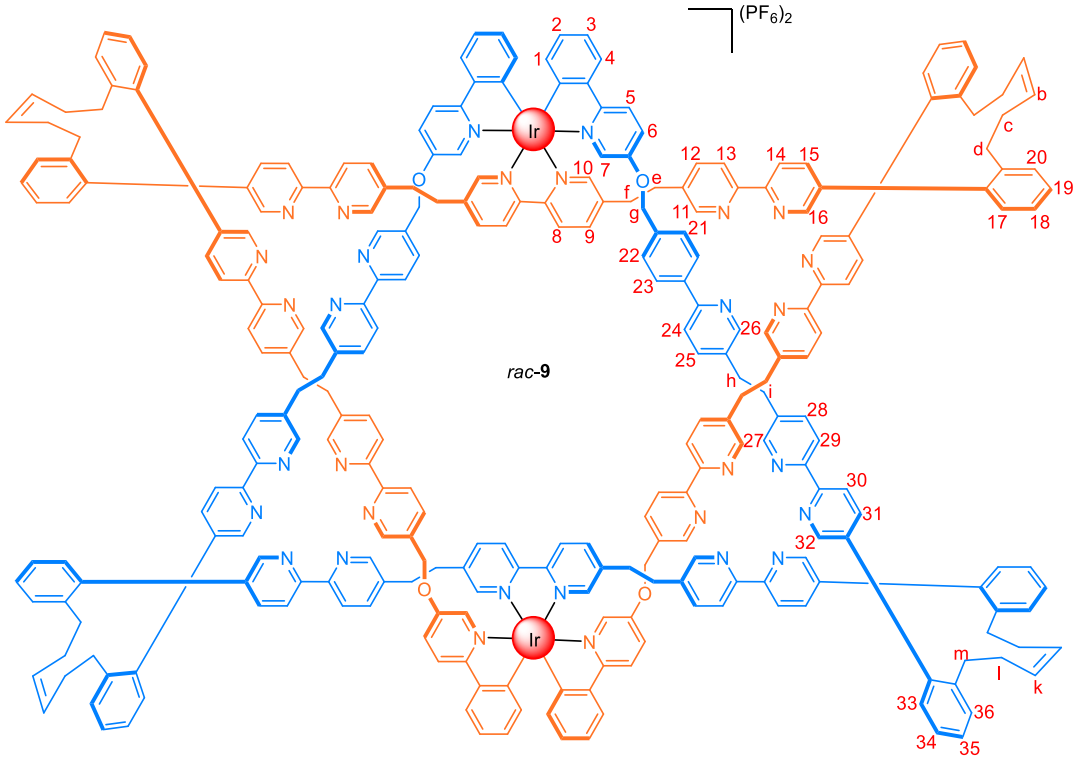

Compound *rac*-**8** (12.2 mg, 2.0 µmol) was dissolved in acetonitrile (1 mL). Li_2S (excess, 250 eq. 22.845 mg) was added and the mixture stirred at room temperature for 10 mins. The mixture was diluted with chloroform (10 mL) and water (10 mL) and heated for 30 mins at 60 °C. The organic layer was separated and extracted with water and brine. The organics were combined, dried over $MgSO_4$ and the solvent was removed under vacuum to yield *rac*-**9** as a bright orange solid (3.8 mg, 41%). DOSY (600 MHz, $CDCl_3$) D = 3.47 x 10^{-10} m^2/s, hydrodynamic radius = 11.7 Å. HRESI-MS: m/z = 2218.3913 $[M-2PF_6]^{2+}$ (calcd. for $C_{276}H_{224}F_{60}Ir_2N_{32}O_4P_{10}Zn_4$ 2218.3817).

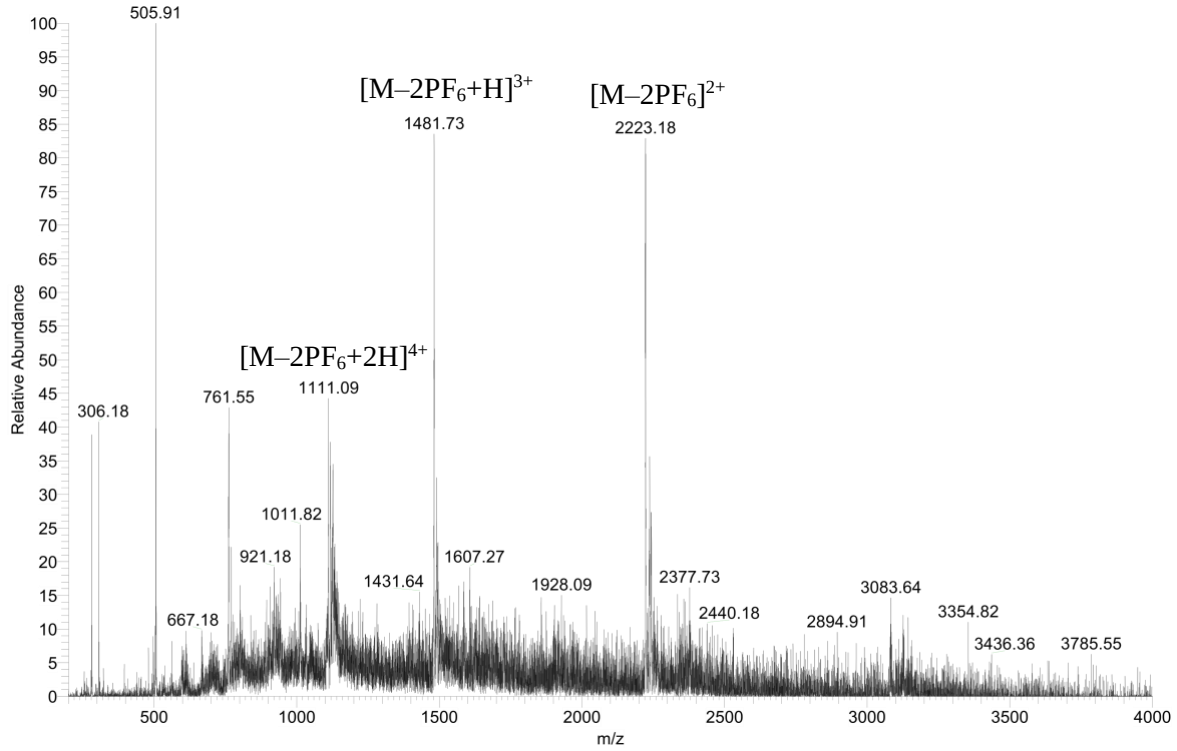

Figure S25. Low-resolution ESI-MS of *rac*-**9**. Calculated peaks (m/z): 2218.39 $[M–2PF_6]^{2+}$; 1479.26 $[M–2PF_6+H]^{3+}$; 1109.70 $[M–2PF_6+2H]^{4+}$.

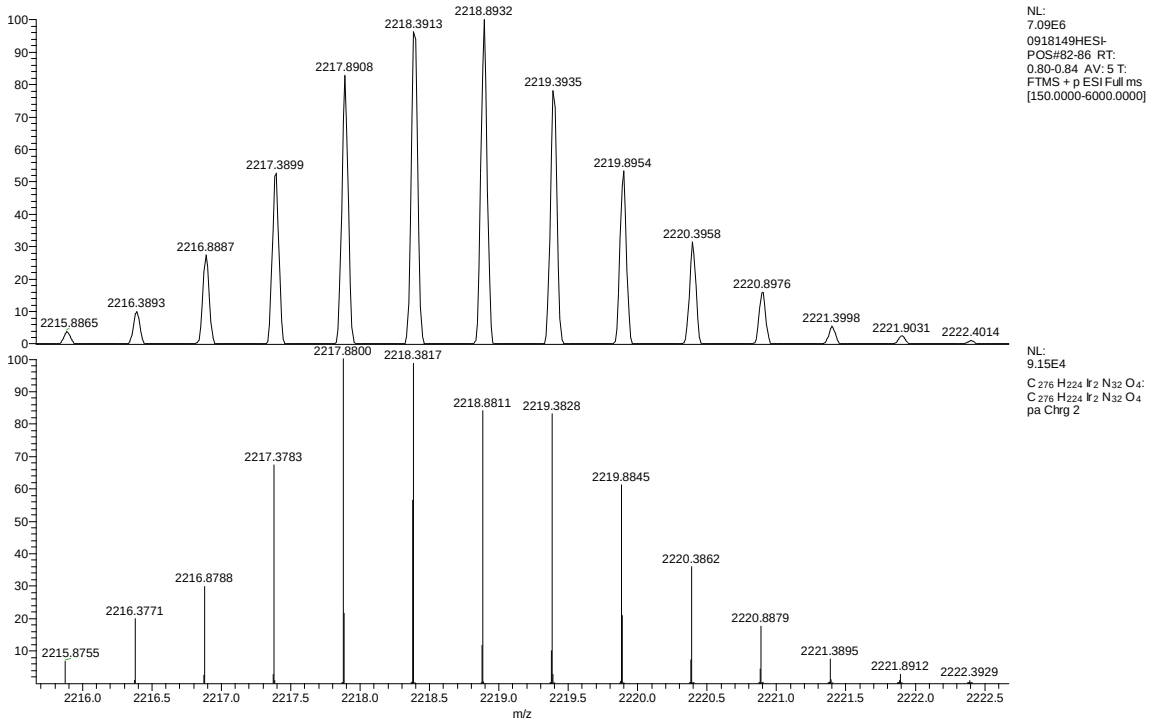

Figure S26. High-resolution ESI-MS of the $[M\text{-}2PF_6]^{2+}$ peak of *rac*-**9**. Experimental spectrum (top, observed m/z 2218.8932) and calculated spectrum (bottom, theoretical m/z 2218.3817).

4. Considerations on Regioisomer Formation and Purification

4.1 Regioisomer removal via helicate formation

Due to the incomplete bias towards the central bipyridine coordination unit in the ancillary ligand introduction step, complex **3** is obtained as a mixture of products. Unfortunately, size exclusion chromatography was unable to fully separate all the formed by-products and one impurity remains (Figure S27a). The complexity and similarity of the different species hampered the NMR analysis of the mixture. Nonetheless, considering that ESI-MS of the product mixture affords a single set of peaks corresponding to the expected **3** (Figures S1, S3 and S5), the remaining impurity was attributed to an inseparable regioisomer of the product **S7** (Figure S28). This unwanted regioisomer should, however, be unable to undergo circular helicate formation. Indeed, while the impurity is still present in the following product **6** (Figure S27b), it can be completely removed based on solubility after circular helicate formation to afford pure helicate **7** (Figure S27c).

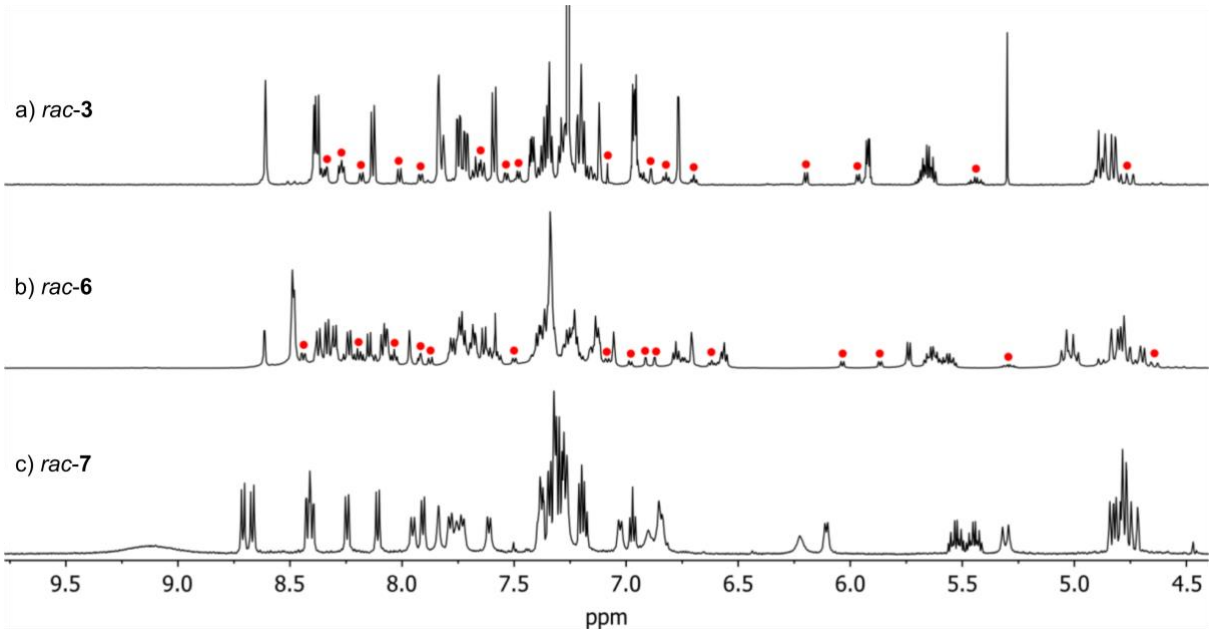

Figure S27. ^{1}H NMR (600 MHz, 298 K) spectra of a) *rac*-**3** after size exclusion chromatography ($CDCl_3$); b) *rac*-**6** after size exclusion chromatography (CD_3CN); c) pure *rac*-**7** (CD_3CN). The peaks corresponding to the unwanted regioisomer are labelled with red circles.

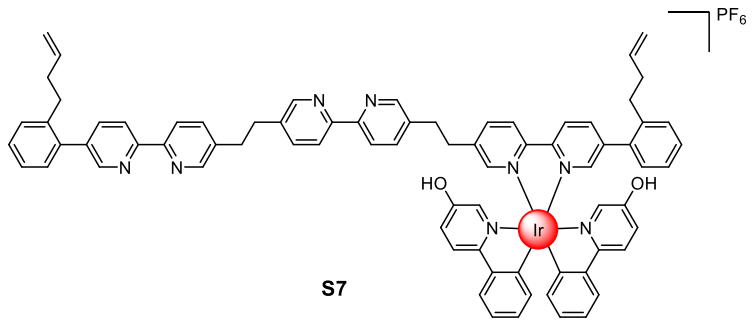

S7

Figure S28. Likely additional regioisomer formed during the synthesis of **3**.

4.2 Purification of *rac*-6 via demetallation of *rac*-7

Since the synthesis involves carrying through the unwanted regioisomer **S7** before removal after helicate formation, compound **6** is usually obtained as a mixture of regioisomers. To allow accurate comparison of the photophysical properties, a sample of *rac*-**6** without the unwanted regioisomer was prepared by removal of Zn(II) from the purified open helicate *rac*-**7** using the Li_2S conditions employed for removal of Zn(II) from the closed helicate **8**.

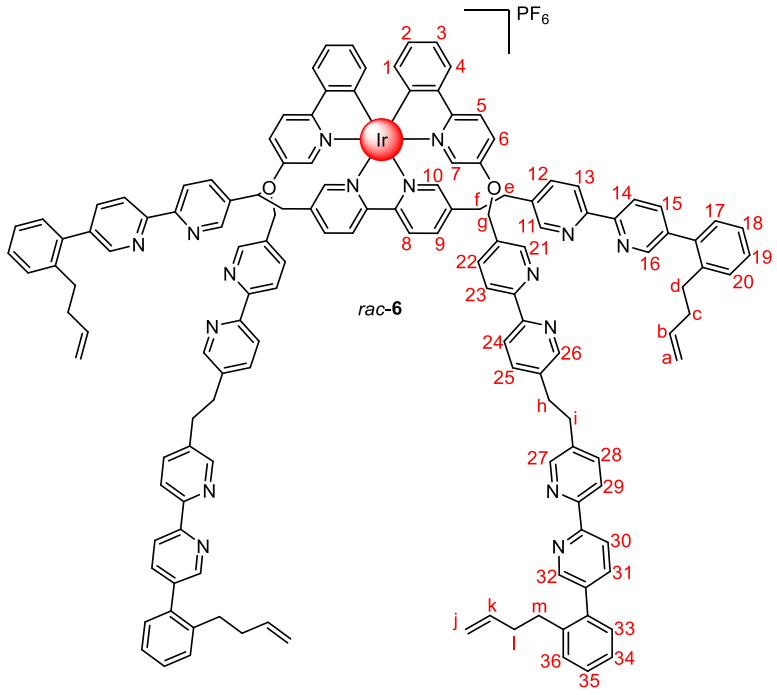

Compound *rac*-**7** (4.8 mg, 0.77 µmol) was dissolved in dry acetonitrile (0.5 mL) under N_2. Excess Li_2S was added and the mixture stirred at room temperature for 5 mins. CH_2Cl_2 (10 mL) and water (10 mL) were added and stirred at room temperature for 16 hours. The organic layer was separated and washed with water (3 x 20 mL) and brine (20 mL). The combined organics were dried over $MgSO_4$, filtered and the solvent removed under vacuum to give pure *rac*-**6** as a bright yellow solid (3.3 mg, 89%). ^{1}H NMR (600 MHz, CD_3CN) δ 8.62 (dd, J = 2.3, 0.9 Hz, 2H, H_{16} or H_{32}), 8.52 – 8.50 (m, 4H, H_{11}, H_{27}), 8.49 (dd, J = 2.3, 0.8 Hz, 2H, H_{16} or H_{32}), 8.38 (dd, J = 8.1, 0.9 Hz, 2H, H_{14} or H_{30}), 8.37 – 8.33 (m, 2H, H_{13} or H_{29}), 8.33 – 8.29 (m, 2H, H_{14} or H_{30}), 8.27 – 8.23 (m, 2H, H_{13} or H_{29}), 8.17 – 8.14 (m, 2H, H_8), 8.11 – 8.08 (m, 2H, H_{23}), 8.07 (d, J = 2.2 Hz, 2H, H_{26}), 8.00 – 7.95 (m, 2H, H_{10}), 7.79 (dd, J = 8.1, 2.3 Hz, 2H, H_{15} or H_{31}), 7.78 – 7.74 (m, 4H, H_{12}, H_{28}), 7.73 (d, J = 8.4 Hz, 2H, H_{24}), 7.69 (dd, J = 8.1, 2.3 Hz, 2H, H_{15} or H_{31}), 7.65 (d, J = 9.1 Hz, 2H, H_5), 7.43 – 7.12 (m, 28H, H_4, H_6, H_9, $H_{17\text{-}20}$, H_{22}, H_{25}, $H_{33\text{-}36}$), 7.06 (d, J = 2.0 Hz, 2H, H_{21}), 6.79 (app td, J = 7.5, 1.2 Hz, 2H, H_3), 6.71 (d, J = 2.7 Hz, 2H, H_7), 6.58 (td, J = 7.4, 1.3 Hz, 2H, H_2), 5.75 (dd, J = 7.6, 1.2 Hz, 2H, H_1), 5.69 – 5.53 (m, 4H, H_b, H_k), 5.09 – 4.97 (m, 4H, H_g, $H_{g'}$), 4.87 – 4.68 (m, 8H, H_a, H_j), 3.21 – 3.12 (m, 8H, H_e, H_i), 2.82 – 2.60 (m, 16H, H_d, H_f, H_h, H_m), 2.13 – 2.08 (m, 8H, H_c, H_l). Despite extensive use of additional 2D and NOE NMR techniques, it was not possible to distinguish between the H_{14}/H_{15}/H_{16} and H_{30}/H_{31}/H_{32} and the H_{11}/H_{12}/H_{13} and H_{27}/H_{28}/H_{29} pyridine ring systems.^{13}C NMR (151 MHz, CD_3CN) δ 161.73, 156.43, 155.31, 155.25, 154.64, 154.45, 154.29, 153.82, 153.67, 150.92, 150.81, 150.69, 150.19, 150.16, 150.03, 149.08, 148.78, 144.24, 141.81, 140.55, 140.52, 139.96, 138.86, 138.82, 138.77, 138.74, 138.49, 138.39, 138.36, 138.34, 138.22, 138.11, 137.74, 137.46, 136.95, 136.43, 136.05, 132.08, 131.85, 131.01,

130.97, 130.67, 130.59, 130.37, 129.27, 129.22, 127.96, 127.17, 127.11, 125.19, 124.81, 123.03, 121.57, 121.28, 121.28, 121.23, 121.12, 120.67, 120.61, 115.44, 115.40, 68.93, 35.84, 35.80, 34.39, 34.22, 33.85, 33.22, 33.17, 33.03. Despite extensive use of 2D experiments (e.g HSQC and HMBC) one of the carbon signals still remains unaccounted for - presumably due to overlap with either the solvent peak or another ^{13}C signal. However, this is unsurprising due to the complexity of the spectrum. DOSY (600 MHz, CD_3CN*)* D = 5.73 x 10^{-10} m^2/s, hydrodynamic radius = 10.3 Å. DOSY (600 MHz, $CDCl_3$*)* D = 3.52 x 10^{-10} m^2/s, hydrodynamic radius = 11.5 Å. HRESI-MS: m/z = 2274.9347 $[M\text{-}PF_6]^+$ (calcd. for $C_{142}H_{120}IrN_{16}O_2$ 2274.9447), 1137.9755 $[M\text{-}PF_6+H]^{2+}$ (calcd. for $C_{142}H_{121}IrN_{16}O_2$ 1137.9720).

5. Variable Temperature NMR

Variable temperature ^{1}H NMR was performed on *rac*-**9** in an attempt to resolve some of the proton signals to aid assignment and analysis. However, whilst a slight sharpening of the signals occurred at high temperatures, the spectrum remained too complex and broad to fully assign. The Ir(III) linked Star of David catenane has numerous similar, yet chemically distinct, pyridine environments.

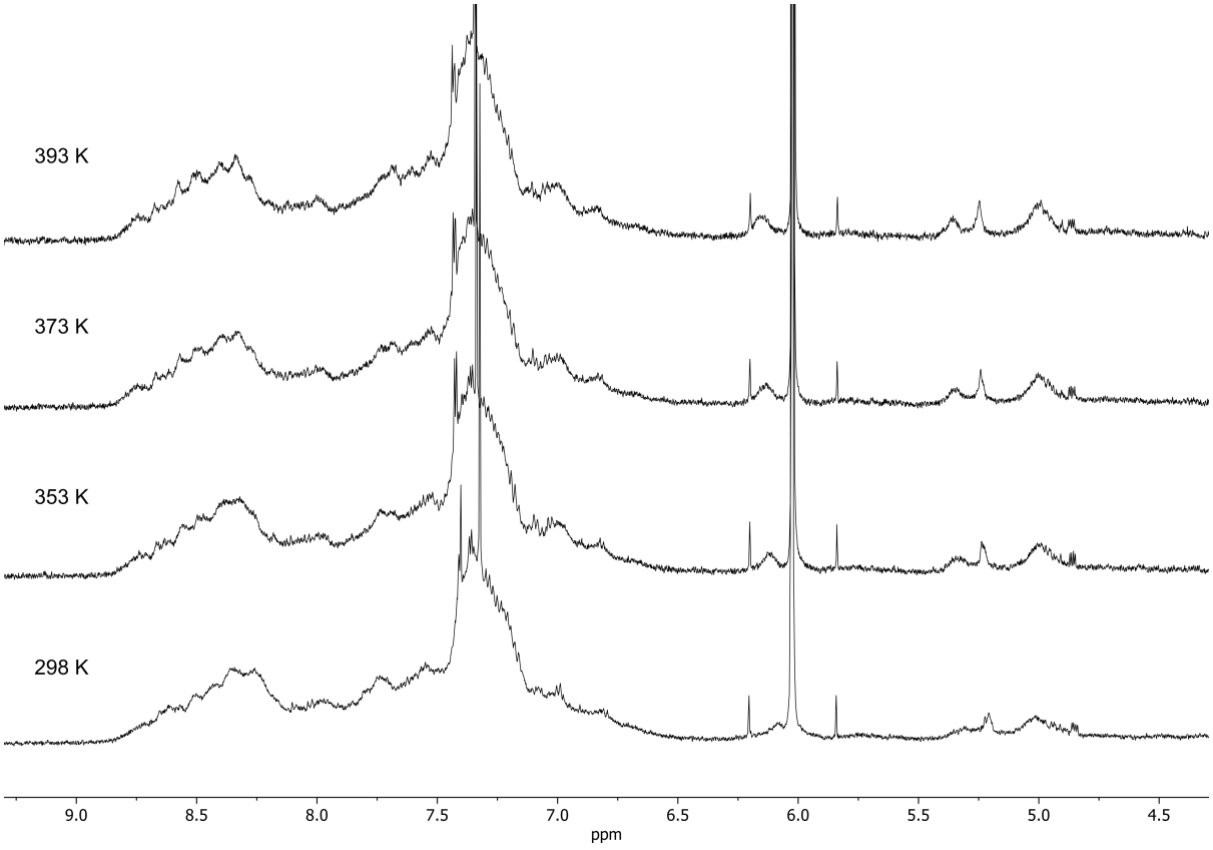

Figure S29. ^{1}H NMR (500 MHz, 1,1,2,2-tetrachloroethane-d_2) spectra of *rac*-**9** at temperatures ranging from 298 K to 398 K.

6. Photophysical Studies

All of the absorption and emission measurements were carried out using either a Cary Eclipse Fluorescence spectrometer or a Cary 50 Bio UV/Visible Varian Spectrophotometer under an air atmosphere. All of the samples were measured in quartz cuvettes with a pathlength of 1 cm. Each sample was dissolved in spectrophotometric grade solvents (acetonitrile for **6**, **7**, **8** and dichloromethane for **9**). All slits were set to 10 nm. For the emission spectra, the emission filter was set to 430-1100 nm to prevent any additional peaks as a result of 2nd order diffraction.

Quantum yields were calculated using $[Ru(bpy_3)](PF_6)_2$ as an external standard due to its similar absorption/emission profile and photophysics.[S4] Emission spectra were recorded with an excitation wavelength of 400 nm as this provided the best overlap between the different species and the external standard. For every sample, the emission peak was integrated using OriginPro 2017 software and plotted versus the corresponding absorbance. In order to minimize inner filter effects, this was repeated for each compound at five different concentrations (5, 10, 15, 20 and 25 µM) such that the absorption ideally varied between 0.01 and 0.2 at a wavelength of 400 nm. A linear fit was then applied to each series and the gradient used to compare the quantum yield via a reference method with the reported values for $[Ru(bpy_3)](PF_6)_2$.

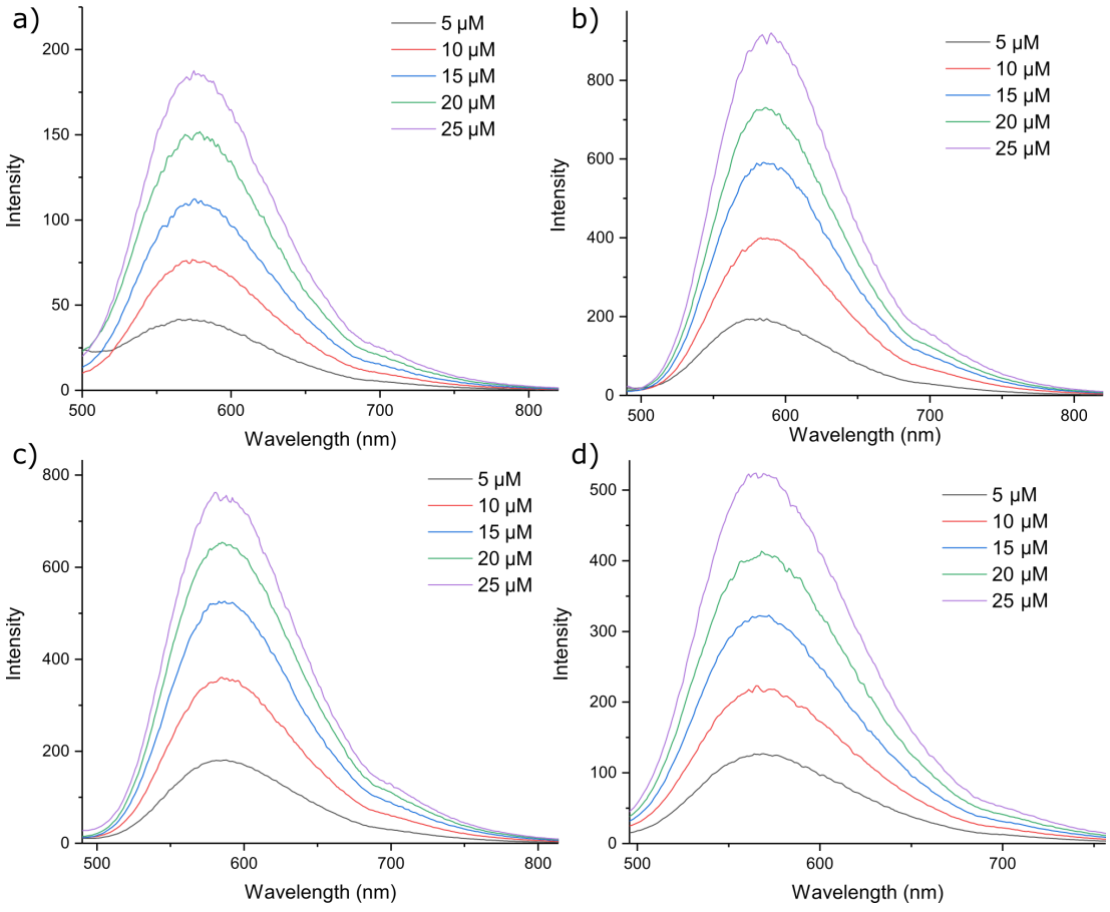

Figure S30. Emmission spectra for compounds a) **6** b) **7** c) **8** (in acetonitrile) and d) **9** (in dichloromethane) at five different concentrations (5, 10, 15, 20, 25 µM) obtained with an excitation wavelength of 400 nm.

Table S1. List of calculated peak areas from the emission spectra and the corresponding absorbance at a wavelength of 400 nm.

Compound	$Ru(bpy)_3(PF_6)_2$[a]		**6**[a]		**7**[a]		**8**[a]		**9**[b]	
Conc. (μM)	**Abs**	**Peak Area**	**Abs**	**Peak Area**	**Abs**	**Peak Area**	**Abs**	**Peak Area**	**Abs**	**Peak Area**
5	0.0294	2959.05	0.0151	1693.3	0.0280	18874.4	0.0507	18756.3	0.0141	11710.4
10	0.0620	6521.73	0.0288	6969.41	0.0555	43172.0	0.0998	38482.5	0.0310	20991.1
15	0.0962	9056.75	0.0444	10466.9	0.0847	65091.1	0.1455	57727.3	0.0500	31005.6
20	0.128	13027.3	0.0586	13539.9	0.1115	79702.5	0.1972	71926.6	0.0636	41541.1
25	0.1580	14998.2	0.0736	17783.2	0.1402	100394	n/a[c]	n/a[c]	0.0824	53214.4

a. in acetonitrile b. in dichloromethane c. at this concentration, the absorption was significantly above 0.2 and therefore not included in the data fitting due to significant inner filter effects

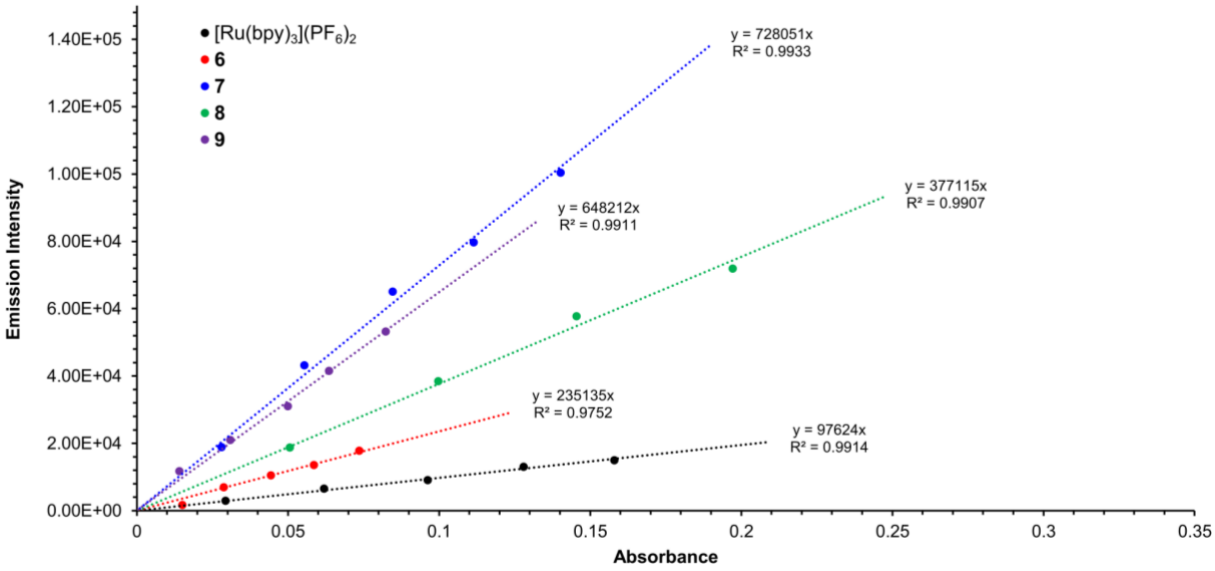

Figure S31. Plot of emission intensity versus absorbance for each of the compounds studied. The gradient of the straight line fits is proportional to the quantum yield.

Equation S1. General equation used to calculate quantum yield via a reference method

$$\frac{gradient\ of\ standard\ (ref)}{gradient\ of\ sample\ x} = \frac{quantum\ yield\ of\ standard\ (\Phi_{ref})}{quantum\ yield\ of\ x\ (\Phi_x)}$$

Table S2. Quantum yield (Φ_{PL}) calculations for the Ir(III) complex **6** and assembled helicates

Compound	**Solvent**	**Gradient**	Φ_{PL}	Φ_{PL} **(%)**
$[Ru(bpy)_3](PF_6)_2$	Acetonitrile	97624	0.018	1.8[S4]
rac-**6**	Acetonitrile	235235	0.043	4.3
rac-**7**	Acetonitrile	728051	0.134	13.4
rac-**8**	Acetonitrile	377115	0.070	7.0
rac-**9**	Dichloromethane	648212	0.120	12.0

All circular dichroism (CD) spectra were recorded on a J-815 Jasco spectrometer (Jasco France, Nantes, France). Spectra were acquired in spectrophotometric grade acetonitrile using a quartz cell with a path length of 2 mm.

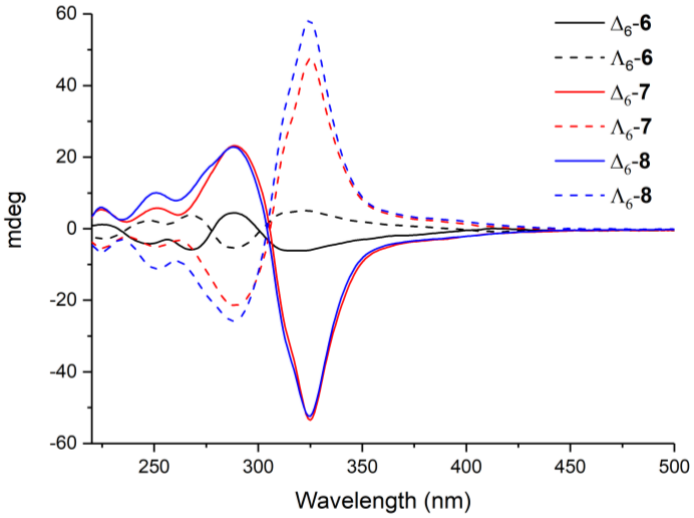

Figure S32. CD spectra (MeCN, 0.01 mM) of the enantiopure iridium species plotted in mdeg.

7. X-Ray Crystal Structures

Data Collection. X-Ray data for compound Δ_6-**8** and Λ_6-**8** were collected at a temperature of 100 K using a synchrotron radiation at single crystal X-ray diffraction beamline I19 in Diamond light Source,[S5] equipped with an Pilatus 2M detector and an Oxford Cryosystems Cobra nitrogen flow gas system. Data was measured using GDA suite of programs.

Crystal structure determinations and refinements. X-Ray data were processed and reduced using CrysAlisPro suite of programmes. Absorption correction was performed using empirical methods (SCALE3 ABSPACK) based upon symmetry-equivalent reflections combined with measurements at different azimuthal angles.[S6] The crystal structures were solved and refined against all F^2 values using the SHELX and Olex 2 suite of programmes.[S7] Despite the highly intense X-ray source, crystals of Δ_6-**8** and Λ_6-**8** present a diffraction limit of 1.25 Å. Only zinc, iridium, nitrogen and oxygen atoms were refined anisotropically. The rest of the atoms were refined isotropically due to a poor reflexions/parameters ratio. Hydrogen atoms were placed in the calculated positions. The phenyl and pyridyl groups were constrained to have idealized geometries using SHELX AFIX commands.

As consequence of the low resolution obtained, the model for crystal structures Δ_6-**8** and Λ_6-**8** were built on ill shaped electron density maps. The C-C and C-O 1,2 and 1,3 distances in the aliphatic chains were restrained using SHELX DFIX and SADI commands. No restraints were applied to force the configuration of the double bonds. The atomic displacement parameters (adp) of the ligands were restrained using SHELX RIGU and SIMU commands. The PF_6 anions were constrained to have the same structure using SHELX RESI command. The adps were also restrained using SIMU and RIGU commands.

Compounds Δ_6-**8** and Λ_6-**8** present large voids filled with a lot of scattered electron density. The solvent mask protocol inside Olex 2 software was used to account for the void electron density corresponding to the disordered solvent placed in the intermolecular space in the crystal structure. 463 and 451 electrons were accounted in a volume of 3454 and 3691 $Å^3$ for Δ_6-**8** and Λ_6-**8** crystals respectively. Both electron counts are compatible with 8 molecules of diisopropyl ether per unit cell.

A large number of A alerts were found in both crystal structures due to the poor resolution (1.25 Å) data obtained. Unfortunately, this resolution is common in big molecules with big intermolecular spaces filled with disordered anions and/or solvent molecules. As we can observe in Figure S32, the structural model was built on broad shaped electron density maps. As consequence the values of R1, wR and wR2 factors are larger than for standard crystal structures. Aliphatic chains were especially poorly resolved due to the most probable disorder of the group, having larger values of U_{ij} than the neighbouring atoms. Despite several attempts, the disorder of the aliphatic chains was not modelled.

CCDC 2035436-2035437 contains the supplementary crystallographic data for this paper. These data can be obtained free of charge *via* www.ccdc.cam.ac.uk/conts/retrieving.html (or from the Cambridge Crystallographic Data Centre, 12 Union Road, Cambridge CB21EZ, UK; fax: (+44)1223-336-033; or deposit@ccdc.cam.ac.uk).

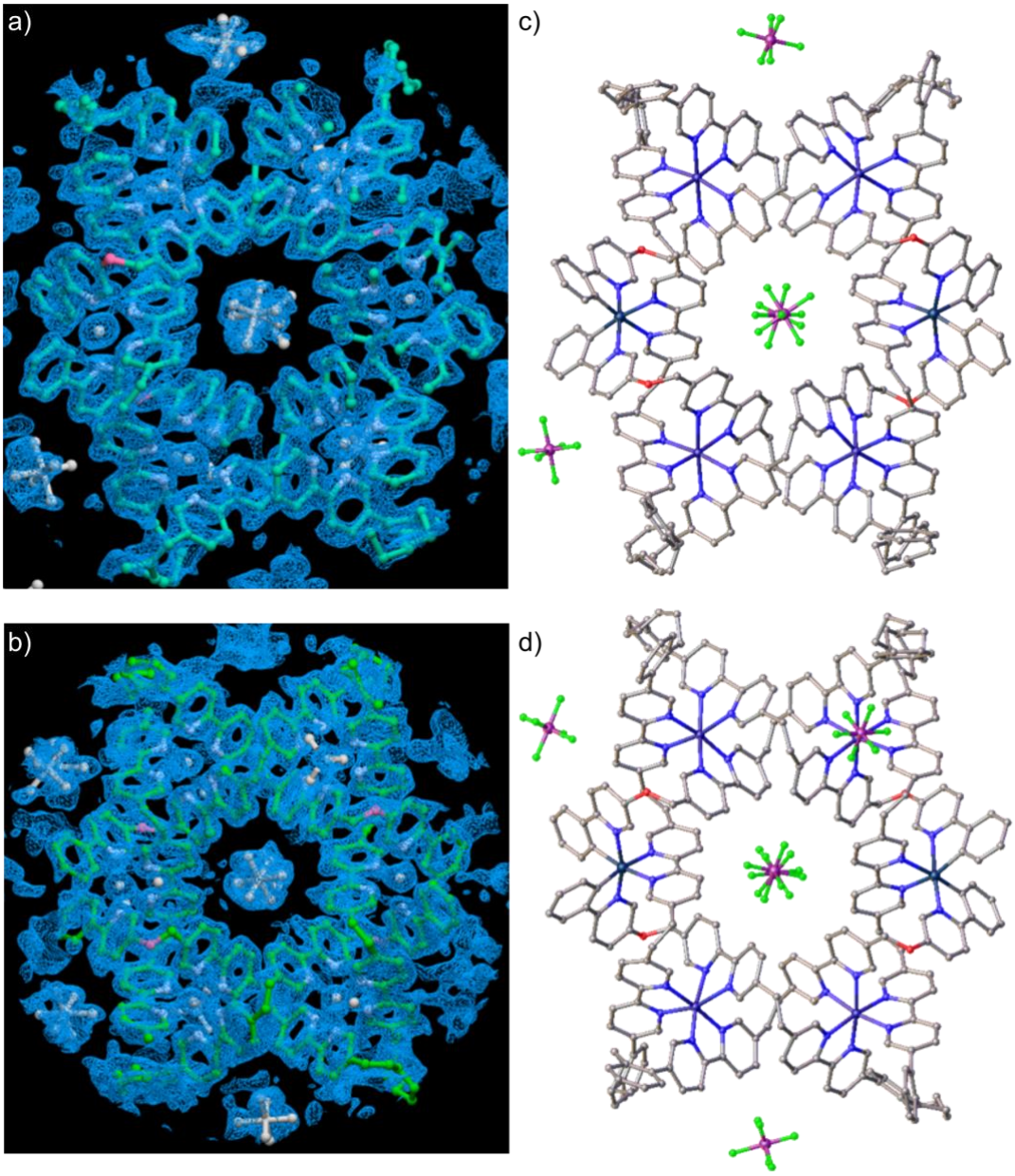

Figure S33. 2Fo-Fc electron density map representation of the central core of a) Δ_6-**8** and b) Λ_6-**8**. Electron density map pictures (4 msd) are represented in blue, carbon atoms are represented in green, nitrogen in light blue, oxygens in pink, PF_6, Zn and Ir in white. Model figures of c) Δ_6-**8** and d) Λ_6-**8** were represented with C in grey, O in red, N in blue, P in magenta, F in green, Zn in purple and Ir in teal. Some of the phenyl-aliphatic chains were omitted for clarity.[S8]

Table S3. Crystallographic information for Λ_6-**8** and Δ_6-**8**

Compound	Λ_6-**8**	Δ_6-**8**
Identification code	m_av434_b_1_3_col1_	m_av435a_3_col1_
Empirical formula	$C_{276}H_{224}F_{60}Ir_2N_{32}O_4P_{10}Zn_4$	$C_{276}H_{224}F_{60}Ir_2N_{32}O_4P_{10}Zn_4$
Formula weight	6148.44	6148.44
Temperature/K	100(2)	100(2)
Crystal system	triclinic	triclinic
Space group	P1	P1
a/Å	23.1012(15)	23.3169(15)
b/Å	27.4445(15)	27.5437(10)
c/Å	27.4980(14)	27.5621(19)
α/°	104.285(5)	104.102(4)
β/°	106.658(5)	106.303(6)
γ/°	107.910(5)	107.895(5)
Volume/Å^3	14781.4(16)	15076.1(17)
Z	2	2
ρ_{calc}g/cm^3	1.381	1.354
μ/mm^{-1}	1.257	1.233
F(000)	6200.0	6200.0
Crystal size/mm^3	0.1 × 0.1 × 0.02	0.1 × 0.1 × 0.1
Radiation	synchrotron (λ = 0.6889)	synchrotron (λ = 0.6889)
2Θ range for data collection/°	2.98 to 31.99	2.942 to 31.99
Index ranges	-18 ≤ h ≤ 18, -21 ≤ k ≤ 21, -21 ≤ l ≤ 21	-18 ≤ h ≤ 18, -22 ≤ k ≤ 22, -22 ≤ l ≤ 22
Reflections collected	56686	63473
Independent reflections	29425 [R_{int} = 0.0787, R_{sigma} = 0.0848]	30691 [R_{int} = 0.0811, R_{sigma} = 0.1154]
Data/restraints/parameters	29425/5562/2067	30691/6149/2429
Goodness-of-fit on F^2	2.190	1.759
Final R indexes [I>=2σ (I)]	R_1 = 0.1498, wR_2 = 0.3489	R_1 = 0.1400, wR_2 = 0.3240
Final R indexes [all data]	R_1 = 0.1994, wR_2 = 0.3738	R_1 = 0.2053, wR_2 = 0.3499
Largest diff. peak/hole / e Å^{-3}	2.22/-0.82	1.46/-0.59
Flack parameter	0.202(12)	0.204(11)

8. NMR Spectra

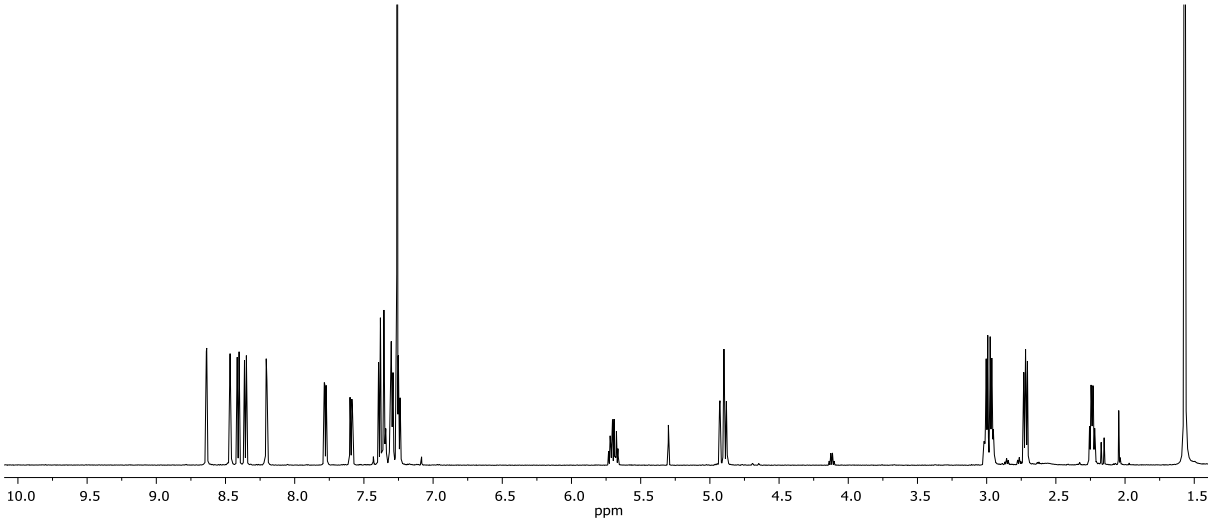

Figure S34. ^{1}H NMR (600 MHz, $CDCl_3$) spectrum of compound **S3**.

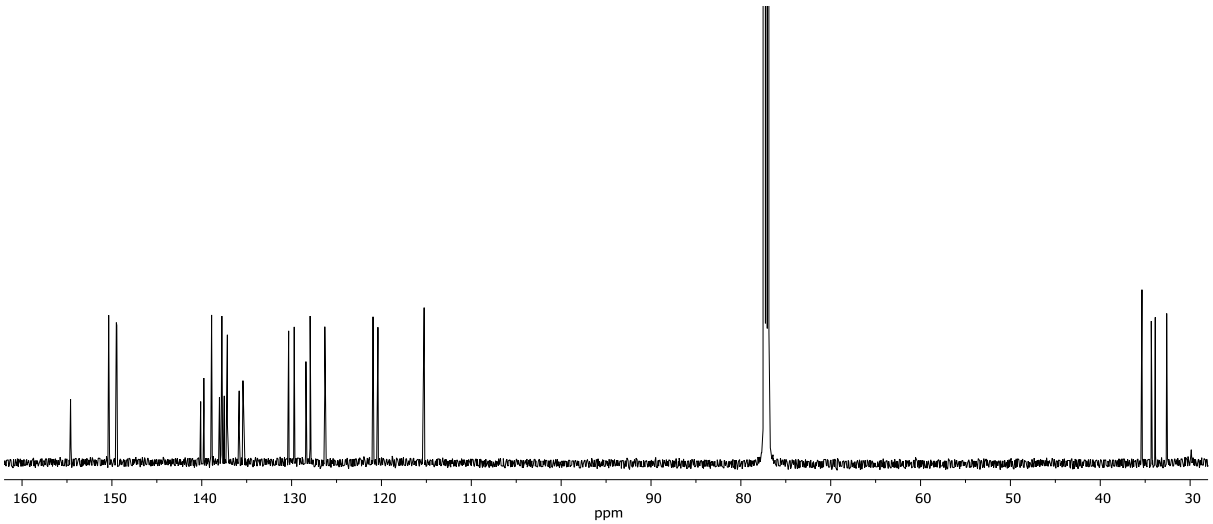

Figure S35. ^{13}C NMR (151 MHz, $CDCl_3$) spectrum of compound **S3**.

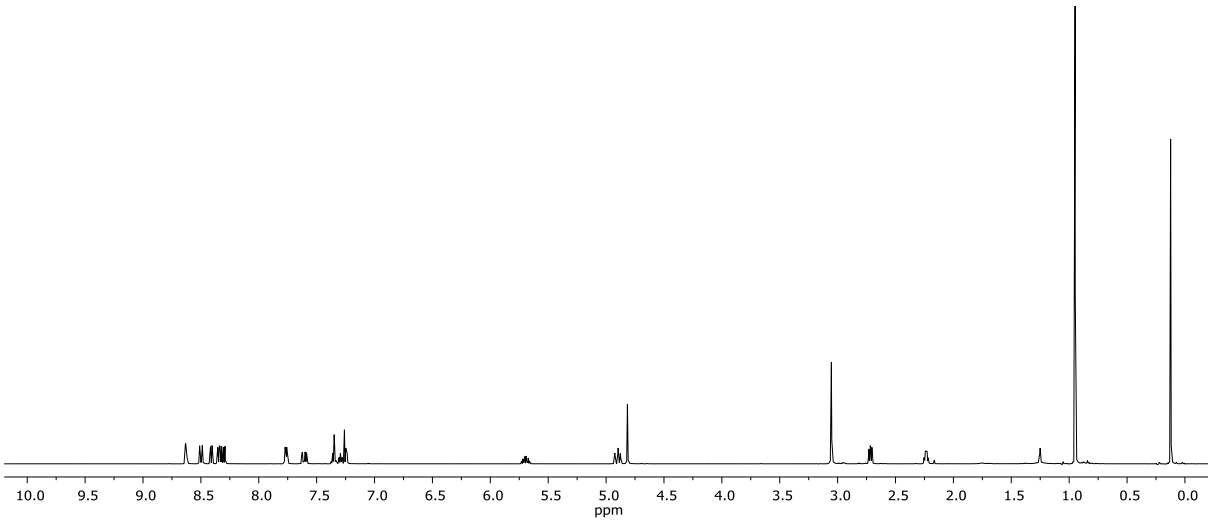

Figure S36. ^{1}H NMR (600 MHz, $CDCl_3$) spectrum of compound **S5**.

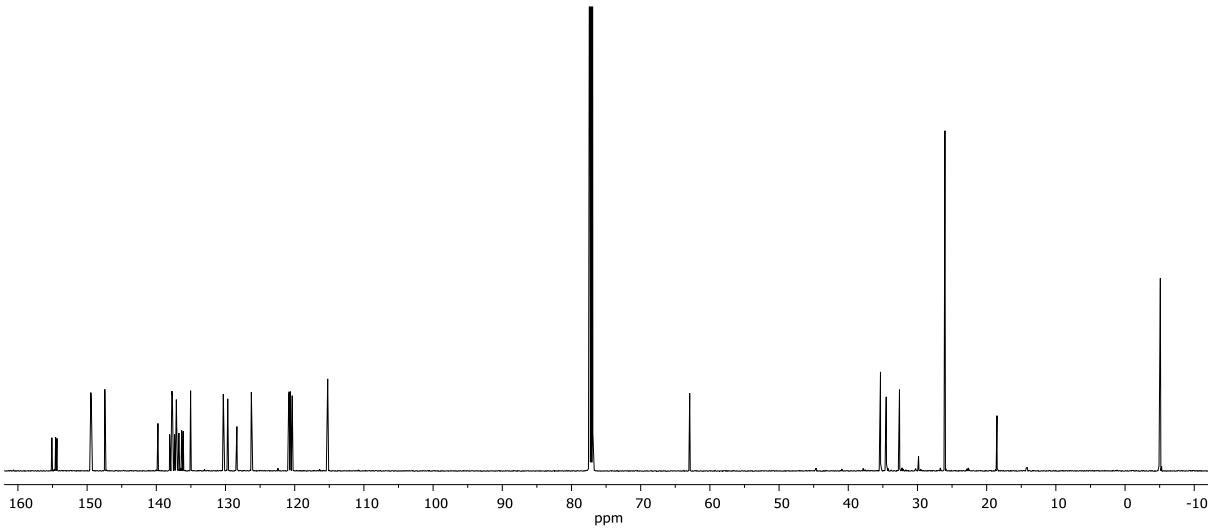

Figure S37. ^{13}C NMR (151 MHz, $CDCl_3$) spectrum of compound **S5**.

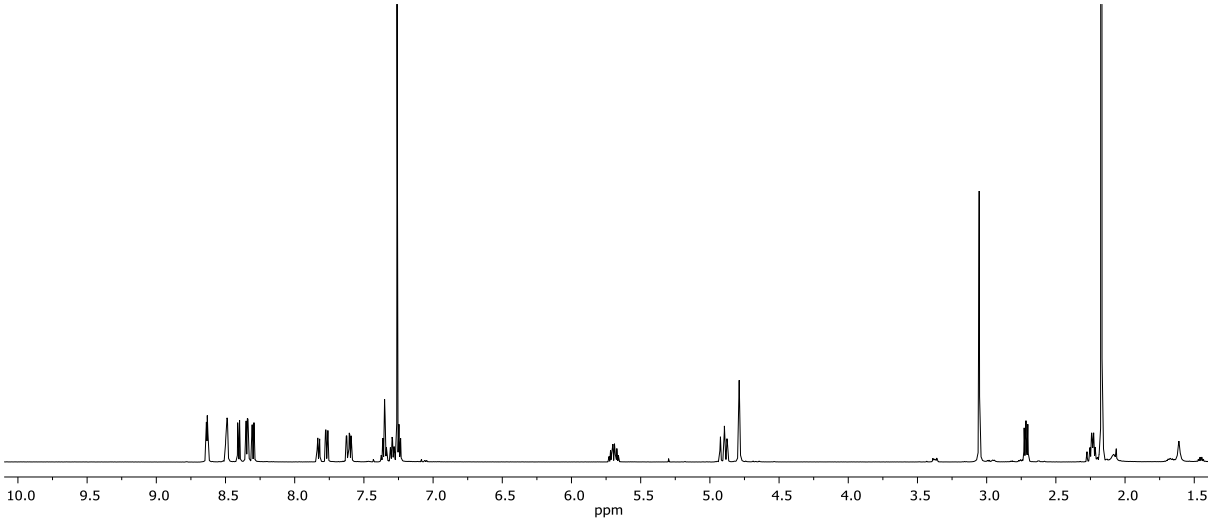

Figure S38. ^{1}H NMR (600 MHz, $CDCl_3$) spectrum of compound **S6**.

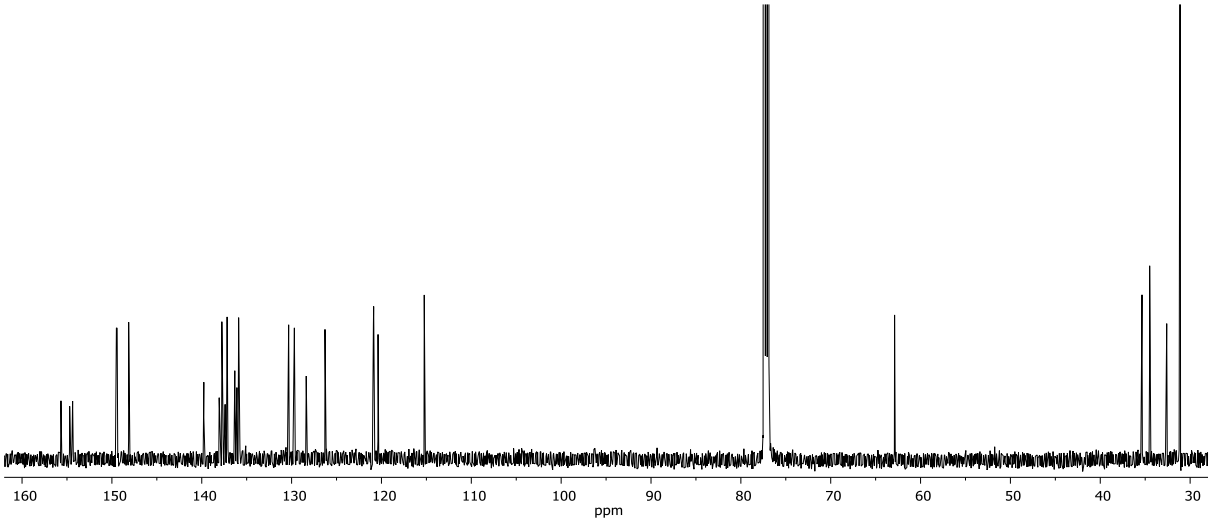

Figure S39. ^{13}C NMR (151 MHz, $CDCl_3$) spectrum of compound **S6**.

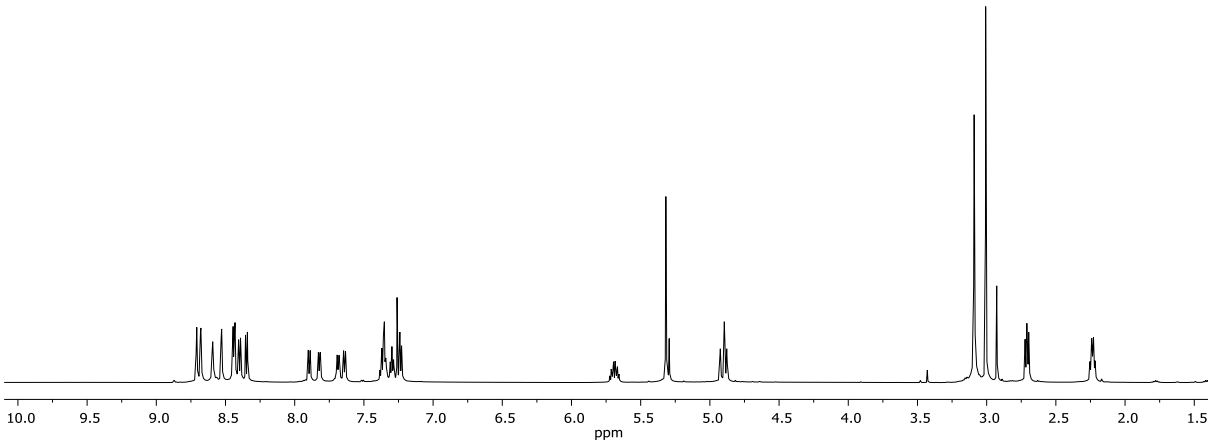

Figure S40. ^{1}H NMR (600 MHz, $CDCl_3$) spectrum of compound **5**.

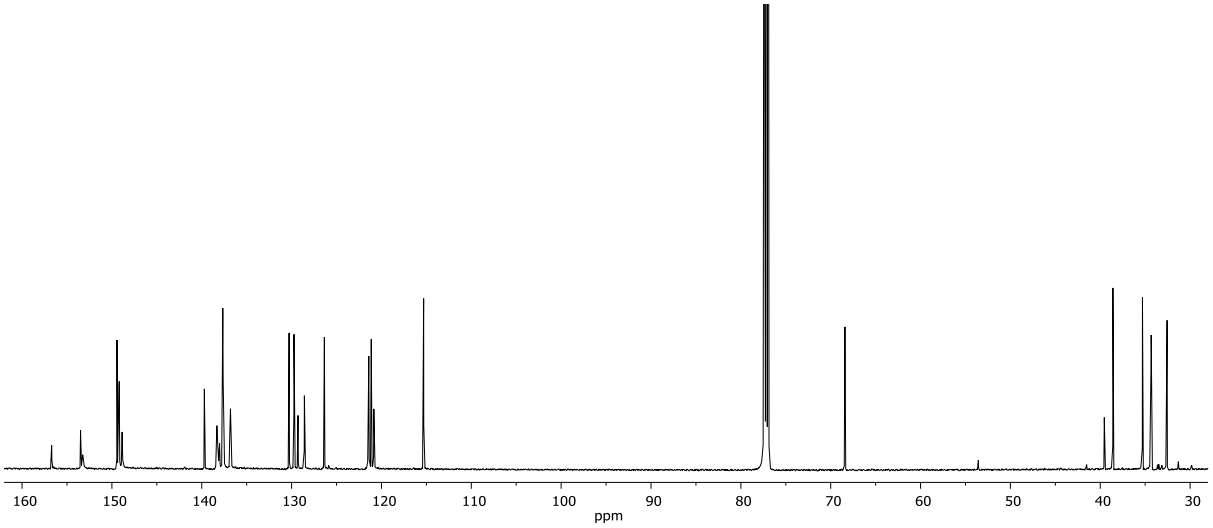

Figure S41. ^{13}C NMR (151 MHz, $CDCl_3$) spectrum of compound **5**.

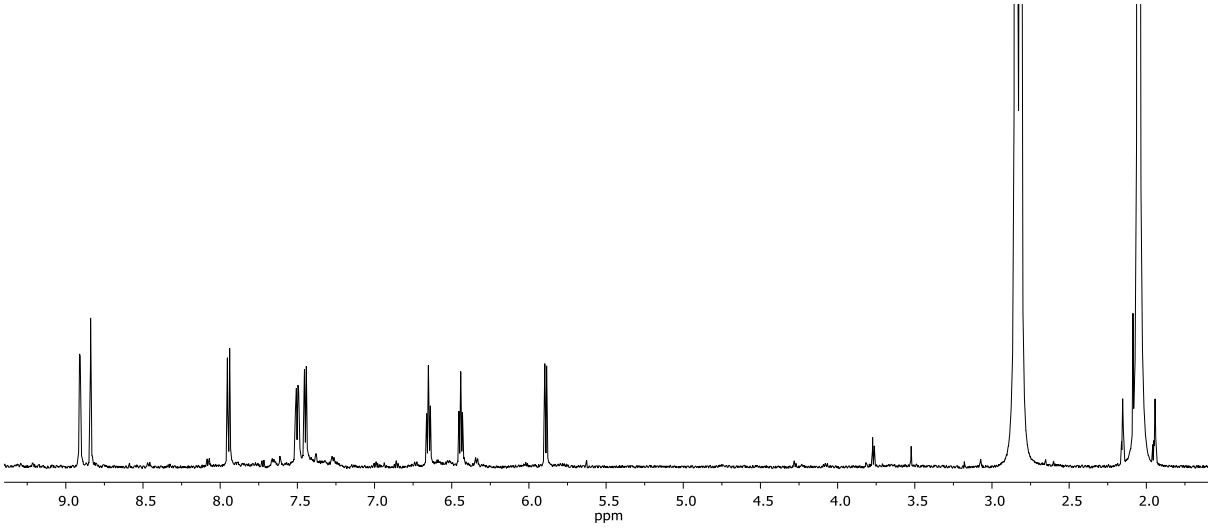

Figure S42. ^{1}H NMR (600 MHz, acetone-d_6) spectrum of compound *rac*-**1**.

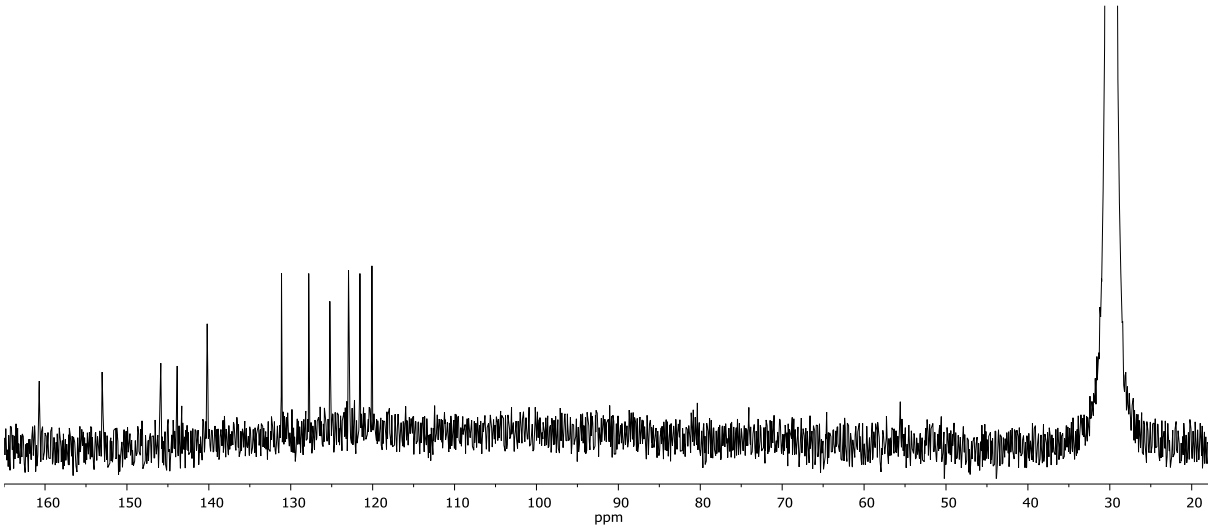

Figure S43. ^{13}C NMR (151 MHz, acetone-d_6) spectrum of compound *rac*-**1**.

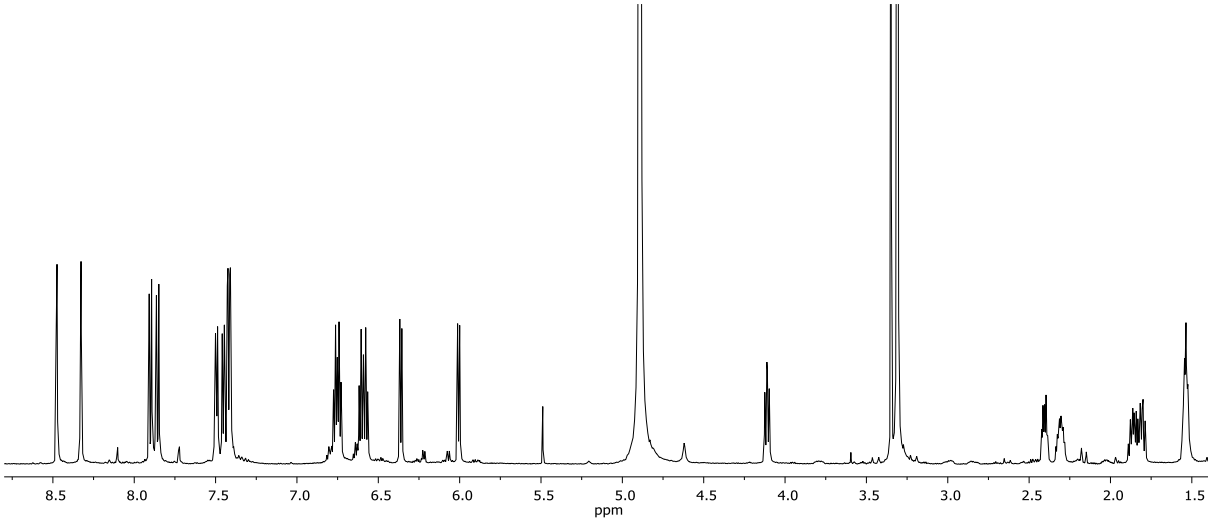

Figure S44. ^{1}H NMR (600 MHz, CD_3OD) spectrum of compound Δ-(D)-**2**.

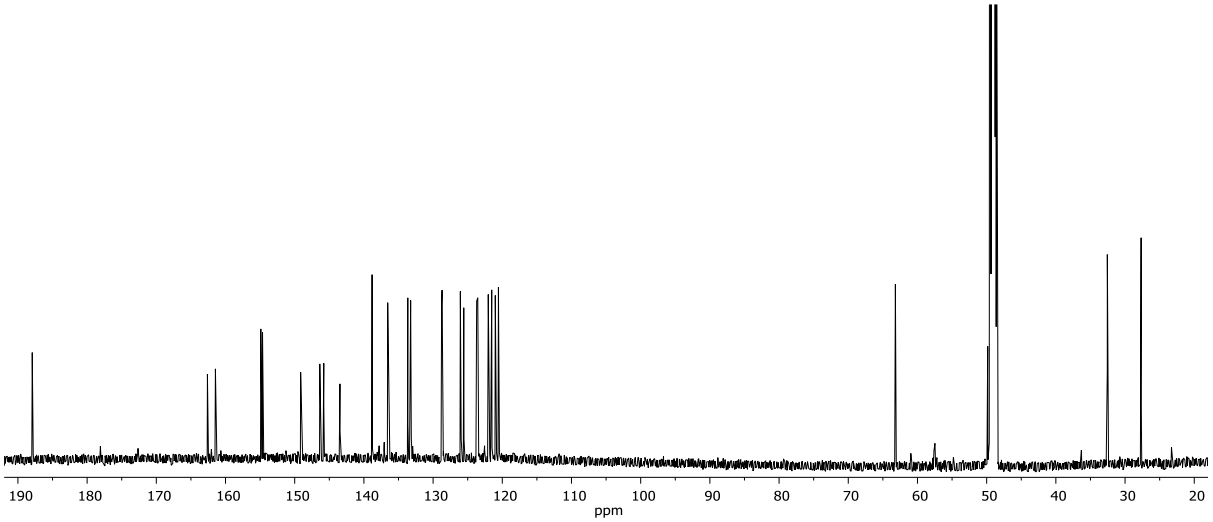

Figure S45. ^{13}C NMR (151 MHz, CD_3OD) spectrum of compound Δ-(D)-**2**.

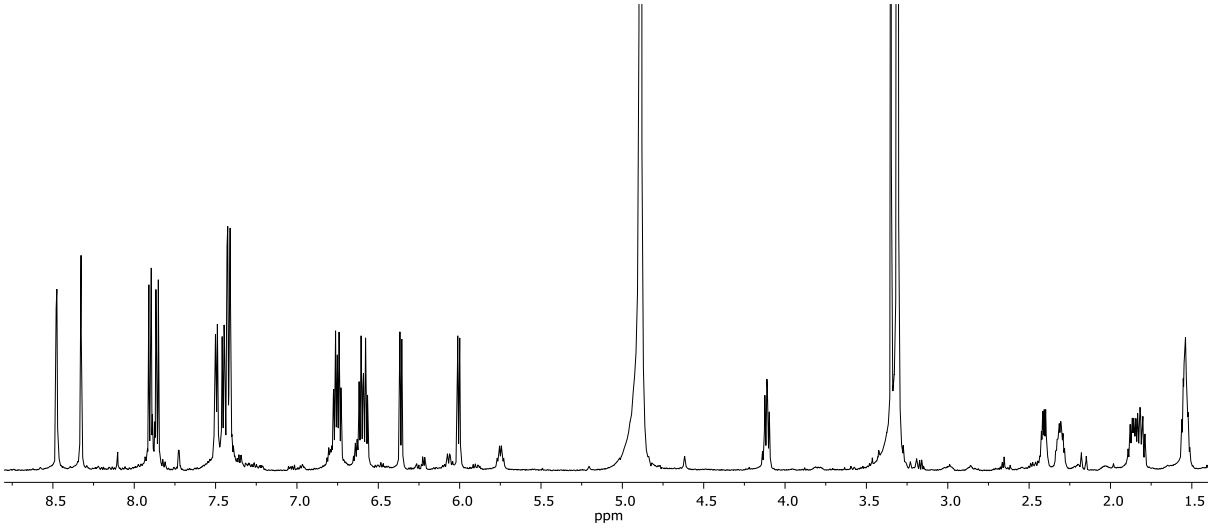

Figure S46. ^{1}H NMR (600 MHz, CD_3OD) spectrum of compound Λ-(L)-**2**.

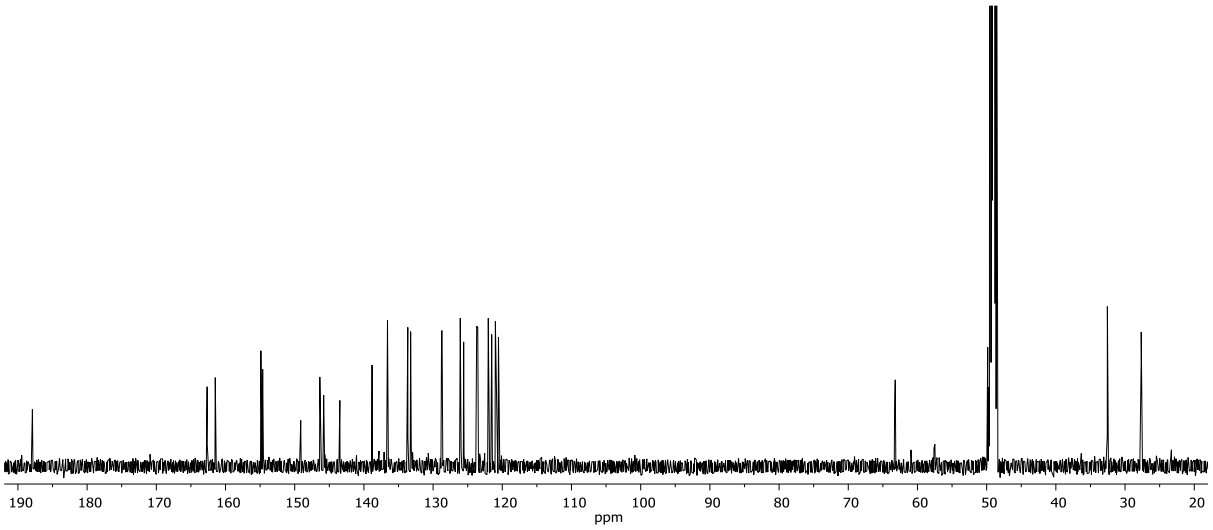

Figure S47. ^{13}C NMR (151 MHz, CD_3OD) spectrum of compound Λ-(L)-**2**.

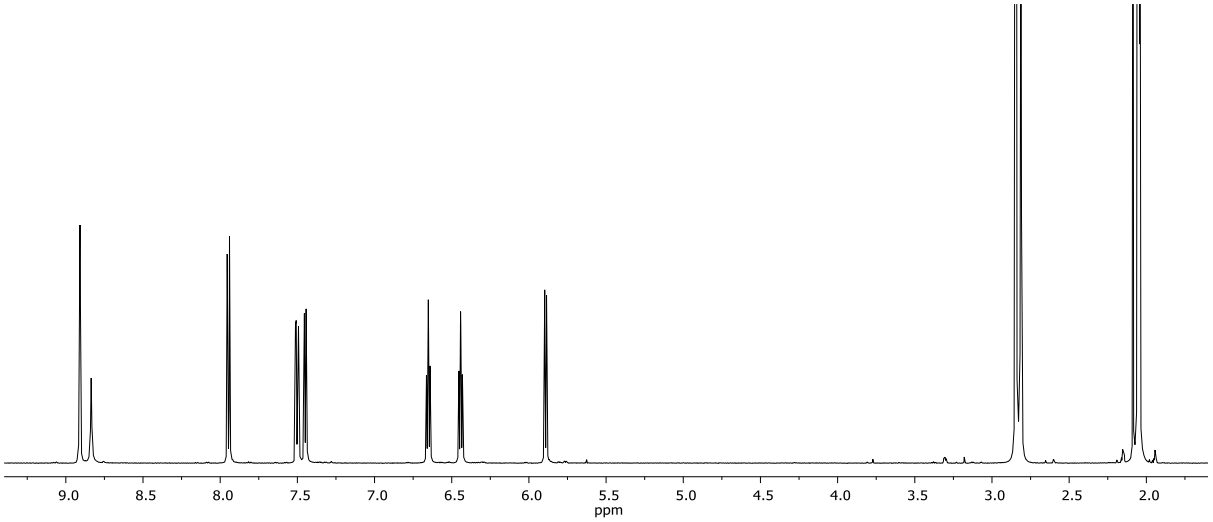

Figure S48. ^{1}H NMR (600 MHz, acetone-d_6) spectrum of compound Δ,Δ-**1**.

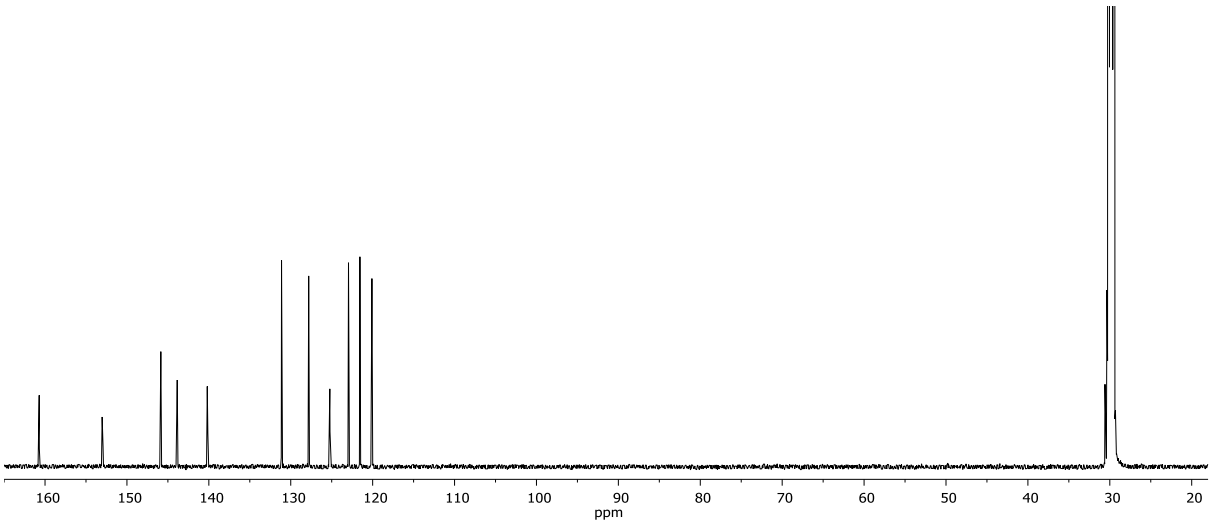

Figure S49. ^{13}C NMR (151 MHz, acetone-d_6) spectrum of compound Δ,Δ-**1**.

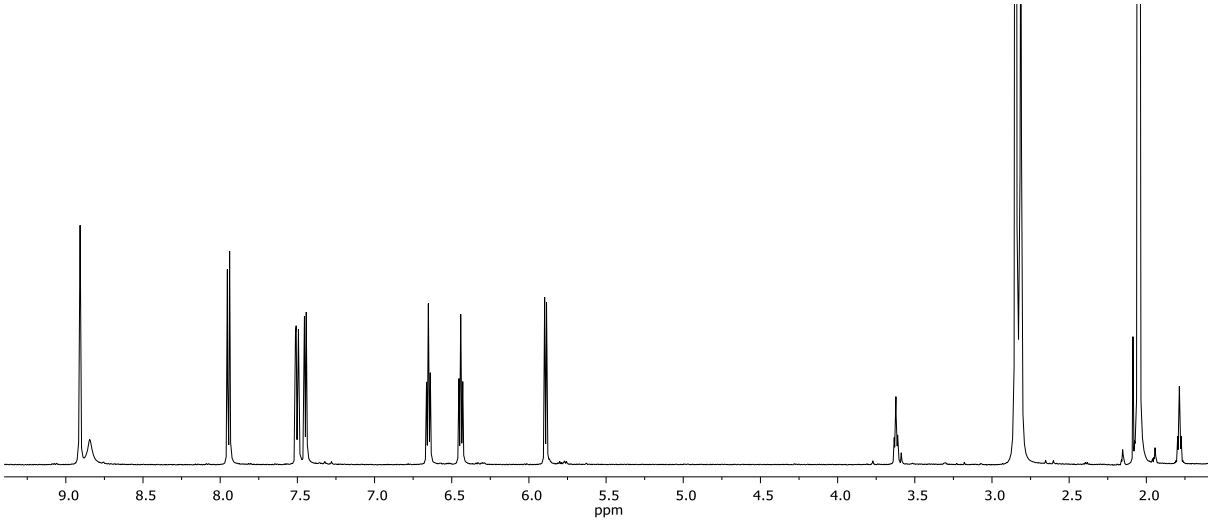

Figure S50. ^{1}H NMR (600 MHz, acetone-d_6) spectrum of compound Λ,Λ-**1**.

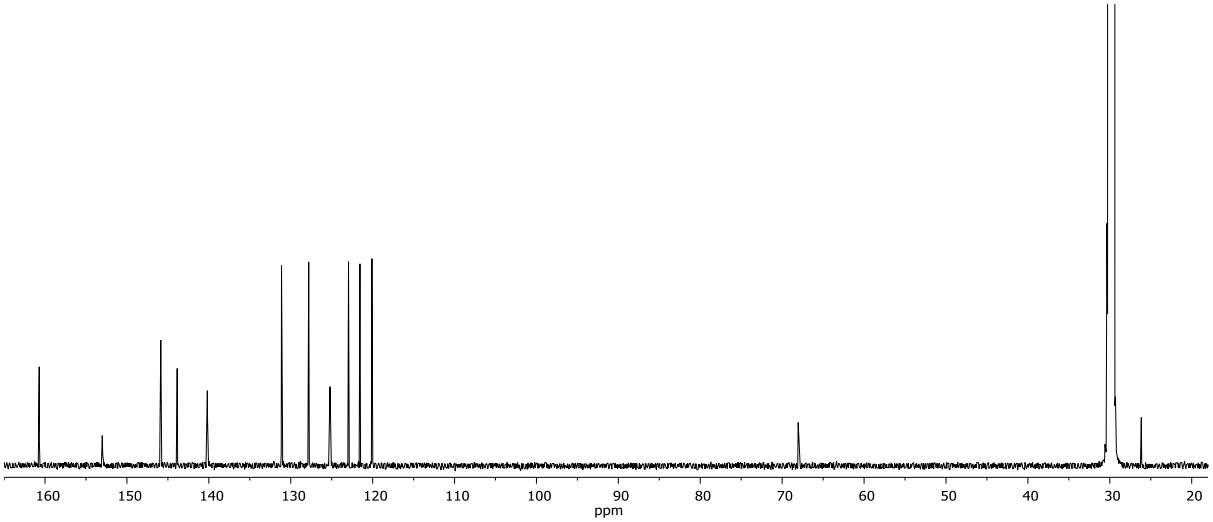

Figure S51. ^{13}C NMR (151 MHz, acetone-d_6) spectrum of compound Λ,Λ-**1**.

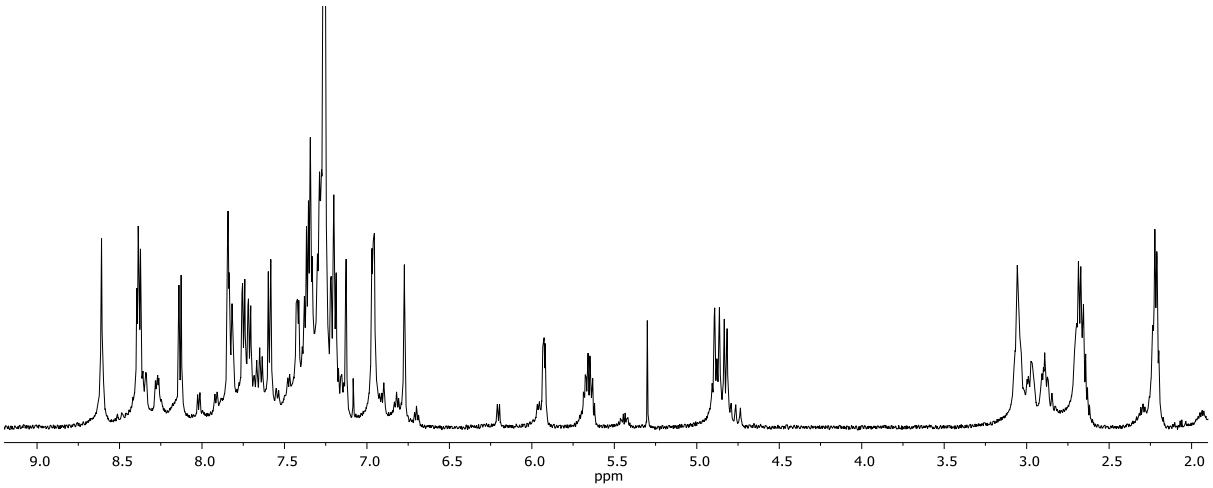

Figure S52. ^{1}H NMR (600 MHz, $CDCl_3$) spectrum of isolated *rac*-**3** used without further purification. Lower intensity peaks correspond to incorrect regioisomer. See Section 4 for a detailed explanation.

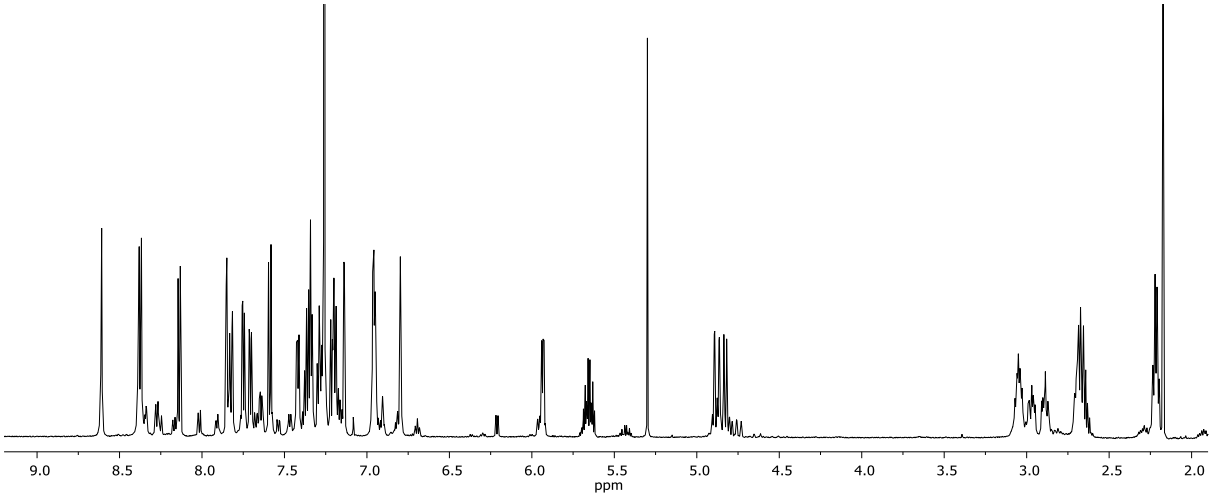

Figure S53. ^{1}H NMR (600 MHz, $CDCl_3$) spectrum of Δ-**3** used without further purification. Lower intensity peaks correspond to incorrect regioisomer. See Section 4 for a detailed explanation.

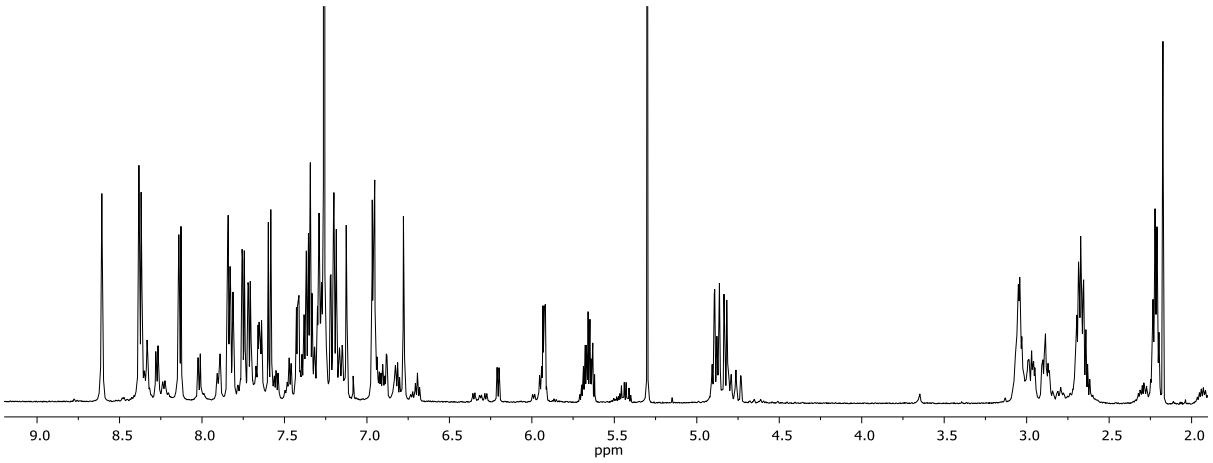

Figure S54. ^{1}H NMR (600 MHz, $CDCl_3$) spectrum of Λ-**3** used without further purification. Lower intensity peaks correspond to incorrect regioisomer. See Section 4 for a detailed explanation.

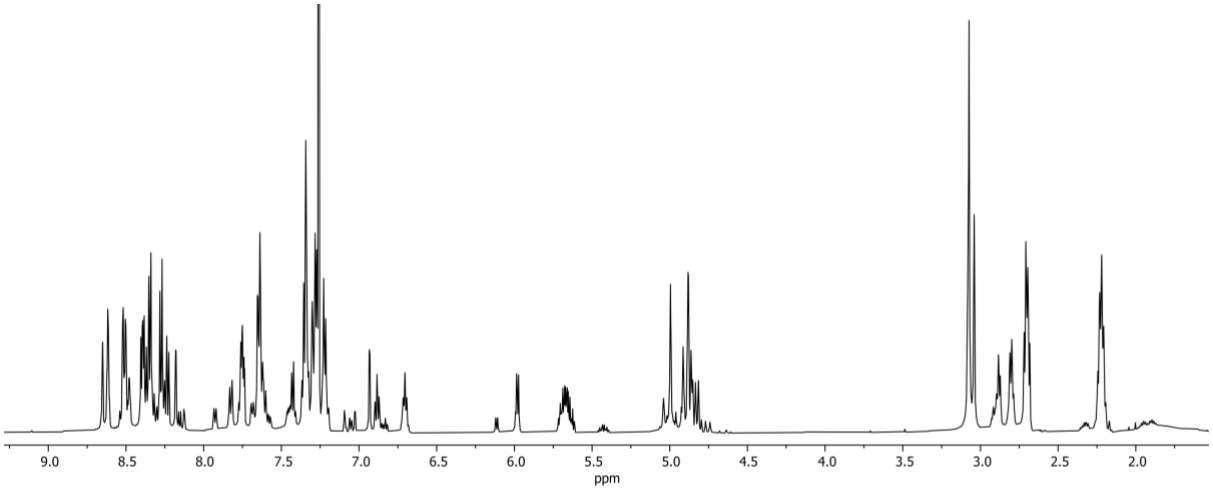

Figure S55. ^{1}H NMR (600 MHz, $CDCl_3$) spectrum of isolated *rac*-**6** used without further purification. Lower intensity peaks correspond to incorrect regioisomer. See Section 4 for a detailed explanation.

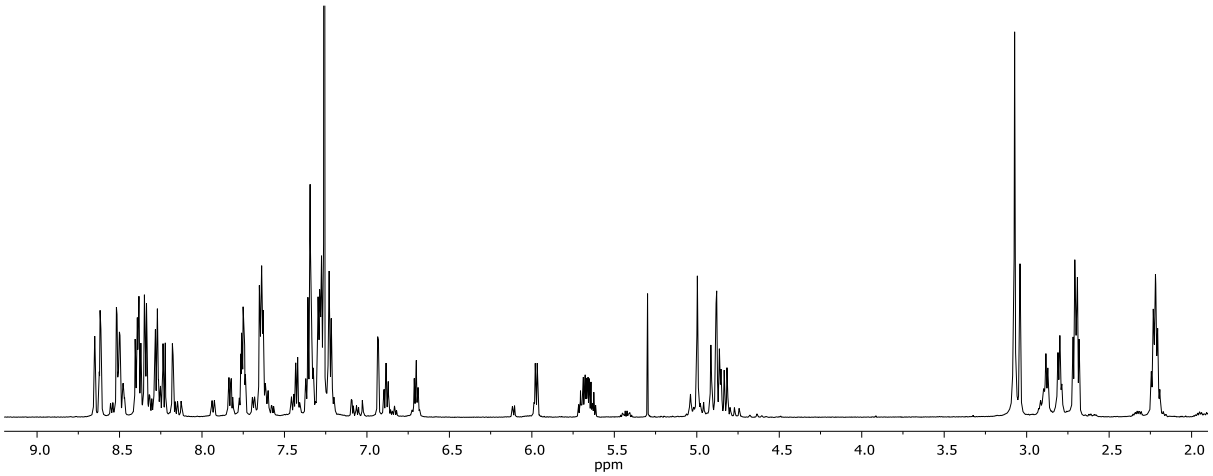

Figure S56. ^{1}H NMR (600 MHz, $CDCl_3$) spectrum of Δ-**6** used without further purification. Lower intensity peaks correspond to incorrect regioisomer. See Section 4 for a detailed explanation.

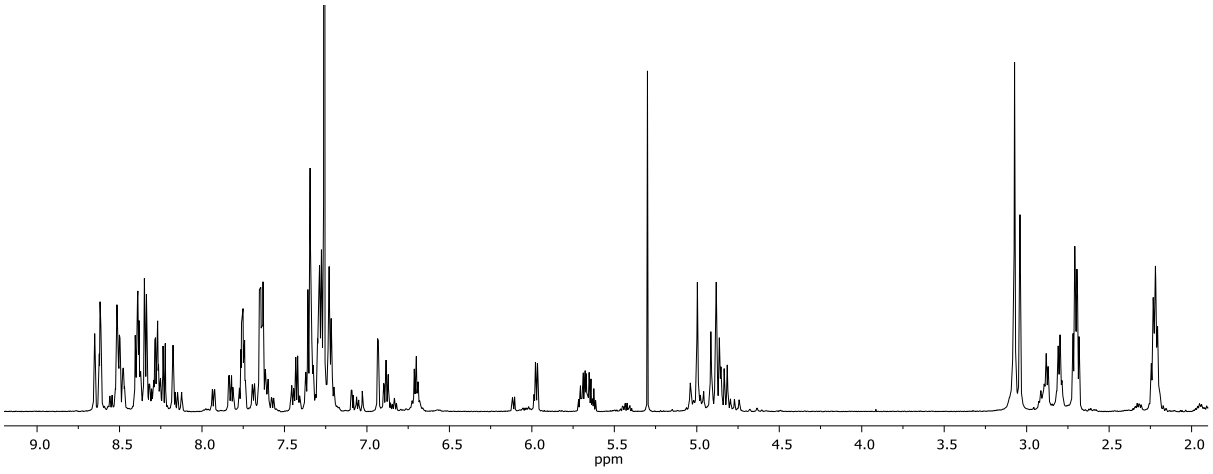

Figure S57. ^{1}H NMR (600 MHz, $CDCl_3$) spectrum of Λ-**6** used without further purification. Lower intensity peaks correspond to incorrect regioisomer. See Section 4 for a detailed explanation.

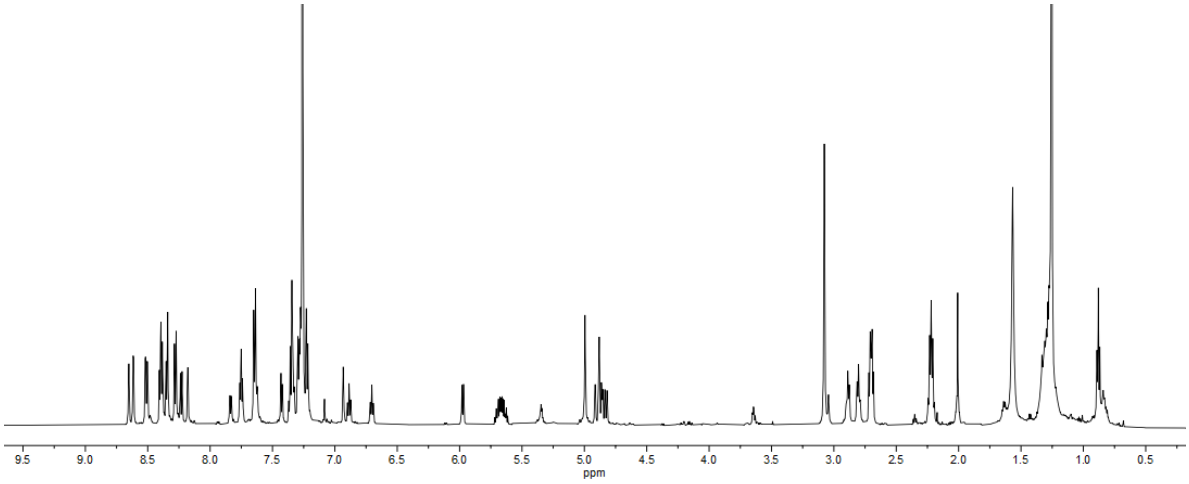

Figure S58. ^{1}H NMR (600 MHz, $CDCl_3$) spectrum of *rac*-**6** purified via demetallation of *rac*-**7**. See section 4.2 for detailed explanation of purification.

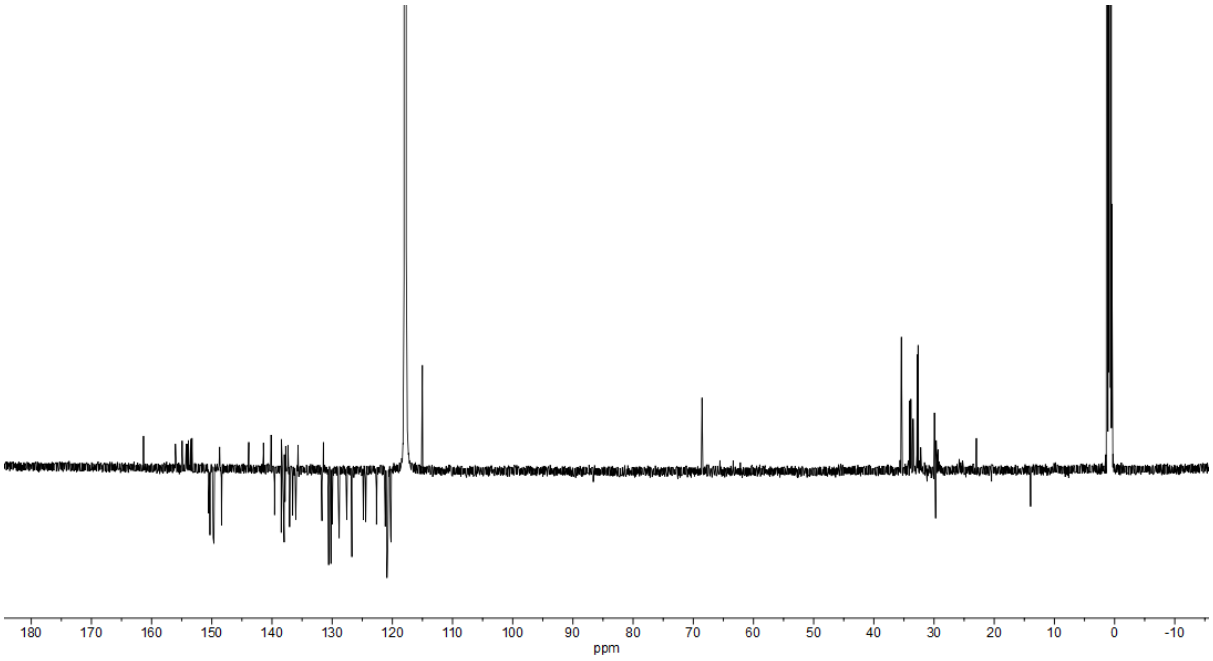

Figure S59. DEPTQ NMR (151 MHz, $CDCl_3$) spectrum of compound *rac*-**6** purified via demetallation of *rac*-**7**. See section 4.2 for detailed explanation of purification.

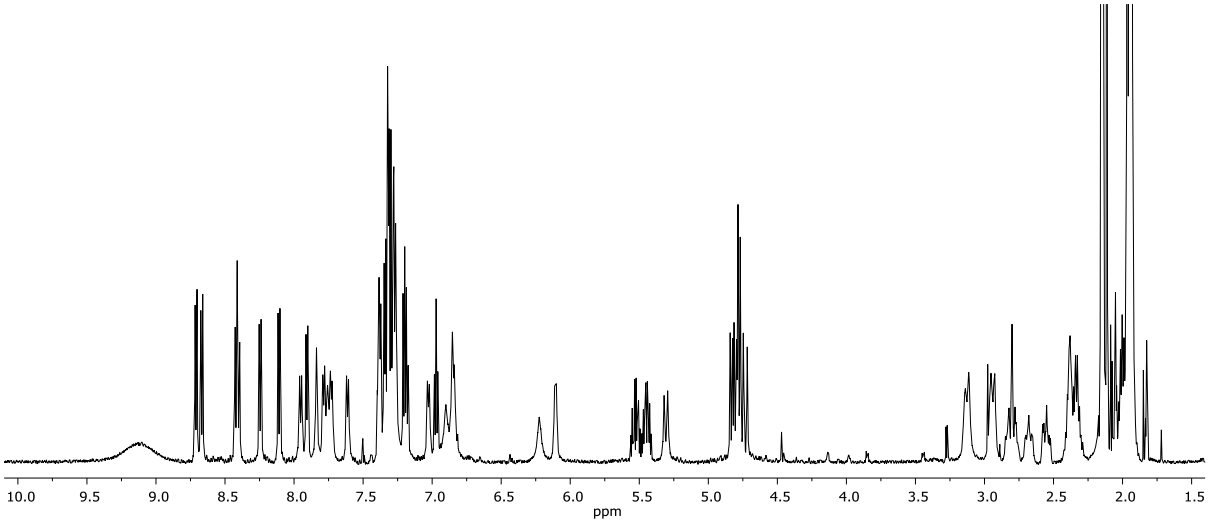

Figure S60. ^{1}H NMR (600 MHz, CD_3CN) spectrum of compound *rac*-**7**.

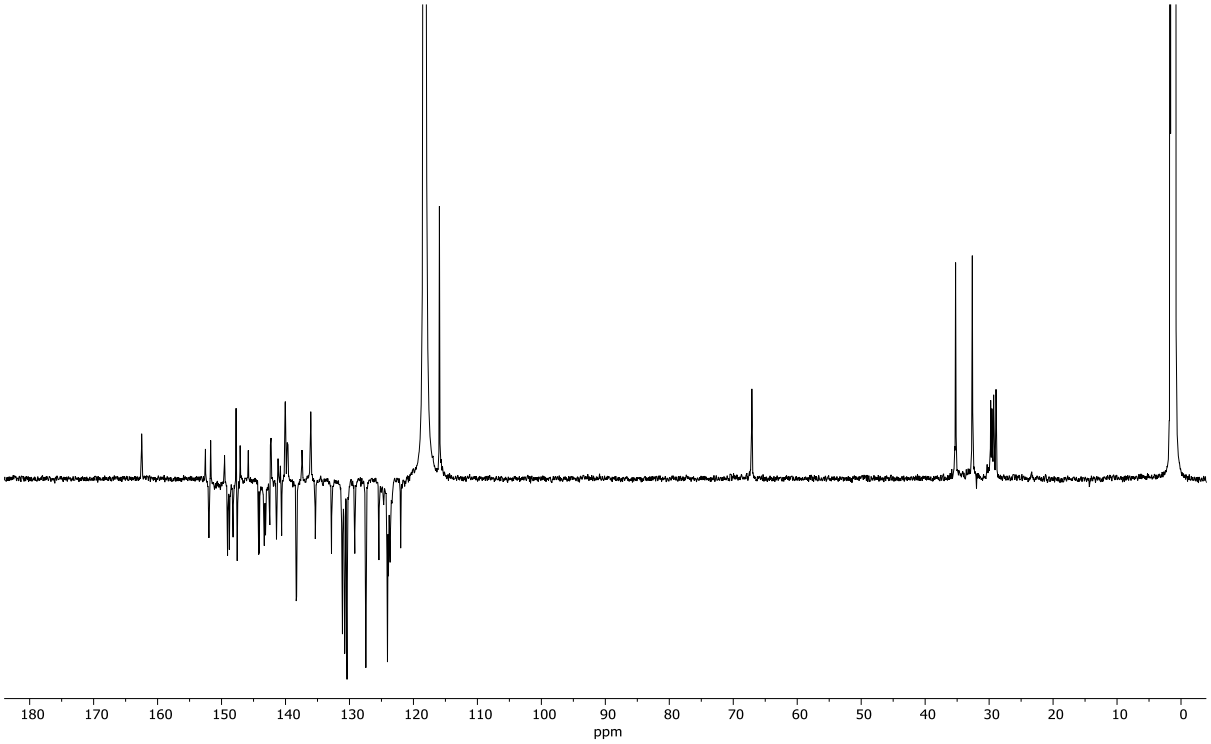

Figure S61. DEPTQ NMR (151 MHz, CD_3CN) spectrum of compound *rac*-**7**.

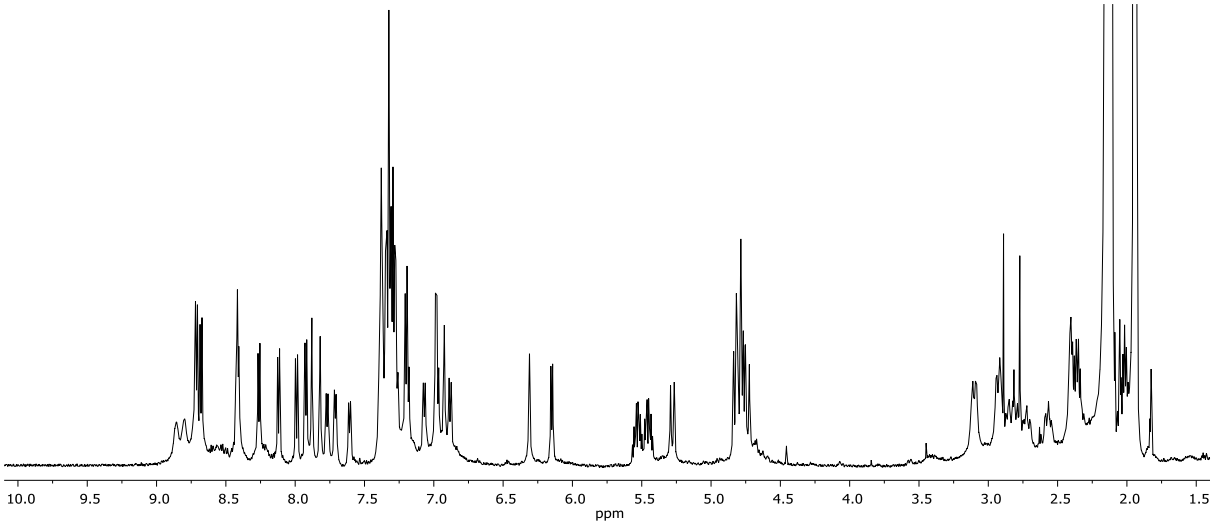

Figure S62. ^{1}H NMR (600 MHz, CD_3CN) spectrum of compound Δ_6-**7**.

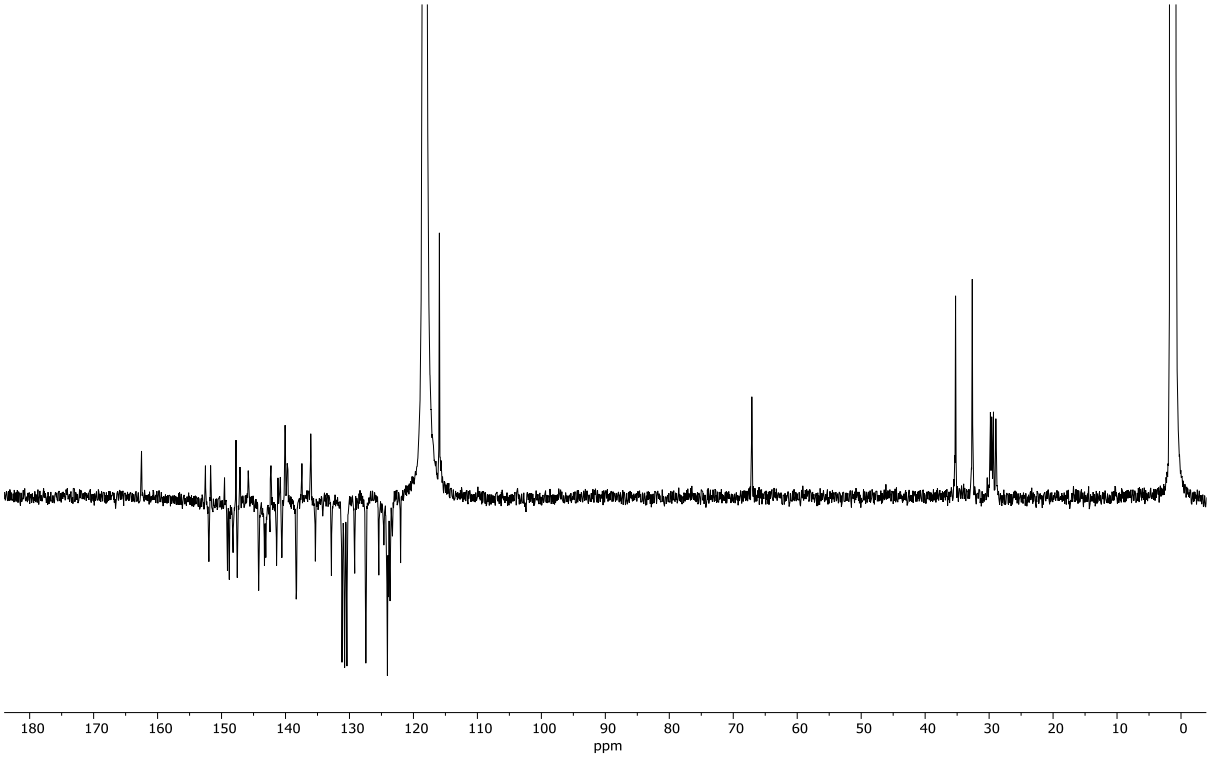

Figure S63. DEPTQ NMR (151 MHz, CD_3CN) spectrum of compound Δ_6-**7**.

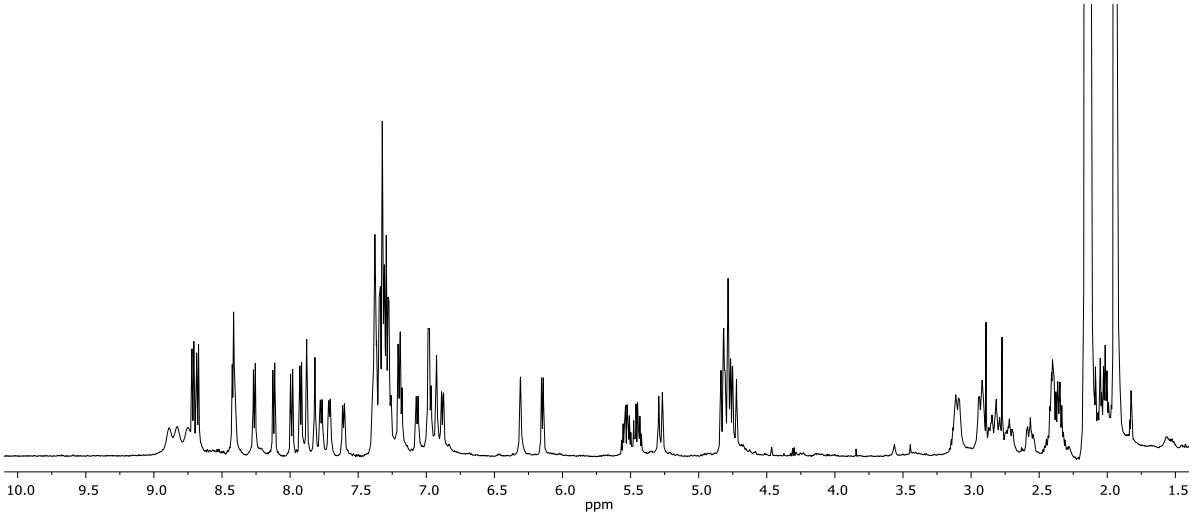

Figure S64. ^{1}H NMR (600 MHz, CD_3CN) spectrum of compound Λ_6-**7**.

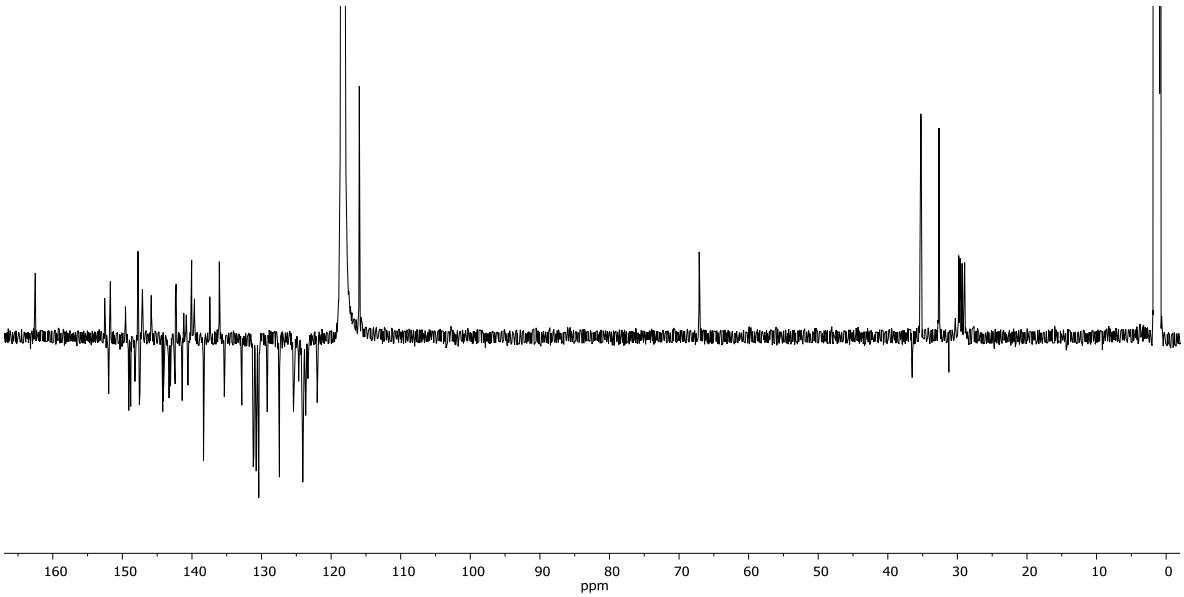

Figure S65. DEPTQ NMR (151 MHz, CD_3CN) spectrum of compound Λ_6-**7**.

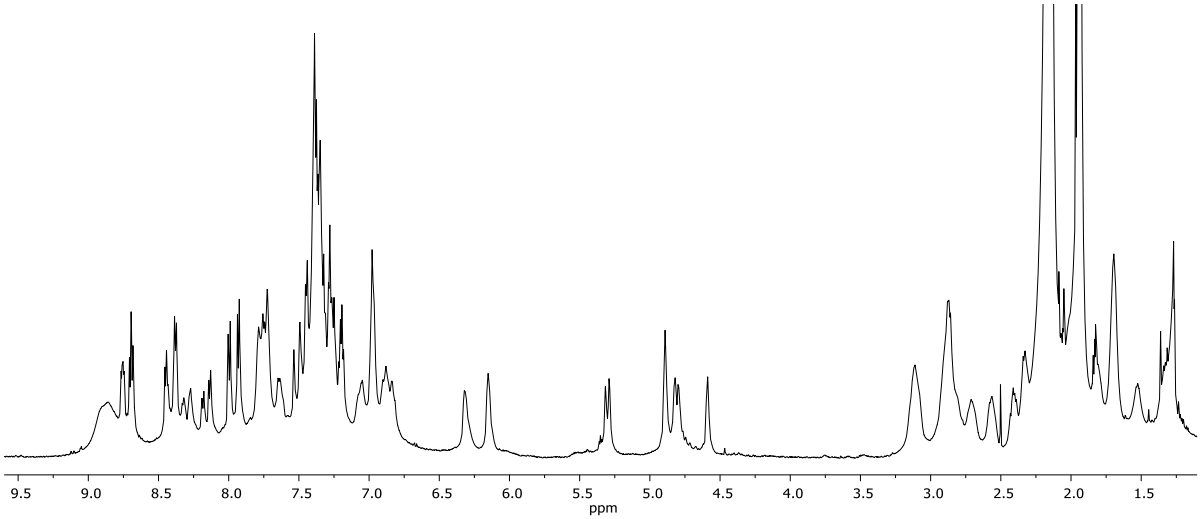

Figure S66. ^{1}H NMR (600 MHz, CD_3CN) spectrum of compound *rac*-**8**.

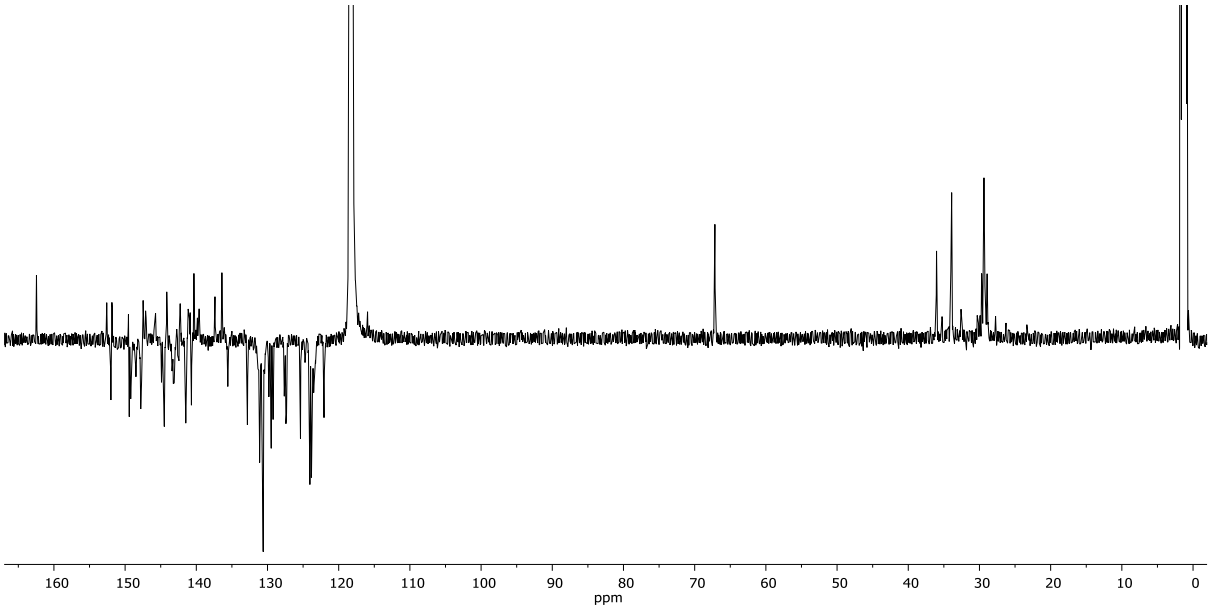

Figure S67. DEPTQ NMR (151 MHz, CD_3CN) spectrum of compound *rac*-**8**.

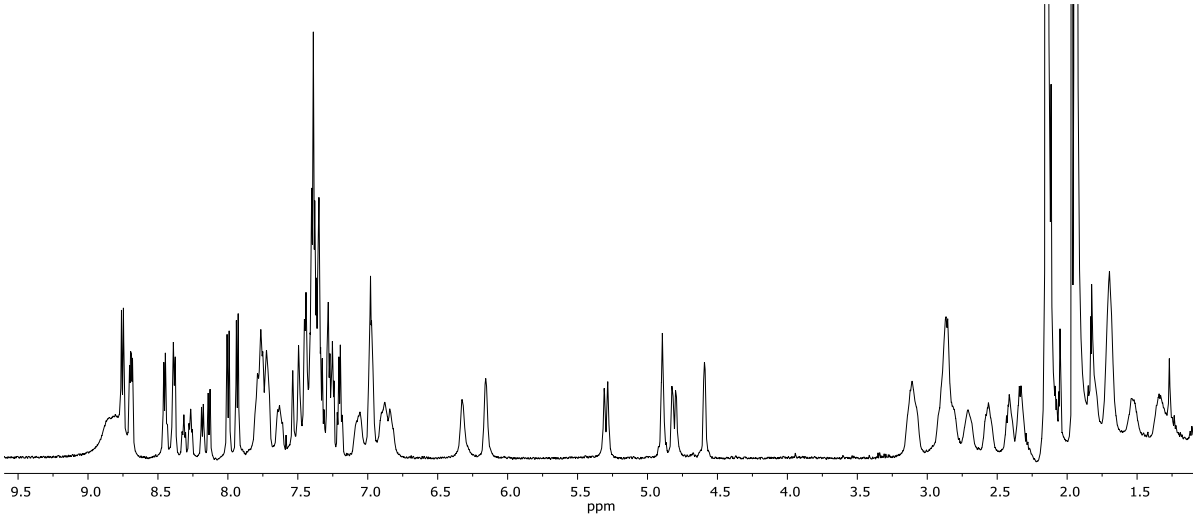

Figure S68. ^{1}H NMR (600 MHz, CD_3CN) spectrum of compound Δ_6-**8**.

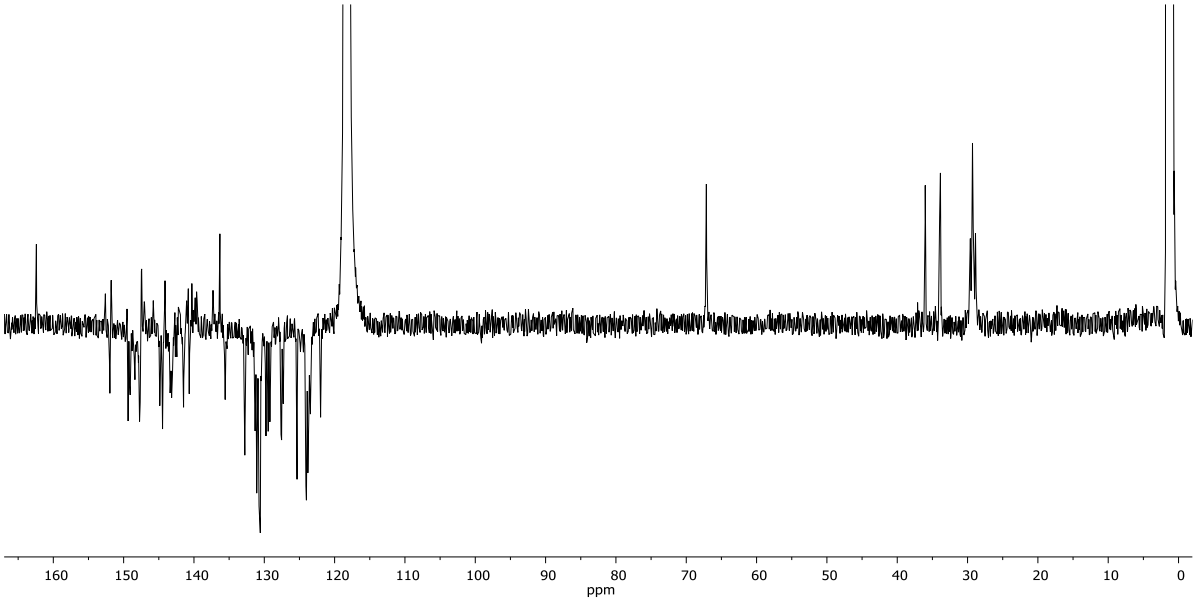

Figure S69. DEPTQ NMR (151 MHz, CD_3CN) spectrum of compound Δ_6-**8**.

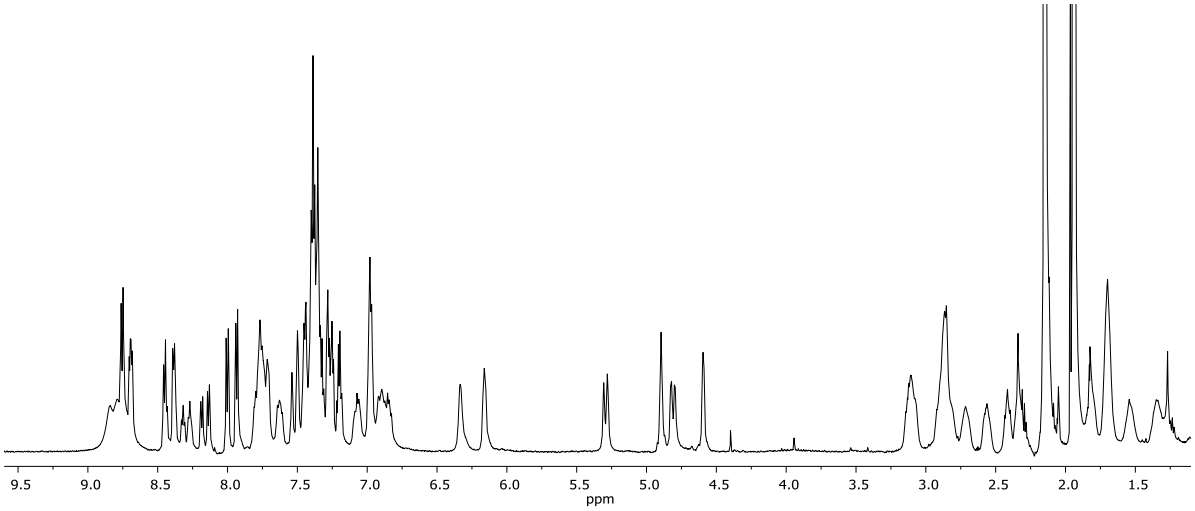

Figure S70. ^{1}H NMR (600 MHz, CD_3CN) spectrum of compound Λ_6-**8**.

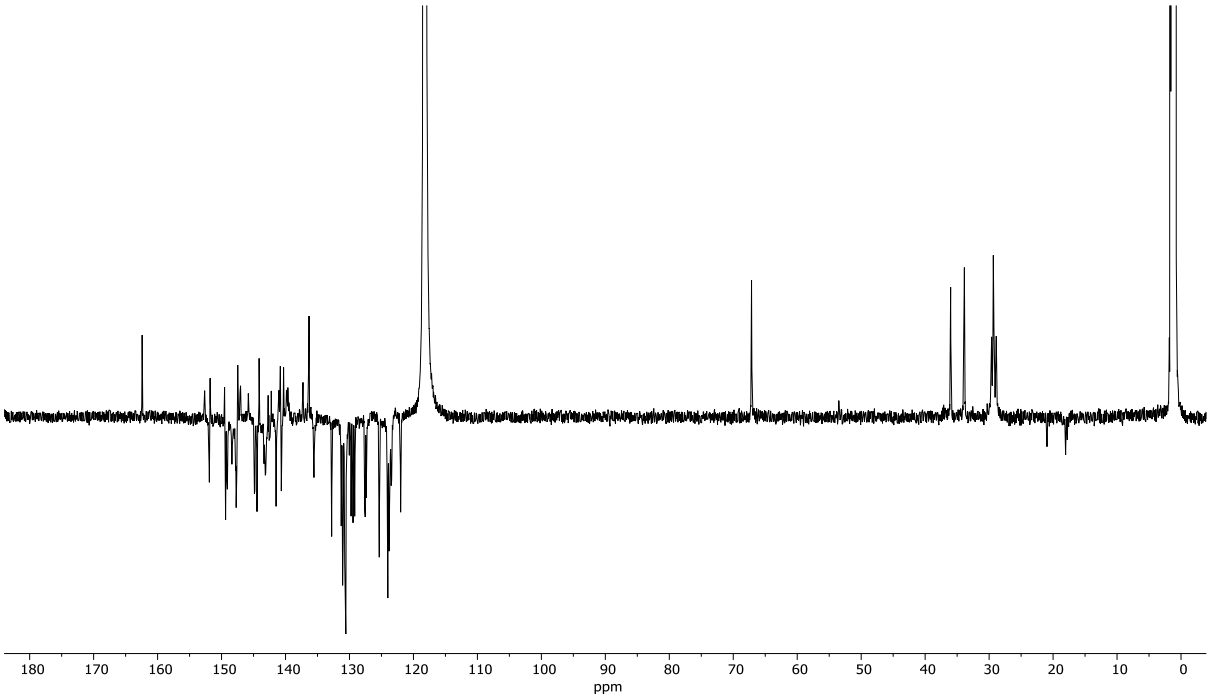

Figure S71. DEPTQ NMR (151 MHz, CD_3CN) spectrum of compound Λ_6-**8**.

References

S1. P. S. Yang, M. T. Tsai, M. H. Tsai, C. W. Ong, *Chem. Asian J.* **2015**, *10*, 849–852.

S2. D. A. Leigh, R. G. Pritchard, A. J. Stephens, *Nat. Chem.* **2014**, *6*, 978-982.

S3. J. W. Ellingboe, M. Antane, T. T. Nguyen, M. D. Collini, S. Antane, R. Bender, D. Hartupee, V. White, J. McCallum, C. H. Park, A. Russo, M. B. Osier, A. Wojdan, J. Dinish, D. M. Ho, J. F. Bagli, *J. Med. Chem.* **1994**, *37*, 542-550.

S4. K. Suzuki, A. Kobayashi, S. Kaneko, K. Takehira, T. Yoshihara, H. Ishida, Y. Shiina, S. Oishi, S. Tobita, *Phys. Chem. Chem. Phys.* **2009**, *11*, 9850-9860.

S5. H. Nowell, S. A. Barnett, K. E. Christensen, S. J. Teat, D. R. Allan, *J. Synchrotron Rad.* **2012**, *19*, 435-441.

S6. a) G. M. Sheldrick, *SADABS*, empirical absorption correction program based upon the method of Blessing; b) L. Krause, R. Herbst-Irmer, G. M. Sheldrick, D. Stalke, *J. Appl. Cryst.* **2015**, *48*, 3-10; c) R. H. Blessing, *Acta Cryst.* **1995**, *A51*, 33-38.

S7. a) Sheldrick. G. M., *Acta Cryst.* **2015**, *C71*, 3-8; b) O. V. Dolomanov, L. J. Bourhis, R. J. Gildea, J. A. K. Howard, H. Puschmann, *J. Appl. Cryst.* **2009**, *42*, 339–341.

S8. 2Fo-Fc electron density maps were obtained using Phenix software. Initially, the reflexions file (.mtz) obtained form CrysAlisPro was edited to include the map coefficients. Then, the maps were calculated from the edited reflexions file and the model (pdb file) obtained from structure solution software (OLEX 2) using phenix.maps software.